

## N O T I C E

THIS DOCUMENT HAS BEEN REPRODUCED FROM  
MICROFICHE. ALTHOUGH IT IS RECOGNIZED THAT  
CERTAIN PORTIONS ARE ILLEGIBLE, IT IS BEING RELEASED  
IN THE INTEREST OF MAKING AVAILABLE AS MUCH  
INFORMATION AS POSSIBLE

**NASA CR-165349**

**SSS-R-81-4847**

**ADDITIONAL APPLICATION OF THE  
NASCAP CODE**

**VOLUME I: NASCAP EXTENSION**

**I. Katz, J.J. Cassidy, M.J. Mandell, D.E. Parks,  
G.W. Schnuelle, P.R. Stannard, P.G. Steen**

**SYSTEMS, SCIENCE AND SOFTWARE**

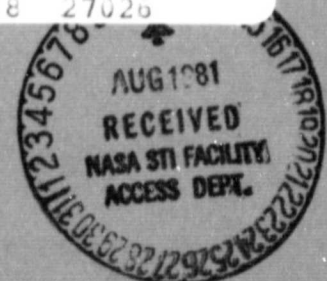
**Prepared for**

**NATIONAL AERONAUTICS AND SPACE ADMINISTRATION**

**NASA LEWIS RESEARCH CENTER**

(NASA-CR-165349) ADDITIONAL APPLICATION OF N81-28136  
THE NASCAP CODE. VOLUME 1: NASCAP  
EXTENSION Final Report, Mar. 1979 - Oct.  
1980 (Systems Science and Software) 126 p. Unclass  
HC A07/MF A01 CSCL 22B G3/18 27026

**Contract NAS3-21762**



1. Report No. NASA CR-165349		2. Government Accession No.		3. Recipient's Catalog No.	
4. Title and Subtitle ADDITIONAL APPLICATION OF THE NASCAP CODE, VOLUME I: NASCAP EXTENSION				5. Report Date February 1981	
				6. Performing Organization Code	
7. Author(s) I. Katz, J. J. Cassidy, M. J. Mandell, D. E. Parks, G. W. Schnuelle, P. R. Stannard, P. G. Steen				8. Performing Organization Report No. SSS-R-81-4847 (Vol. I)	
9. Performing Organization Name and Address Systems, Science and Software P. O. Box 1620 La Jolla, CA 92038				10. Work Unit No.	
				11. Contract or Grant No. NAS3-21762	
12. Sponsoring Agency Name and Address National Aeronautics and Space Administration Lewis Research Center 21000 Brookpark Road, Cleveland, OH 44135				13. Type of Report and Period Covered Contractor Report 3/1979-10/1980	
				14. Sponsoring Agency Code 5532	
15. Supplementary Notes  Project Manager, James C. Roche, NASA-Lewis Research Center, Cleveland, OH					
16. Abstract  NASCAP is a computer program that comprehensively analyzes problems of spacecraft charging. Using a fully three-dimensional approach, it can accurately predict spacecraft potentials under a variety of conditions. Under Contract NAS3-21762, several changes were made to improve NASCAP, and a new code, NASCAP/LEO, was developed. In addition, detailed studies of several spacecraft-environmental interactions and of the SCATHA spacecraft were performed (see companion reports, References 1 and 2).  The changes made to NASCAP make it run faster - execution time has been cut by more than half. It is now more accurate - photosheath approximations and many other features have been added. It is easier to use - a new user unfamiliar with the host computer can learn NASCAP in a matter of days. Auxiliary codes have also been developed to improve NASCAP flexibility and reduce problem turnaround time.  A NASCAP/LEO program has been written. This handles situations of relatively short Debye length encountered by large space structures or by any satellite in low earth orbit (LEO). This preliminary model has already been applied to two important high voltage interaction problems.					
17. Key Words (Suggested by Author(s)) NASCAP, Spacecraft Charging, Solar Power Satellite, Photosheath, Plasma Collection, Spacecraft Sheath, Computer Simulation				18. Distribution Statement  Publicly Available	
19. Security Classif. (of this report) Unclassified		20. Security Classif. (of this page) Unclassified		21. No. of Pages 134	22. Price*

\* For sale by the National Technical Information Service, Springfield, Virginia 22161

## TABLE OF CONTENTS

		<u>Page</u>
	SUMMARY . . . . .	1
1.	INTRODUCTION . . . . .	3
2.	PHYSICAL MODEL EXTENSIONS . . . . .	6
	2.1 PHOTOSHEATH . . . . .	6
	2.1.1 Effective Photosheath Conductivity . . . . .	6
	2.1.2 Self-consistent Photosheath . . . . .	7
	2.2 MATERIAL PROPERTIES . . . . .	9
	2.3 SCREENING LENGTH . . . . .	10
	2.4 ROTATING MAGNETIC FIELD . . . . .	10
	2.5 DETECTOR UPDATE . . . . .	11
	2.6 EMITTER ROUTINE KINENG . . . . .	19
	2.7 BOOM CELL MODELING . . . . .	24
3.	USABILITY . . . . .	32
	3.1 INPUT . . . . .	33
	3.1.1 Free Format Input . . . . .	33
	3.1.2 Surface Cell Specifications . . . . .	34
	3.1.3 Boom Input . . . . .	35
	3.1.4 Default Material Properties . . . . .	36
	3.2 OUTPUT . . . . .	37
	3.2.1 Current Balance Printout . . . . .	38
	3.2.2 Flux Breakdown . . . . .	38
	3.2.3 Print Flags . . . . .	39
	3.2.4 Contour Plot Flexibility . . . . .	40

TABLE OF CONTENTS (Continued)

	<u>Page</u>
3.3 NEW FEATURES . . . . .	41
3.3.1 DEADLINE and TIMER . . . . .	41
3.3.2 Automatic Convergence Monitor - MAXITR . . . . .	42
3.3.3 SPIN Command . . . . .	43
4. CODE REVIEW . . . . .	46
4.1 CENTERING . . . . .	46
4.2 FASTER INTERFACE ROUTINES . . . . .	47
4.3 1250 SURFACE CELLS . . . . .	48
4.4 CODE CLEANUP AND COMMENTS . . . . .	48
4.5 SHADOWING (HIDCEL) IMPROVEMENTS . . . . .	49
4.6 'TYPE' CONFLICT . . . . .	49
5. AUXILIARY CODES . . . . .	51
5.1 TERMTALK . . . . .	52
5.2 MATCHG . . . . .	71
5.2.1 Bulk Conductivity . . . . .	71
5.2.2 Aligned Fluxes . . . . .	71
5.2.3 Emission Table . . . . .	73
5.2.4 Initial Voltage . . . . .	73
5.2.5 Multiple Maxwellian Plasmas . . . . .	73
5.3 WORKSHOP CODES . . . . .	74
5.3.1 FILES . . . . .	74
5.3.2 OBJCHECK . . . . .	76
5.3.3 POTPLT . . . . .	80

TABLE OF CONTENTS (Continued)

	<u>Page</u>
6. PRELIMINARY LOW EARTH ORBIT (LEO) MODEL . . . . .	82
6.1 LANGMUIR PROBE THEORY COMPARISON . . . . .	83
6.2 NASCAP/LEO LIMITATIONS . . . . .	85
6.3 THE EFFECT OF SOLAR ARRAY VOLTAGE PATTERNS ON PLASMA POWER LOSSES . . . . .	86
6.4 PLASMA COLLECTION BY HIGH VOLTAGE SPACECRAFT AT LOW EARTH ORBIT . . . . .	91
APPENDIX A - REPLACEMENT OF SECTION 7.3 OF NASCAP USER'S MANUAL, NASA CR-159417 . . . . .	99
APPENDIX B - DEFAULT MATERIALS AND PARAMETERS . . . . .	115
REFERENCES . . . . .	120

## LIST OF FIGURES

<u>Figure No.</u>		<u>Page</u>
2.1	Particle detector on boom cell. . . . .	13
2.2	2-D illustration of surface cell/ dielectric interface . . . . .	20
2.3	Initial and final particle velocity for case $\Delta E > 0$ . . . . .	22
2.4	Quadrant of a boom section enclosed in the cubical mesh . . . . .	26
2.5	Potential contours around a thin boom with $R = 0.01$ . . . . .	28
2.6	Potential contours around a thin boom with $R = 0.03$ . . . . .	29
2.7	Potential contours around a thin boom with $R = 0.10$ . . . . .	30
2.8	Potential contours around a thin boom with $R = 0.32$ . . . . .	31
3.1	Examples of "Surface Cell" and "Surface At" keyword options . . . . .	35
3.2	Flux breakdown printout . . . . .	38
3.3	Keyword values for contour plots . . . . .	40
3.4	Potential contours around satellite at equilibrium in sunlight, with conductor potential at -700 volts . . . . .	44
3.5	Same conditions as in Figure 3.4 . . . . .	45
4.1	Centering scheme. . . . .	47
4.2	Illustration of a shadowing case . . . . .	50
5.1	Diagram of TERMTALK . . . . .	54
5.2	Example of use of the FILES.ASSIGN program . . . . .	75
5.3	Example of OBJCHECK use . . . . .	77

LIST OF FIGURES (Continued)

<u>Figure No.</u>		<u>Page</u>
5.4	Example of POTPLT use . . . . .	81

LIST OF TABLES

<u>Table No.</u>		<u>Page</u>
2.1	Suggested NASCAP Material Parameters for Six Metals . . . . .	10
6.1	Langmuir Probe Theory Comparison . . . . .	84

**"Page missing from available version"**

## SUMMARY

NASCAP is a computer program that comprehensively analyzes problems of spacecraft charging. Using a fully three-dimensional approach, it can accurately predict spacecraft potentials under a variety of conditions. Under Contract NAS3-21762, several changes were made to improve NASCAP, and a new code, NASCAP/LEO, was developed. In addition, detailed studies of several spacecraft-environmental interactions and of the SCATHA spacecraft were performed (see companion reports, References 1 and 2).

The changes made to NASCAP this year make it run faster - execution time has been cut by more than half. It is now more accurate - photosheath approximations and many other features have been added. It is easier to use - a new user unfamiliar with the host computer can learn NASCAP in a matter of days. Auxiliary codes have also been developed to improve NASCAP flexibility and reduce problem turnaround time.

A NASCAP/LEO program has been written. This handles situations of relatively short Debye length encountered by large space structures or by any satellite in low earth orbit (LEO). This preliminary model has already been applied to two important high voltage interaction problems.

**"Page missing from available version"**

## 1. INTRODUCTION

This is the Final Report on Tasks 5 and 6 of Contract NAS3-21762, "Additional Application of the NASCAP Computer Code". The work was performed by Systems, Science and Software between 26 March 1979 and 9 October 1980.

This report includes much of the information from monthly reports published throughout the contract, as well as some new items. There are two other volumes of the final report. One contains environmental interaction studies of three space systems, Tasks 1, 2, and 3; the other describes work done on Task 4 - SCATHA spacecraft study.

NASCAP (NASA Charging Analyzer Program) is a powerful computer program for studying spacecraft charging. It is intended as a tool for spacecraft designers to help them avoid the problems of electrical charging in space. It has also been used by scientists associated with the SCATHA satellite to interpret the results of on-board experiments.

Since there is now a group of researchers using NASCAP on a day-to-day basis, there is now a need for code extensions, improvements, and miscellaneous modifications. The changes we have made to NASCAP this year fall into five categories: physical model extensions, usability, code review, auxiliary codes, and NASCAP/LEO.

One way to improve the accuracy of a model code is to expand the range of physical situations it can handle. Chapter 2 reports on the changes to the physics of NASCAP. This includes new treatments of the photosheath, and improvements in detector and emitter modeling.

Chapter 3 reports on changes that make NASCAP easier to use. These changes, along with the new auxiliary codes of Chapter 5, make it much easier for a new user to learn

NASCAP. More than that, they free the experienced user to think more about the actual problem and less about the details of code mechanics. The changes involve simplified input, more informative output, and a few new features. The most visible of the changes allows all NASCAP input to be in free format - input parameters are no longer card-column sensitive.

Chapter 4 gives the details of a comprehensive code review. We have made NASCAP faster and cleaner. A particular problem that used to take eight hours of computer time now takes two hours. We also put in comments to make the source code clearer and made minor improvements. NASCAP now can handle up to 1250 surface cells and can handle certain shadowing cases that formerly were prohibited.

Chapter 5 is titled "Auxiliary Codes". These are codes to be used in conjunction with NASCAP. In general, each auxiliary code takes a single isolated function of NASCAP, and performs it easier, faster, and cheaper. MATCHG, used before NASCAP is run, allows the user to try various combinations of material properties and environments, interactively. TERMTALK is an interactive post-processor that culls surface cell potential histories from NASCAP files. Three more codes - OBJCHECK, POTPLT, and FILES - were designed for new users in a workshop situation. These are not interactive, but provide turnaround an order of magnitude faster than otherwise possible.

The most important change in the NASCAP model is the development of an alternate code - NASCAP/LEO. This is described in Chapter 6. NASCAP analyzes standard sized objects in deep space or in geosynchronous orbit. For very large objects, or those in low earth orbit (LEO), the NASCAP physical models are inadequate. NASCAP/LEO is designed to handle these situations. It is a brand new code, and

presently has none of the sophistications or convenient user features that have been built into NASCAP over the years. NASCAP/LEO calculates an equilibrium solution to high voltage-dense plasma interaction problems. It handles objects that are built from cubes. The code has already been used to study ion focusing, and to calculate the effects of solar voltage array patterns on plasma power losses.

NASCAP/LEO is not ready for general distribution. NASCAP is currently available through COSMIC.

## 2. PHYSICAL MODEL EXTENSIONS

This chapter describes several modifications or extensions to the physical models employed in NASCAP to calculate the charging response of an object in space. The changes described below represent fine tuning of existing physical models rather than fundamental revisions.

Enhancements in the treatment of space charge around the NASCAP objects due to photoelectrons or the ambient plasma are described in Sections 2.1 and 2.3. Updated default material parameters are given in Section 2.2. Miscellaneous modifications to the ROTATE, DETECTOR, and EMITTER routines are described in Sections 2.4 through 2.6. Section 2.7 documents the finite element interpolants used in cells containing thin booms.

### 2.1 PHOTOSHEATH

NASCAP has incorporated two new options for calculating effects of the photosheath. They are: effective photosheath conductivity and self-consistent photosheath.

The effective photosheath conductivity causes a change in surface conductivity. It depends on rate of photoemission, external electric field, and surface cell voltage.

The self-consistent photosheath is a feature to be used only in very specialized applications. It requires certain preconditions and is expensive to use.

#### 2.1.1 Effective Photosheath Conductivity

A formulation for effective surface conductivity by low energy electrons has been incorporated into NASCAP. The option may be invoked by specifying the option 'EFFCON ON' and turned off by specifying 'EFFCON OFF'. (The default

value is 'EFFCON OFF'.) The photosheath conductivity is added to the intrinsic (material property) surface conductivity at each cycle. It is not operative for those cells for which surface conductivity is to be ignored.

The value of the effective photosheath conductivity is dependent on  $J$  (current of low energy emitted electrons,  $A/m^2$ ),  $E$  (external electric field, volts/meter),  $V$  (cell potential), and  $X$ , the code mesh size. The conductivity,  $\sigma$  (ohms $^{-1}$ ) is given by

For  $E \leq 0$

$$\sigma = \frac{1}{2} J X^2 e^{E/2}$$

For  $E > 0$  and  $V > 0$

$$\sigma = (J/E^2) \left( 4 - (4-2V) e^{-V/2} \right)$$

For  $E > 0$  and  $V \leq 0$

$$\sigma = (J/E^2) \left( 4 - (4-2EX) e^{-EX/2} \right)$$

Additionally,  $\sigma$  is forced into the range

$$10^{-7} \geq \sigma \geq 10^{-20} .$$

### 2.1.2 Self-consistent Photosheath

One aspect of spacecraft charging that has not been thoroughly investigated using NASCAP has been the structure of the space charge barrier formed by photoelectrons. This barrier, while small in voltage compared to substorm induced charging, is of interest both theoretically and experimentally. Experiments, such as SC-10 and SC-2 can make inferences about

the sheath structure. The extent and magnitude of the sheath can be important in unfolding ambient electric field data.

Previous NASCAP calculations did not take the space charge of the photosheath into account because the voltage perturbations of the sheath are extremely small compared to the kilovolt/meter fields set up by differential or spacecraft charging during substorms. However, for the case of the unfolding of SC-10 during quiescent conditions, the space charge sheath is the dominant source of field differentials between the two halves of the dipole. This experiment has provided electric field strength as a function of distance in front of SCATHA.

In order to predict the space charge barrier, a slight modification of the NASCAP explicit photosheath treatment was necessary. The 'SHEATH' option in NASCAP predicts photocharge densities, but does not use them for potential calculations. The space charge calculations run for SCATHA were made using the calculated space charge, and the potentials and charge densities were iterated on until self-consistency was obtained between the potentials and the charge densities obtained from particle tracking. This procedure converged quite rapidly. Another improvement in the 'SHEATH' routine, that is, emission of photoelectrons at several angles rather than just normal to the surface, was made to calculate more accurate charge densities.

These modified SHEATH routines are not designed for general use with NASCAP for several reasons. First, the self-consistent routines are presently implemented only for fixed spacecraft ground potentials, since the net photosheath currents are not available to the LONGTIMESTEP features of the code. Secondly, to track particles and iterate on the potentials would make this procedure prohibitive to use on a production basis because of computer time requirements.

However, for those interested in scientific investigations of the low energy sheath structure the keyword in the RDOPT file is 'SHEATH SELF CONSISTENT'. A number can be included on the card after these keywords to specify the charge density relaxation parameter,  $\alpha$ ;

$$\rho = \alpha \rho_{\text{new}} + (1-\alpha) \rho_{\text{old}}$$

A value of unity for  $\alpha$  would correspond to explicit iteration. The default value is

$$\alpha_{\text{default}} = 0.5$$

With the default value of the relaxation parameter a typical run converged to within  $\pm 5$  percent in the charge density after five iterations.

For an example of the use of this feature, see Schnuelle, et al. [2]

## 2.2 MATERIAL PROPERTIES

In NASCAP, surface material properties are in a state of frequent revision. Earlier this year, we conducted a comprehensive reworking of material property parameters. These were incorporated into the default values. We are again restructuring our material parameters.

One of the major changes during the contract year was a revision of subroutine PROSEC to give reduced proton secondary yields for protons incident at 1 keV and below.

Another change was to incorporate emission coefficients for protons on metals from Reference 3. Table 2.1 shows the new values of NASCAP properties 11 and 12 for best fit to data between 10 and 50 keV.

TABLE 2.1. SUGGESTED NASCAP MATERIAL PARAMETERS  
FOR SIX METALS

<u>Metal</u>	<u>Property 11</u>	<u>Property 12</u>
Li	.335	91.
Al	.244	230.
Cr	.247	250.
Cu	.257	320.
Ag	.49	123.
Au	.413	135.
(average)	.33	191.

### 2.3 SCREENING LENGTH

NASCAP now correctly takes into account the interaction between screening length and boundary conditions. It also performs a capacitance rescaling when a sudden change of screening length takes place. (This procedure is less exact than a fresh call to CAPACI, but is far faster and more flexible.) An interactive program is available to insert necessary information into files created prior to September 1979.

### 2.4 ROTATING MAGNETIC FIELD

ROTATE now causes any constant magnetic field to be rotated along with the sun direction. Any magnetic dipoles are not rotated, since they are assumed to be generated by the object, and hence would be locked to the object's reference frame. ROTATE assumes that the initial, unrotated magnetic field has been specified using the BFIELD keyword in a preceding RDOPT.

## 2.5 DETECTOR UPDATE

The NASCAP detector routines have been modified to include a number of new features. This section is intended to augment the detector routine documentation contained in Katz, I., et al. [4]

### Summary of New Features:

1. Particle tracking is now performed in all NG computational grids of NASCAP.
2. Particle tracking beyond the highest computational grid may be performed using a  $1/R$  monopole potential.
3. New I/O buffering scheme permits virtually unlimited numbers of particle trajectory line segments to be plotted.
4. The correct potential interpolation function is now employed to obtain the electric field for particles which pass into boom cells.
5. Routines have been implemented which correctly determine when a trajectory terminates on a boom. (Prior to this booms were transparent to NASCAP particle detectors.)
6. Particle detectors may now be placed on booms.
7. The energy aperture of NASCAP particle detectors has been modified (by popular request) to provide constant % energy  $\Delta E/E$  width in preference to the old fixed  $\Delta E$  for all energies.
8. In addition to the standard energy flux plot produced by NASCAP detectors a point-by-point breakdown of the flux may (optionally) be printed.

9. Optional detailed printout of each discrete particle trajectory calculation is available.
10. Optionally omit flux and trajectory plot headings for quick on-line plotting display terminals.
11. Optional user modification of particle charge and mass. Permits tracking heavy ions, for example.
12. Particle trajectory 2-D projection views may optionally be plotted more than once, each time using a different maximum grid boundary. This permits the fine details of particles returning to the satellite to be viewed while also displaying the details of particles circling in large radii due to the presence of a magnetic field, for example.
13. All detector keyword input may now be made using free format. (The user should still pay attention to keyword variable types since a decimal point or exponent specified for an integer variable will result in errors.)

#### Placement of Particle Detectors on Boom Cells:

In addition to satellite object surface cells NASCAP now permits the user to place a particle detector on a boom cell. Placement of a detector on a boom cell is done in a way very similar to that used for surface cells. The NASCAP user must first have performed an OBJDEF run on the boom-containing object which he intends to use. Then referring to the boom surface cell list printed by the OBJDEF run he can choose the cell number of the boom cell on which he desires to place a detector. This cell number is then placed on the ICELL keyword card in the detector keyword file. The detector will be located at the axial center of the boom surface cell specified by ICELL. In addition, the user must specify the

direction of the vector normal to the surface of the boom cell. This vector is restricted to lie in that plane which is perpendicular to the boom axis and passes through the boom surface cell axial center. The vector is specified in terms of the angle  $\zeta$  (ZETA) as illustrated in the following diagram for a boom along the z-axis. The definition of  $\zeta$  for booms lying along either of the other two coordinate axis may be obtained by cyclic permutation of axis labels in the figure. (Note that the coordinate axis are those of the Satellite Coordinate System.)

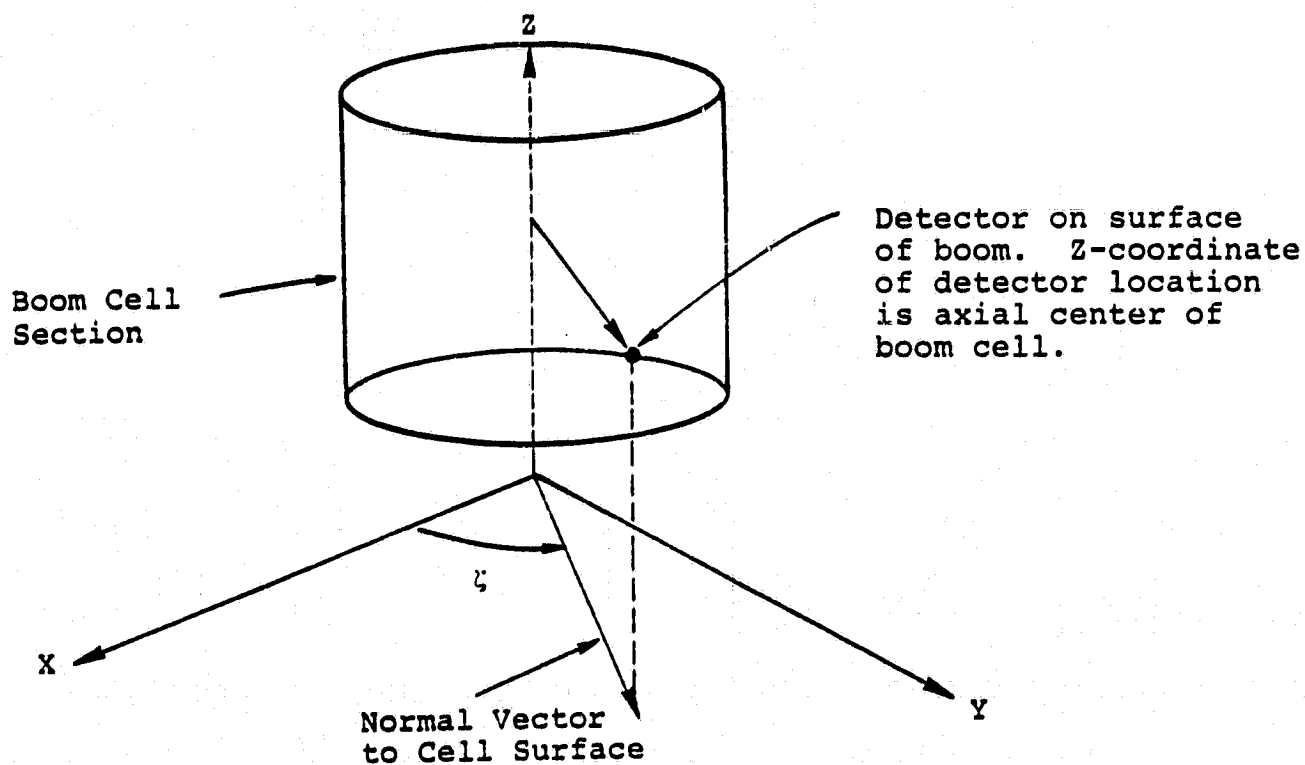


Figure 2.1. Particle detector on boom cell.

The boom cell normal vector defined by the selection of ICELL and ZETA plays the same role as the surface cell normal vector which defines the Surface Cell Coordinate System as described on p. 145-146 of Reference 4, the only difference being that the cell normal vector may point in any direction within one of the three coordinate planes rather than being restricted to one of the 26 mesh symmetry directions listed in Table 8.1, p. 147.

Description of New Detector Parameter Options by Keyword:

Detector Independent Parameters

- LABABV Inclusion of this card in a detector keyword definition sequence will cause the detector energy flux and particle trajectory plot heading labels to be suppressed. This feature is useful to the user who has access to a Tektronix graphics display terminal and desires to speed up his on-line plotting process. If multiple detectors have been defined, then this option is not recommended since label omission in such cases is apt to be confusing.
- PRBMAT Inclusion of this card causes the inverse matrices relating grid potentials to interpolating function coefficients in boom cells to be printed. (Not intended for user applications.)
- PRTRAJ Modulo number for printout of particle trajectory steps. (This variable must be an INTEGER even though the variable type indicates a real parameter.) If this card is included then for every PRTRAJ<sup>th</sup> point of each particle trajectory a line will be printed containing the trajectory step number (ISTP), index of NASCAP computational grid (IR), index of boom whose cells the particle is

currently in (if it is in a boom cell) (IB), coordinates of particle (X) in inner mesh units, particle velocity (V) in inner mesh units/timestep, electric field (E) in volts/inner mesh unit, and magnetic field (B) in gauss. Also printed is the electrostatic potential (VBOOMC) which is only valid if the particle is within a boom cell (IB > 0). If IB = 0 then the value given for VBOOMC is not relevant.

{ The user is cautioned against careless use of the PRTRAJ option since there is a potential for a tremendous amount of printed output - namely a maximum of about  $N \cdot NSTP$  lines where N is the number of independent variable points! }

PRFLUX Inclusion of this card will result in a tabulated listing of the detector energy flux values in addition to the standard plot. (If the PRTRAJ option is concurrently active then the listing will be interspersed with particle pushing trajectory information - a possibly undesirable condition.)

#### Detector Dependent Parameters

Normally the boundary of a particle trajectory plot is adjusted to correspond to the boundary of the highest grid into which any of the N emitted particles fell during tracking. Unfortunately particles circling in small magnetic fields tend to make very large loops, i.e., into grid 12 or higher. Thus the automatic plot boundary selection can obscure details of individual particles returning to the object in grid 1. (The object silhouette is only plotted if the boundary of the plot corresponds to grid 6 or lower and fine details are usually only apparent if the boundary of the plot is set to grid 4 or lower.) In addition there may be some

cases in which it is desirable to have the same set of particle trajectories plotted more than once, each time using a different maximum grid boundary for the plot. The following three keywords provide the user with the capability to deal with these problems and special requirements.

**NGBND**      Grid number to which the boundary of the particle trajectory plots corresponds to. (Note that all grids which are higher than 2 but fall inside the plot edge are automatically outlined for reference on the trajectory plots.) Acceptable range is integral  $\text{NGBND} \geq 0$ , i.e.,  $\text{NGBND} = 0, 1, 2, \dots$ . If  $\text{NGBND} = 0$  then the boundary of the plot will be automatically adjusted to correspond to the highest grid into which any of the  $N$  particles fell during tracking. Default value is  $\text{NGBND} = 0$ .

**NGPLOT**     Number of different plots of same set of trajectories desired (only has an effect if  $\text{NGBND} \geq 0$ ). Each trajectory plot is made using a different grid boundary (see **NGINC**). The acceptable range is integral  $\text{NGPLOT}$  such that  $1 \leq \text{NGPLOT} \leq 4$ . The default is  $\text{NGPLOT} = 1$ .

**NGINC**      Increment factor for grid boundaries of successive trajectory plots. If  $\text{NGPLOT} > 1$  then the same trajectories will be drawn on  $\text{NGPLOT}$  different plots. The grid boundaries are incremented for each successive plot as follows:  
$$\text{IG} = \text{NGEND} + (\text{I}-1) * \text{NGINC} \text{ for } \text{I} = 1, \dots, \text{NGPLOT}$$
Acceptable range is integral  $\text{NGINC} \geq 0$ . Default is  $\text{NGINC} = 0$ .

Note that the highest grid value selected for plotting boundaries by **NGBND**, **NGPLOT**, and **NGINC** should not exceed **LIMGRD** if useful plots are to be obtained.

**MODPAR** Modulo number for particle trajectory line segment plotting (significant only if PLPART option active). MODPAR > 0 results in every MODPAR<sup>th</sup> trajectory point being plotted. MODPAR = 0 or keyword option omitted will result in the default of every  $2^{IR-1}$ <sup>th</sup> point being plotted where IR is the index number of the NASCAP computational grid in which the particle is located. Thus the default is for dynamic adjustment of MODPAR.

**LIMGRD** Highest grid in which particle tracking is permitted. If particle passes outside this grid it will be assumed to have escaped to infinity. Default value is LIMGRD = NG, the highest NASCAP computational grid. Acceptable range is LIMGRD  $\geq$  1. (Note that particles which exit from the highest NASCAP computational grid NG are tracked using a monopole potential.)

**ZETA** Angle of particle detector on a boom cell. (Default is ZETA = 0.0°.) Not relevant if ICELL is the index of a surface cell of the satellite.

{ If the user intends to modify particle mass and/or charge using the following four keywords then he must be certain that the same particle masses and charges are specified on the environment FLUX definition file! }

**ELMASS** Electron mass used for reverse trajectory tracking. (Default is ELCH =  $9.1091 \times 10^{-31}$  kg.)

**PRMASS** Proton mass used for reverse trajectory tracking. (Default is PRCH =  $1.67252 \times 10^{-27}$  kg.)

**ELCH** Electron charge. (Default is ELCH =  $-1.602 \times 10^{-19}$  coul.)

PRCH Proton charge. (Default is PRCH =  $+1.602 \times 10^{-19}$  coul.)

Description of Old Detector Keyword Options Which Have Been Modified:

ICELL Now may be index number of a boom surface cell.

NSTP Maximum number of steps per particle allowed during reverse trajectory tracking. Acceptable range is  $1 \leq NSTP \leq 30,000$ . Default is NSTP = 500. As a rule of thumb, assuming VCODE = 0.3, NSTP should be increased by at least 400 for each additional NASCAP grid used. If NG = 3 then NSTP = 1200 is probably not unreasonable.

DE Deleted keyword. Function superseded by DEK.

DEK Width of detector energy aperture in percent. Acceptable range is DEK  $\geq 0.0$ . Default is DEK = 0.0. If the energy the detector is looking at is E then the flux value will be obtained from Eq. (8.9), p. 156, of Reference 4, where

$$\Delta E = E \times \left( \frac{DEK}{100} \right) \quad (\text{constant \% energy window}).$$

VCODE If ICELL is the index number of a boom surface cell then the value specified for VCODE is automatically scaled by  $2^{(IG-1)}$  where IG is the index number of the grid in which the boom cell is located.

N Definition of this keyword is same as before but default value has been changed from 100 to 20.

PSCALE Definition of this parameter is same as before except that documentation incorrectly stated that the proton flux multiplication factor was  $10^{**PSCALE}$  when in fact it is just PSCALE. The default is PSCALE =  $10^5$ .

## 2.6 EMITTER ROUTINE KINENG

### Definitions:

- $\phi_C$  = electrostatic potential of emitter conductor
- $\phi_L$  = electrostatic potential at top of dielectric layer covering conductor
- $E_O$  = particle kinetic energy at conductor surface
- $\theta_O$  = polar emission angle of particle at conductor surface
- $E_L$  = particle kinetic energy at top of dielectric layer covering conductor
- $\theta_L$  = polar emission angle of particle at top of dielectric layer covering conductor
- $m$  = particle mass
- $q$  = particle charge
- $v_x', v_y'$  particle velocity components at conductor surface
- $v_x'', v_y''$  particle velocity components at top of dielectric layer covering conductor

### Motivation:

Particles are conceptually emitted from the geometric center of the conductor underlying the surface cell on which the low-density NASCAP particle emitter is located. In NASCAP potential nodes which lie on surface cells are considered to represent potentials on the surface of the thin dielectric coating which overlays the surface cell conductor rather than the potentials of the conductor itself (see Figure 2.2). Therefore, it is not possible to numerically solve the equations of motion for a particle in the dielectric coating region using electric fields obtained from the NASCAP routine EFIELD. (EFIELD does not know about the dielectric region.) NASCAP emission routine EMITER circumvents this difficulty by

employing an approximate analytic treatment within the dielectric region.

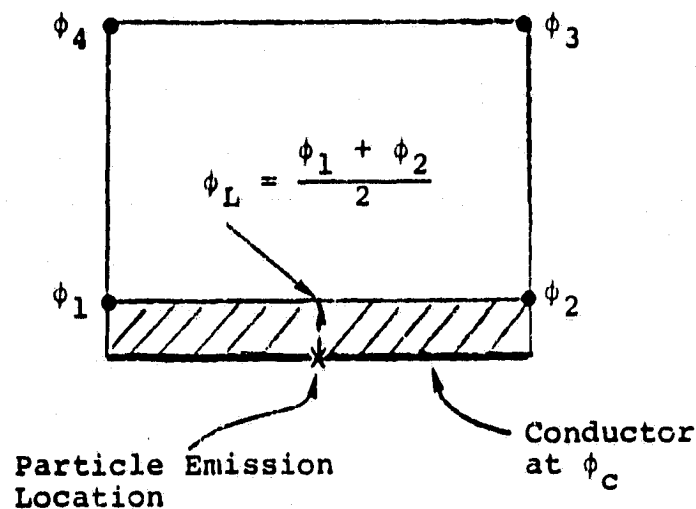


Figure 2.2. 2-D illustration of surface cell/dielectric interface. Shaded area is dielectric region.

Analysis:

The analytic treatment of particle motion in the dielectric layer covering an emitter surface cell conductor is made using the following set of assumptions:

1. Particles in the dielectric region are accelerated only by an electric field which is normal to the plane of the conductor.
2. The point on the dielectric surface where the particle passes into free space lies on that line which is normal to the plane of the conductor and passes through the geometric center of the surface cell. (This is an approximation.)

Energy conservation applied to Figure 2.3 yields the relation between initial particle kinetic energy  $E_0$  and emission polar angle  $\theta_0$  at the conductor surface and the kinetic energy  $E_L$  and polar emission angle  $\theta_L$  of the particle at the top of the dielectric layer as follows:

$$E_0 = m/2 (v_x^2 + v_y^2) \quad (\text{initial kinetic energy})$$

$$E_L = m/2 (v_x'^2 + v_y'^2) \quad (\text{final kinetic energy})$$

$$= m/2 (v_x'^2 + v_y^2) \quad (\text{since } v_y' = v_y, \text{ a consequence of normal electric field})$$

or rewriting

$$v_x'^2 = \frac{2E_L}{m} - v_y^2$$

But

$$v_y^2 = \frac{2E_0}{m} \left( \frac{v_y^2}{(v_x^2 + v_y^2)} \right) = \frac{2E_0}{m} \sin^2 \theta_0$$

so

$$v_x'^2 = \frac{2}{m} (E_L - E_0 \sin^2 \theta_0) \quad (2.1)$$

Also

$$\cos^2 \theta_L = \frac{m v_x'^2}{2 E_L} \quad (2.2)$$

and

$$E_L = E_0 + \Delta E \quad (2.3)$$

where  $\Delta E = q(\phi_C - \phi_L)$ .

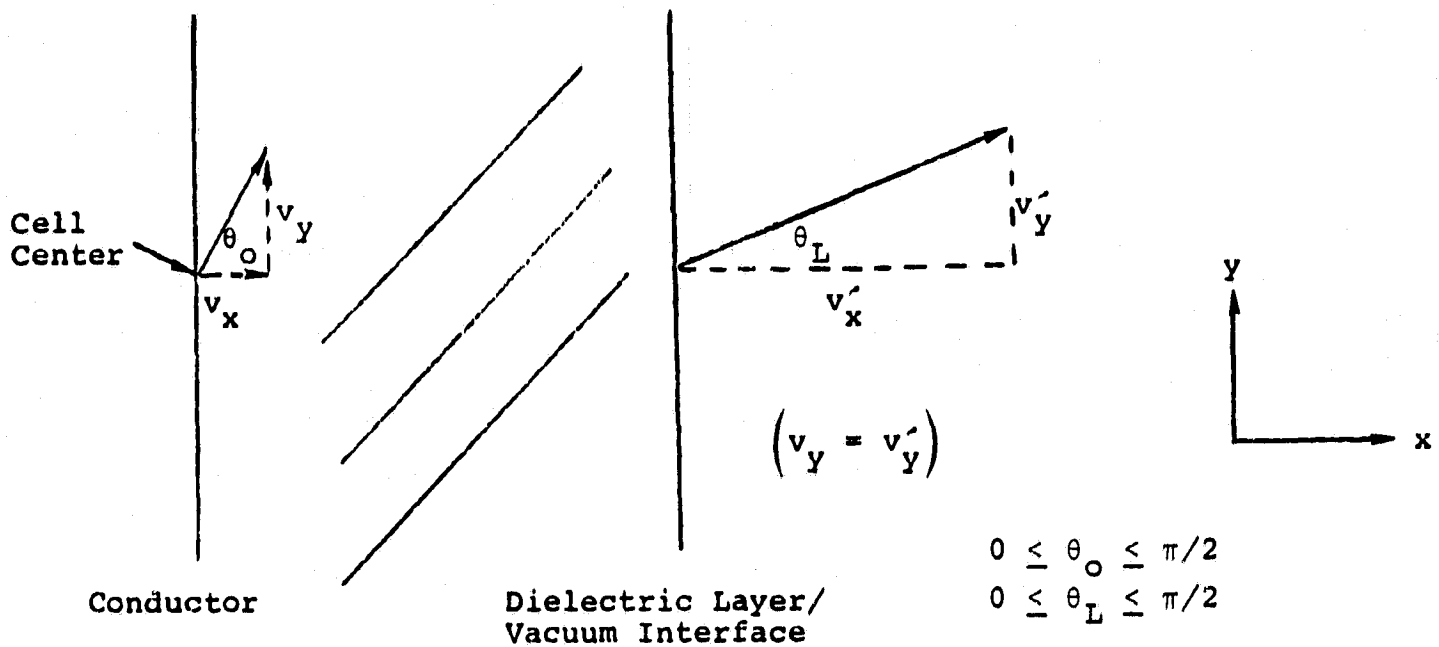


Figure 2.3. Initial and final particle velocity for case  $\Delta E > 0$ .

Putting Eq. (2.3) into Eq. (2.1) gives

$$\begin{aligned}
 v_x'^2 &= \frac{2}{m} \left( E_0 + \Delta E - E_0 \sin^2 \theta_0 \right) \\
 &= \frac{2}{m} \left( E_0 \cos^2 \theta_0 + \Delta E \right)
 \end{aligned}$$

Then using this in Eq. (2.2) we obtain:

$$\cos^2 \theta_L = \frac{E_0 \cos^2 \theta_0 + \Delta E}{E_0 + \Delta E}$$

or

$$\theta_L = \cos^{-1} \sqrt{\frac{E_0 \cos^2 \theta_0 + \Delta E}{E_L}} \quad (2.4)$$

### Implementation:

The analytic treatment presented above is implemented in the NASCAP particle emitter routines via subroutine KINENG. Given the emission energy  $E_0$  and angle  $\theta_0$  at the conductor surface, KINENG returns the particle energy  $E_L$  and angle  $\theta_L$  at the dielectric/vacuum interface as given by Eqs. (2.3) and (2.4).

In the event that Eq. (2.3) yields a negative energy or Eq. (2.4) has no real solution, KINENG sets a flag to indicate that the particle can never reach the dielectric surface and hence its emission is suppressed.

Note that an acceptable solution of either equation alone is not sufficient to guarantee that a valid solution of the other equation exists!

#### Examples:

1.  $E_L = E_0/2$  satisfies Eq. (2.3) but (2.4) has solution only for  $\theta_0 \leq 45^\circ$ .
2.  $\theta_0 = 0 \rightarrow \theta_L = 0$  for any  $\Delta E$ , but some  $\Delta E$  will make  $E_L < 0$  violating conditions on Eq. (2.3).

#### Operational Note: (add to p. 182 of Reference 4)

If the NASCAP user includes the IPRNT option card in his particle emitter keyword file then prior to the one-line summary for each particle trajectory completion KINENG will print one of two possible informative messages pertaining to the trajectory. The two possible messages are of the form

1. \*\*\*EMISSION SUPRESSED BY KINENG\*\*\* -----  
is printed if Eq. (2.3) and/or (2.4) had no valid solution.
2. \*\*IN KINENG THETA = --- CHANGED TO ---  
VANOD = --- CHANGED TO ---

Message 1 may appear up to a maximum of 50 times. If this limit is exceeded a warning is issued and no further such messages will be printed.

The variables in these messages correspond to the definitions as follows:

$$\text{THETA} = \theta_0 \text{ (radians)} \quad \text{PAVG} = \phi_L \text{ (volts)}$$

$$\text{VANOD} = E_0 \text{ (eV)} \quad \text{VC} = \phi_C \text{ (volts)}$$

The "changed to" variables are  $\theta_L$  and  $E_L$ .

If message 1 is not printed by KINENG it is still possible to receive another similar message:

**\*\*EMISSION SUPRESSED BY LOCAL FIELD\*\*** .

This message is generated by the EMITER routine in response to a flag which is set within the PUSHER routine. The PUSHER routine contains a preliminary test to determine (based on the emitter local surface cell field) whether or not the particle has sufficient energy to travel a distance of more than one cell. If it doesn't then there is no point in explicitly tracking such a particle.

## 2.7 BOOM CELL MODELING

(This section describes a feature that has been in NASCAP for some time, but it was not included in last year's Final Report.)

To treat the boom one constructs a mixed geometry (cylindrical-Cartesian) finite element solving technique, starts by enclosing each section of the cylindrical boom in four cubes of sides of unit length, which are part of the cubical 3-D mesh. It is apparent that it is enough to treat only one quadrant.

The object is to construct the finite element matrix that represents the finite element interpolation potential in the region of Figure 2.4.

The interpolation potential has to have the following properties:

- a. It has to be constant on the circular section of the boom.
- b. It has to satisfy Laplace's equations in the region of Figure 2.4.

One such interpolation potential is

$$V(r, \phi, z) = A(r, \phi) (1-z) + B(r, \phi) z ,$$

where the coordinates system is that defined in Figure 2.4 with

$$A(r, \phi) = \alpha_4 + \alpha_1 \ln \frac{r}{R} + \alpha_2 \cos \phi \left( \frac{r}{R} - \frac{R}{r} \right) + \alpha_3 \sin \phi \left( \frac{r}{R} - \frac{R}{r} \right) ,$$

and  $B(r, \phi)$  is the same functional expression with  $\alpha$ 's replaced by  $\beta$ 's.

We call  $a_1, a_2, a_3$  the potentials on the three available corners of the square (counting counterclockwise) and  $a_4$  the potential over the quarter circle (see Figure 2.4) on the plane  $z = 0$ , and on the other hand  $b_1, b_2, b_3$  the equivalent entities on the plane  $z = 1$ . Then the  $\alpha$ 's bear a linear relationship with the  $a$ 's obtained by asking  $A(r, \phi)$  to take the values  $a_4, a_1, a_2, a_3$  on the quarter circumference and the three corners respectively and equivalently for the  $\beta$ 's and  $b$ 's.

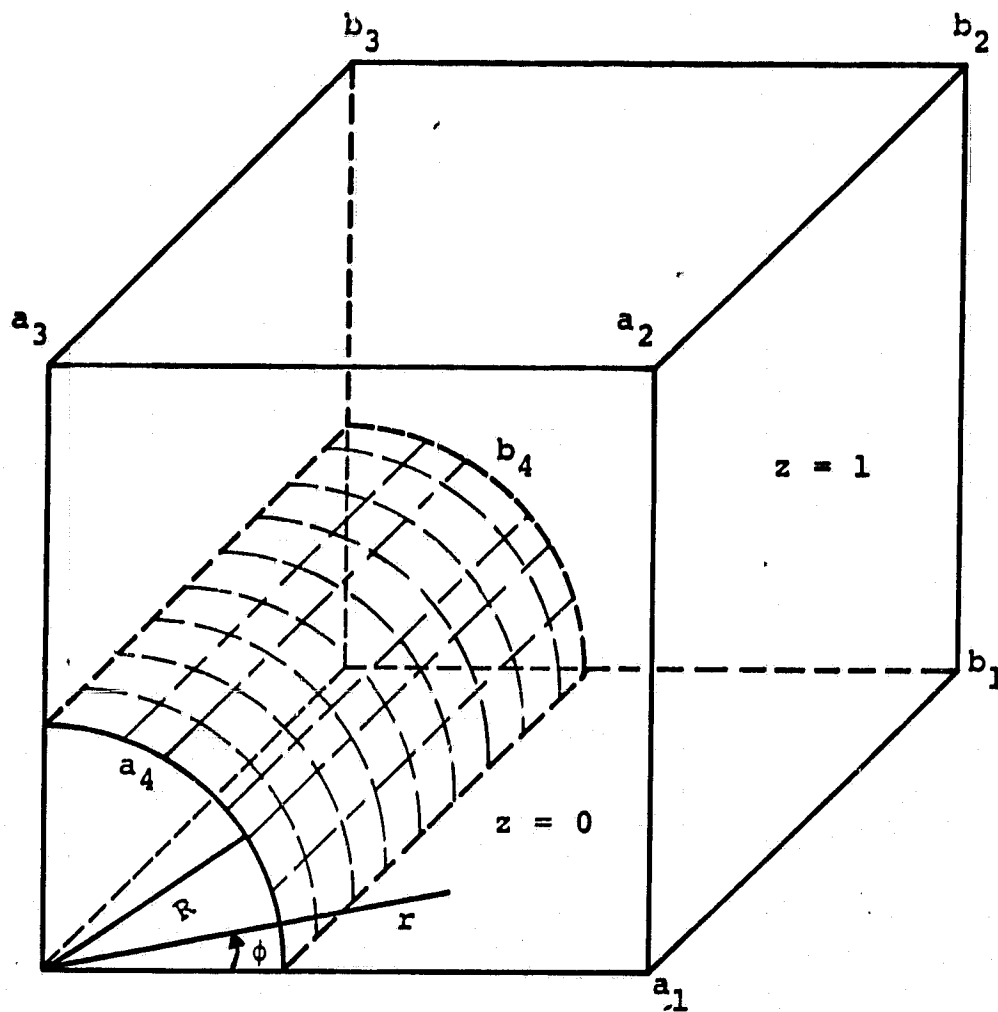


Figure 2.4. Quadrant of a boom section enclosed in the cubical mesh.

Then we construct the 8 x 8 matrix, to be used as a submatrix of the total mesh, such that

$$\int_{\Omega} |\nabla V|^2 r dr d\phi dz = \tilde{X} S X ,$$

where

$$\tilde{X} = (a_1 \dots, a_4, b_1 \dots, b_4)$$

and X is the associated column vector.  $\Omega$  is given by

$$\left\{ \begin{array}{l} R \leq r \leq \frac{1}{\cos\phi} , \quad 0 \leq \phi \leq \frac{\pi}{4} \\ R \leq r \leq \frac{1}{\sin\phi} , \quad \frac{\pi}{4} \leq \phi \leq \frac{\pi}{2} \\ 0 \leq z \leq 1 \end{array} \right.$$

We have written a subroutine to obtain S as a function of R with arbitrary accuracy, because we have done the quadratures needed analytically.

Figures 2.5-2.8 present potential contours resulting from a two-dimensional calculation on a 9 x 9 mesh containing a central boom and a grounded outer conductor having diameter equal to the mesh diagonal. The boom radii range from 0.01 to 0.32 mesh units. In the figures the boom outline is represented by the second innermost contour. With increasing boom size the fields at the boom surface decrease, and the fields in the surrounding space increase. The calculated boom capacitances are one to two percent larger than the theoretical values. Distortion of equipotentials near the boom cell boundaries results from the differences in interpolation functions between boom and bilinear cells.

R = .010000

ZMIN = .11921-06 ZMAX = .20000+01 ΔZ = .50000+00

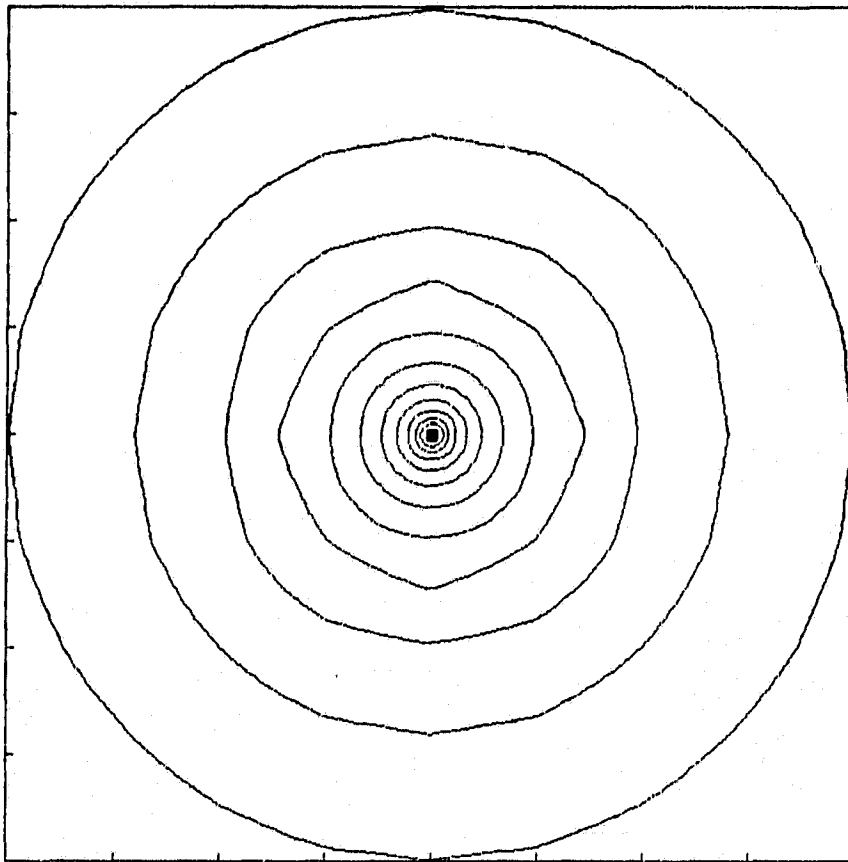


Figure 2.5. Potential contours around a thin boom with  $R = .01$ . The tic marks indicate the mesh spacing.

R = .031623

ZMIN = .11921-06 ZMAX = .90000+01 ΔZ = .50000+00

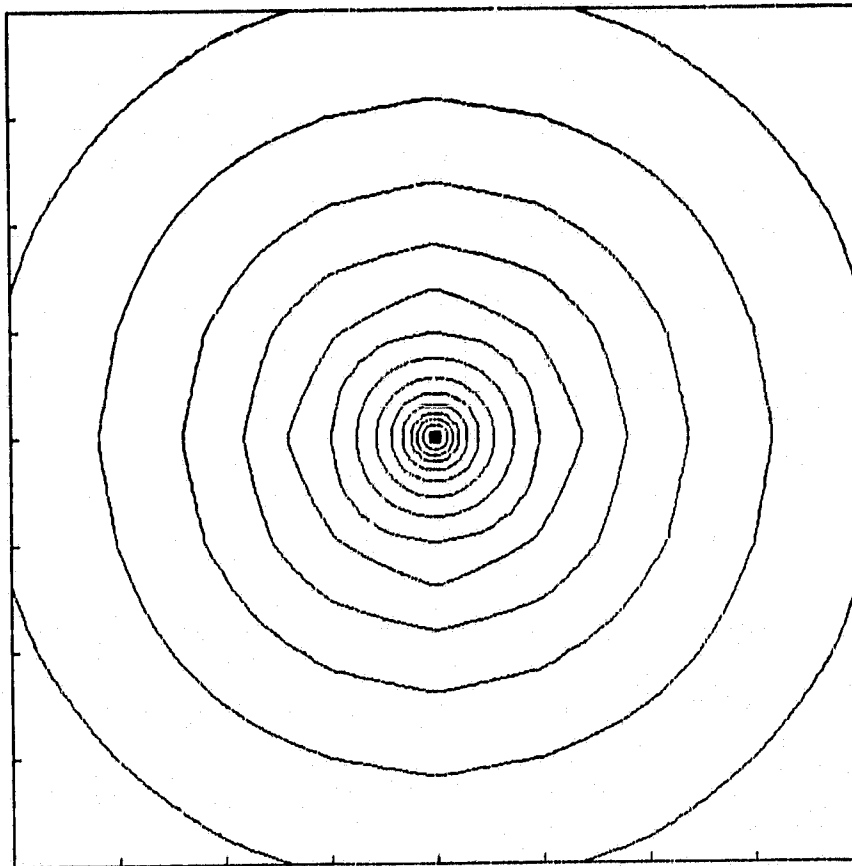


Figure 2.6. Potential contours around a thin boom with  $R = .03$ . The tic marks indicate the mesh spacing.

R = .100000

ZMIN = .11921-06 ZMAX = .90000+01 ΔZ = .50000+00

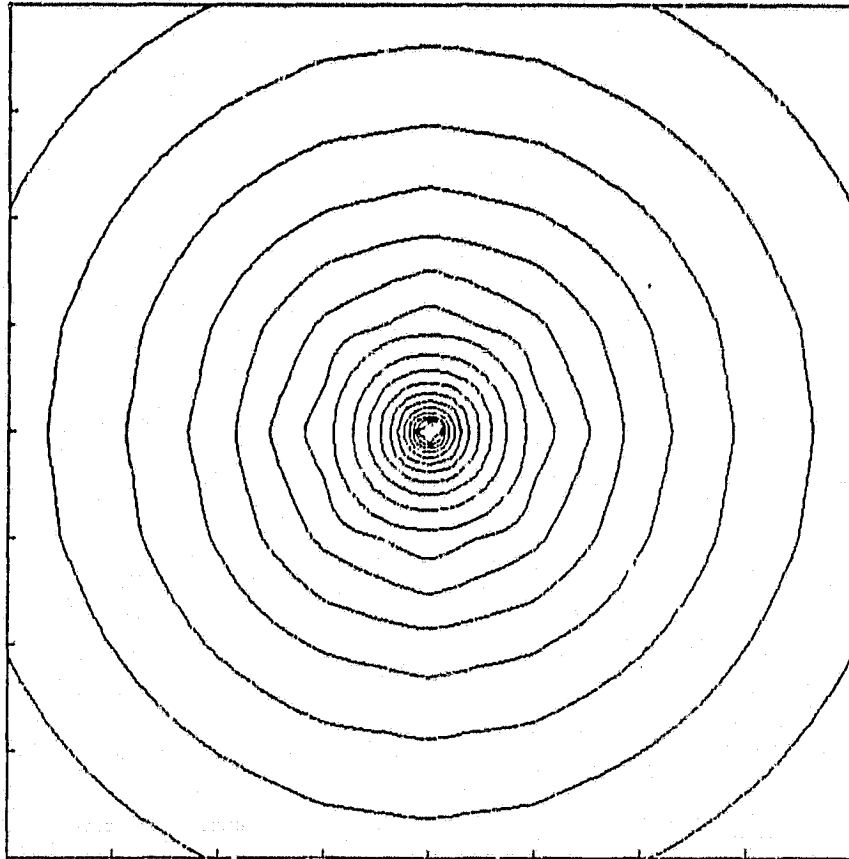


Figure 2.7. Potential contours around a thin boom with  $R = .10$ . The tic marks indicate the mesh spacing.

R = .316228

ZMIN = .11921+06 ZMAX = .90000+01 ΔZ = .50000+00

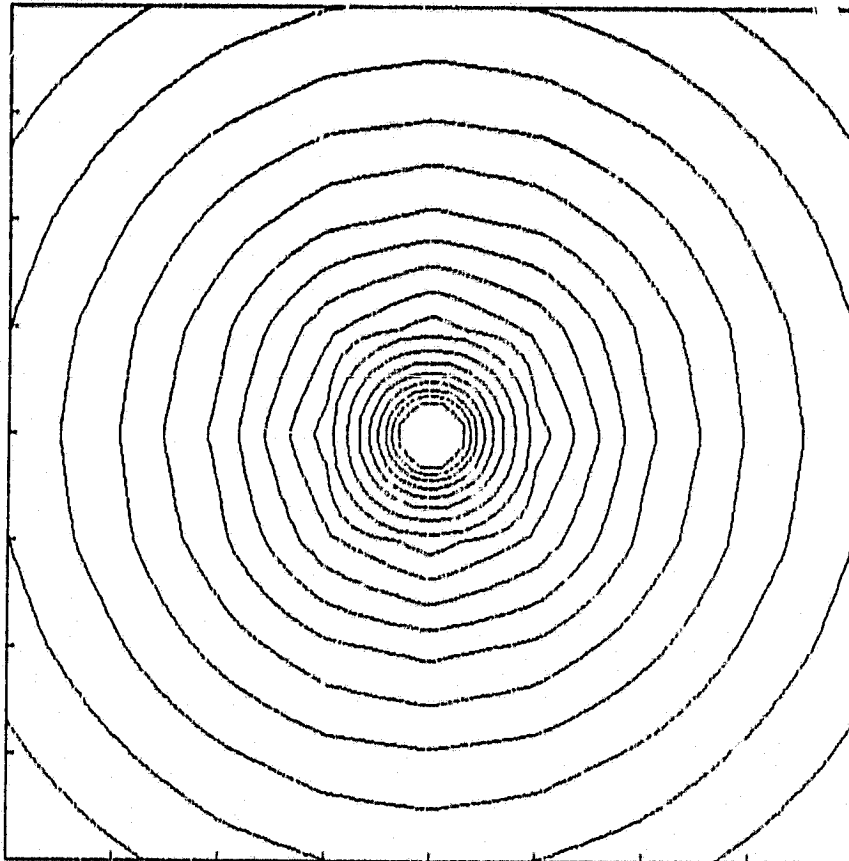


Figure 2.8. Potential contours around a thin boom with  $R = .32$ . The tic marks indicate the mesh spacing.

### 3. USABILITY

NASCAP is constantly being improved to fit the needs of users. No matter how accurate a computer program may be, it is only useful to those who can run it. The changes we have made to make NASCAP more usable, fall into three categories: input, output, and new features.

"Input" includes all those changes for which NASCAP still does the same thing, but with far less persuasion and patience on the user's part than was previously necessary. First, these changes reduce problem set-up time. They allow users to concentrate on physics more, and keypunching less. Second, they save computer time by reducing the number of wasted problem runs necessary to produce a good one.

"Output" changes improve the selection of information available to the user. Most of the changes take information that NASCAP already stores internally, and make it available as printout or graphics plots. One of the changes (print flags) also concerns some information that NASCAP already prints out. It lets the user say, "Keep it to yourself, NASCAP. I don't want to hear about it."

The "New Features" in this section (Deadline and Timer, Spin Command, and Automatic Convergence) are some of the most widely asked-for improvements. In their various ways, they also save computer time and simplify the job of running NASCAP.

### 3.1 INPUT

While the NASCAP code is constantly becoming more sophisticated, it is at the same time becoming easier to use. As the number of users grows, the new users suggest ways to simplify input procedures.

Perhaps the biggest procedural change made in the last year is the new free format input. This allows users to ignore column numbers and format statements.

Another big change is the introduction of default material properties. NASCAP now provides a set of material properties automatically.

The user input for defining booms and the input for special cell selection have been improved.

In all of these cases, the old input procedures work as before. The new, simplified procedures offer an additional alternative.

Finally, there is a new way to specify the flux pattern for a test tank electron beam. The old method (which still works) requires a polar coordinate pattern. The new method uses a beam pattern specified in cartesian coordinates. Appendix A of this report is a replacement of Section 7.3 (Flux Definition File) of the NASCAP User's Manual. It describes both techniques in full.

#### 3.1.1 Free Format Input

This year's NASCAP has incorporated a Free Format feature. This means that you can scatter your input lines right across the page, without paying any attention to column numbers.

No longer will NASCAP change your number of computational grids from 2 to 20, just because you put your 2 in the wrong column. You can now ignore the Format statements in the NASCAP User's Manual.

There must be a space or a comma separating each input value, but otherwise NASCAP doesn't care how close together or far apart they are. The card images:

```
SUNDIR 2,2,1
```

```
SUNDIR      2      2 1
```

are equivalent.

There are still a few input restrictions. You must put the right number of items on each card. You can't leave blanks to indicate zeroes. And don't put a decimal point on a number that NASCAP expects to be an integer. The forms "2" and "2." are both acceptable for REAL number (floating point) input. But for INTEGER (fixed) numbers, only "2" would be acceptable.

If NASCAP doesn't like your input, then subroutine FREED or subroutine CLASY will probably print out angry error messages.

### 3.1.2 Surface Cell Specifications

NASCAP prints a flux breakdown and other information for surface cells that are specified by the user. There are two ways to specify which surface cells are of interest, the SURFACE CELL card and the SURFACE AT card. Both cards go in the "options" file to be read at RDOPT time.

The SURFACE CELL card has one integer - a surface cell number. This number can be obtained by finding the desired cell on the surface cell list printed by OBJDEF.

The SURFACE AT card has three or six integers to describe the geometrical location of a surface cell. The format is

```
SURFACE AT ix jy kz
```

or

```
SURFACE AT ix jy kz nx ny nz,
```

where (ix,jy,kz) is lower-left corner (in absolute coordinates) of the volume cell in which the surface is located or out of which it points, and (nx,ny,nz) (optional) is the surface normal. Some examples are shown in Figure 3.1. Note that an invalid cell specification is interpreted as cell 1251, so as not to interfere with validly specified cells.

```

surface at 10 10 15
SURFACE AT 10 10 15
FNDCEL FOUND CELL NO. 288: 111212176041.
CELL 288 INFORMATION TO BE PRINTED.

surface at 10 10 16
SURFACE AT 10 10 16
FNDCEL FOUND CELL NO. 289: 011212206001.
CELL 289 INFORMATION TO BE PRINTED.

surface at 9 9 14
SURFACE AT 9 9 14
FNDCEL FOUND CELL NO. 244: 011111160101.
CELL 244 INFORMATION TO BE PRINTED.

surface at 4 9 17
SURFACE AT 4 9 17
FNDCEL ---000411210000 NOT FOUND
CELL 1251 INFORMATION TO BE PRINTED.

surface cell 48
SURFACE CELL 48
CELL 48 INFORMATION TO BE PRINTED.

surface cell 49
SURFACE CELL 49
CELL 49 INFORMATION TO BE PRINTED.

surface cell 13
SURFACE CELL 13
CELL 13 INFORMATION TO BE PRINTED.

```

Figure 3.1. Examples of "Surface Cell" and "Surface At" keyword options. An invalid cell specification is interpreted as cell 1251.

### 3.1.3 Boom Input

A new form of input is available for the AXIS card in BOOM definition in NASCAP. The new form is (free format)

```

AXIS IBX IBY IBZ IEX IEY IEZ

```

where (IBX,IBY,IBZ) and (IEX,IEY,IEZ) are the beginning and ending locations of the boom axis, respectively. The locations are all assumed to be in first grid coordinates using

this form (even if the boom extends outside the first grid). Any offset is applied to both beginning and ending locations. Locations in outer grids must, of course, correspond to nodal points. The old form of the AXIS card is still valid:

```
AXIS  IBX  IBY  IBZ  IBG  IEX  IEY  IEZ  IEG
```

where IBG and IEG are the grid number of the starting and ending axis locations, respectively, and where any offset is applied only to locations in the first grid.

An example of the new input form: a boom extends from the center of the inner mesh along the negative X axis just one node into the third grid. The default offset grid center is used.

New form:

```
AXIS  0,0,0  -20,0,0
```

Old form:

```
AXIS  0,0,0  1  4,0,0  3
```

Both axis cards will describe the same boom. NASCAP knows which form you are using by the number of integers on the AXIS card.

### 3.1.4 Default Material Properties

Default values for material properties of twelve materials have been provided in NASCAP. A list of the default materials and parameters is given in Appendix B. The routine MATDEF contains the default values in the code. If properties are not read in for a material during object definition, the first reference to that material name will cause the default values to be used. The default values will be ignored whenever a set of properties is specifically read in for a material in the default list.

A new command has been added to NASCAP to allow material properties to be changed without redoing OBJDEF. The

command card 'NEWMAT LUN', where LUN is an integer, causes revised material parameters to be read from unit LUN. For each material, LUN should contain a card with the material name, followed by three cards with the revised parameters exactly as during OBJDEF. An 'END' card terminates reading from LUN. The NEWMAT segment reprocesses material parameters, recalculates the large capacitances between surface cells and the underlying conductors, and recalculates the conductivity matrix elements. There is one restriction on parameter changes: the sign of parameter 3 (bulk conductivity) and 14 (surface conductivity) cannot be changed. Therefore, a material initially treated as a perfect conductor (parameter 3 negative) cannot subsequently be treated as an insulator (parameter 3 positive), or vice-versa. Also, a material for which surface resistivity was ignored (parameter 14 negative) cannot subsequently be assigned a surface resistivity (parameter 14 non-negative), or vice-versa.

NEWMAT may be called any time after OBJDEF.

### 3.2 OUTPUT

The major change in NASCAP output has been the development of post processor codes through which the user can interactively request specific information. However, the basic NASCAP output has been improved in four areas - current balance printout, flux breakdown, print flags, and contour plot flexibility.

The current balance printout shows, for each conductor, where the current is coming from. The flux breakdown does the same for surface cells, with some additional information about cell geometry and fields. The new print flags allow a user to control the amount of NASCAP printout. And the contour plot flexibility feature lets the user tell NASCAP how many grids should be shown in potential contour plots.

### 3.2.1 Current Balance Printout

An analysis of current balance to conductors is provided at the end of the LIMCEL section. For each conductor, the quantities provided are:

- a. Net current (implicit)
- b. Plasma current (explicit, taking account of limiting of low-energy electrons)
- c. Conductivity current (implicit)
- d. "Battery" current = [Net current] - [Plasma current] - [Conductivity current]

In steady state, the "battery" current represents current supplied to maintain biased or fixed potentials on conductors.

### 3.2.2 Flux Breakdown

The flux breakdown printout has been modified to display more information, as shown below:

SURFACE CELL NO. 237	CODE = 011310050302
	LOCATION = 11 8 5
	NORMAL = 0 0 -1
	MATERIAL = SOLAR
	POTENTIAL = 7.441+00 VOLTS
	STRESS = -1.067+04 VOLTS/METER
	EXTERNAL FIELD = 8.867+00 VOLTS/METER
FLUXES IN A/M**2	
INCIDENT ELECTRONS	1.98-07
RESULTING BACKSCATTER	8.48-08
RESULTING SECONDARIES	1.30-07
INCIDENT PROTONS	7.25-09
RESULTING SECONDARIES	5.29-09
BULK CONDUCTIVITY	-1.07-13
PHOTOCURRENT	6.04-06
NET FLUX	6.06-06

Figure 3.2. Flux breakdown printout.

STRESS is the internal field for insulating surfaces (previously labeled 'FIELD' in the printout). The external field was not printed before; this value is used (when positive) in the field limiting of low energy emission. The initial bulk conductivity is now also printed for insulating surface cells.

To request a flux breakdown printout for any surface cell, the user inserts a card in the options file, read by RDOPT. There are two forms for this card - one is 'SURFACE CELL n' where 'n' is the surface cell number. The other is 'SURFACE AT i,j,k' where 'i,j,k' is the cell location. Both are described in Section 3.1.2, "Surface Cell Specifications".

### 3.2.3 Print Flags

Keyword input may be used to vary the print level from various portions of NASCAP.

'PRINT POTENT' results in an increased level of output from the large Scaled Conjugate Gradient potential solver. This is intended mainly for debugging purposes. 'NOPRINT POTENT' restores the default.

'PRINT OBJDEF' results in printing of the element table and some point-lists which are now by default suppressed. 'NOPRINT OBJDEF' suppresses printing of the surface cell list and list of material properties.

'PRINT LIMCEL' causes the results of the preliminary charging analysis to be printed prior to entering the final charging analysis. For each insulating surface cell and conductor the initial and trial potentials, external field, current level, and status (fixed or not fixed) are given. 'NOPRINT LIMCEL' causes reversion to the default. Also, some obsolete debugging prints have been removed from the LIMCEL section.

### 3.2.4 Contour Plot Flexibility

A new keyword, NGPLOT, has been added to NASCAP's RDOPT routine. This allows the user to specify the number of grids to be considered in potential contour plots. Using the keywords ICON, NCON, and NGPLOT, contour plots will be generated as indicated below:

ICON	NCON	NGPLOT	
0	0	any	None
0	any	0	None
>0	0	0	Three views each of 1 and NG grids when ICYC = 1 mod ICON.
0	>0	>0	Extra views only plotted in NGPLOT grids every timestep.
>0	>0	>0	Three default views plus extra views plotted in NGPLOT grids every timestep.
>0	>0	0	Three default views plus extra views plotted in 1 and NG grids when ICYC = 1 mod ICON.
>0	0	>0	Three default views plotted in NGPLOT grids when ICYC = 1 mod ICON.

Figure 3.3. Keyword values for contour plots.

Note that additional flexibility is available through use of the interactive routine POTPLT.

### 3.3 NEW FEATURES

Three new features in NASCAP for the 1980's are: deadline and timer, automatic convergence monitor, and the spin command.

The deadline is quite useful in allowing for scheduled computer down time. Rather than worry every night that the computer will dump you before your NASCAP run finishes, you can set a NASCAP deadline, after which the program gracefully terminates. Timer shows the user how much execution time is used by various parts of NASCAP.

The automatic convergence monitor eliminates another uncertainty for the NASCAP user. It eliminates the old keyword MAXITR, which was hard to figure out, and was also critical to the successful running of NASCAP.

The SPIN command will save much computer time analyzing satellites that turn in relation to the sun. It is often desirable to run NASCAP timesteps of ten minutes or more. But a spinning satellite used to require several timesteps per rotation to properly figure solar illumination. Now, an average illumination can be calculated.

The SPIN command is one example of a code change that appeared to be quite simple, but ended up causing changes in many parts of the code, including the hidden line routines (HIDCEL) and the longtimestep routines (LIMCEL).

#### 3.3.1 DEADLINE AND TIMER

The keyword specification  
DEADLINE hhmss  
will cause TRILIN to exit rather than start another timestep after the host computer's internal system clock has passed through the DEADLINE time.

Examples:

```
DEADLINE 235959
```

will not allow a timestep to start after midnight of the day the deadline card is read.

DEADLINE 060000

will not allow a timestep to start after 6:00 a.m. (the next day, if the DEADLINE card is read during the evening).

Remember that the effect of the DEADLINE is gone after exiting (and re-executing) NASCAP.

The TIMER option gives the user a better idea of how NASCAP execution time is used up. If you insert a card reading "TIMER" in the options (RDOPT) file, then NASCAP will print out the accumulated amount of execution time, at various points in the calculation.

### 3.3.2 Automatic Convergence Monitor -- MAXITR

It is no longer necessary for the NASCAP user to guess how large to set MAXITR to achieve convergence of the potential solver. MAXITR can be totally left out of the options file.

NASCAP now keeps track of the measure of convergence and its rate of decrease. The iteration procedure terminates if the following three conditions are satisfied:

1. The number of iterations is at least  $8 \cdot (\text{no. of grids})$ .
2. The measure of convergence is decreasing.
3. The measure of convergence has been reduced POTCON orders of magnitude from its initial value.

The parameter POTCON is set by default to 8 in CAPACI and to 4 in TRILIN. It may be changed by keyword input in the options file. As a "measure of convergence" in the potential iterations, the square of the length of the residual vector is used (i.e.,  $\rho'$  in Figure 7.1 of the NASCAP User's Manual<sup>[5]</sup>). Since MAXITR will now not be normally used to terminate the convergence process, its default value has been changed to 99.

### 3.3.3 SPIN Command

A SPIN command has been added to the main NASCAP routine. This command generates a table of averaged solar illumination for each surface cell of a rapidly spinning satellite. SPIN performs a straightforward numerical average of solar illumination factors for a sequence of sun directions about a specified rotation axis.

The SPIN routines require specification of NIEWS, the number of sun directions to include in the averaging, and SPINAX(3), a vector specifying the rotation axis. The default values are NIEWS = 8 and SPINAX = (0.0.1.); these values are used when LUN = 0 is supplied on the SPIN command card. If LUN = 5, SPIN reads two cards from the input runstream. For any other positive value the cards are read from the specified file. The first card read contains NIEWS (an integer) and the second card contains the x, y, and z components of the spin axis. The spin axis vector need not be normalized. Tests with NIEWS = 8 indicate that the numerical averaging procedure is accurate to within a few percent for simple objects.

The SPIN driver routine generates NIEWS calls to HIDCEL, with the sun initially at the original input sun direction, and then rotated uniformly thereafter. If the CONVEX option is specified, calls to HIDCEL are not required. Once the SPIN command is invoked, NASCAP assumes all later TRILIN cycles (including restarts) for the satellite will use the resulting tables of averages illumination, unless HIDCEL is explicitly called at a later point.

Figures 3.4 and 3.5 illustrate the equilibrium potentials reached using the SPIN option for a one-grid SCATHA model.

POTENTIAL CONTOURS ALONG THE X-Y PLANE OF Z = 17

MIN = -.70000E+03 MAX = -.12945E+03 ΔE = .50000E+02

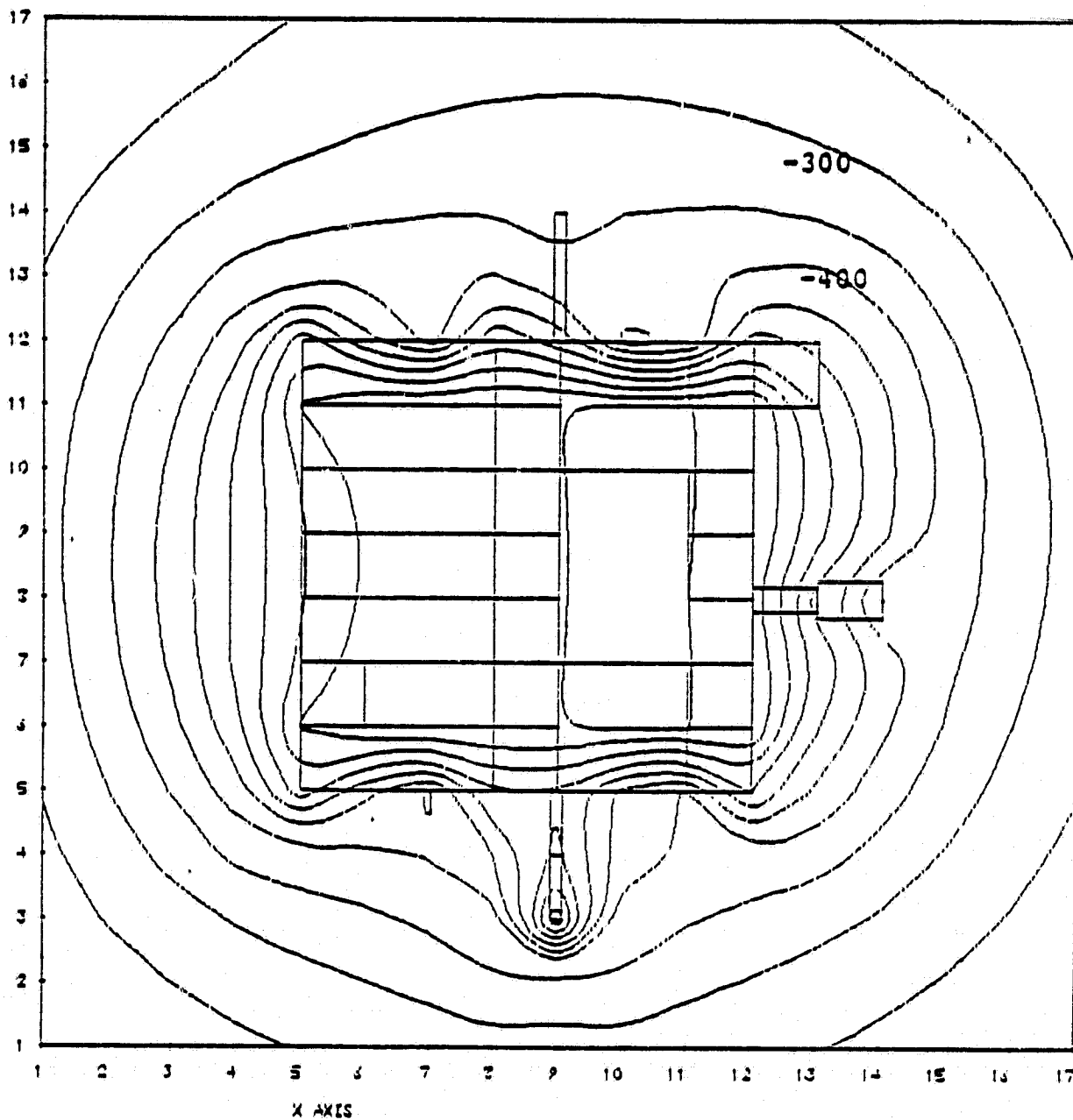


Figure 3.4. Potential contours around satellite at equilibrium in sunlight, with conductor potential at -700 volts. Average solar illumination applied with initial sun direction = (.1,1.,1.) and spin axis = (1.,0.,0.).

POTENTIAL CONTOURS ALONG THE Y-Z PLANE OF X = 9

MIN = -.70000E+03 MAX = -.12410E+03 ΔS = .20000E+02

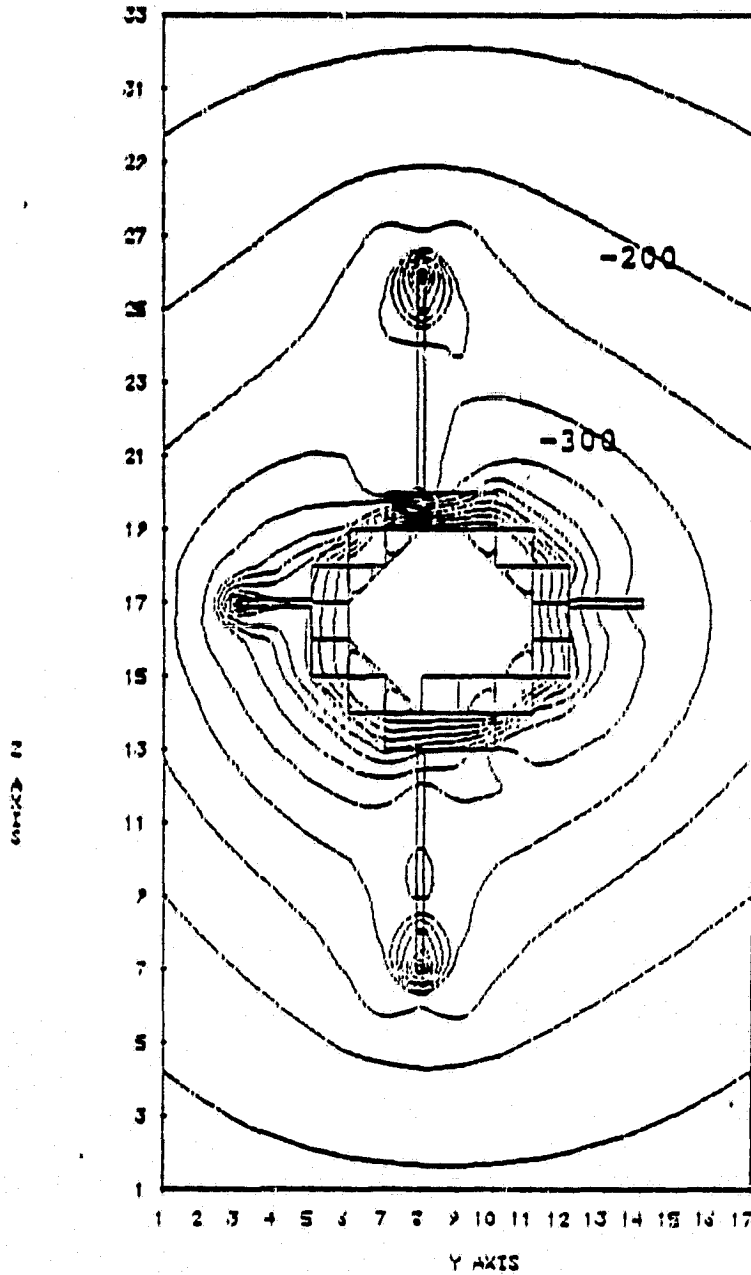


Figure 3.5. Same conditions as in Figure 3.4. Note absence of any dipole potential field since averaged solar illumination has been used.

## 4. CODE REVIEW

In a large sense, all of the changes made to NASCAP are a result of code review. This section of the report is devoted to those changes which are general or miscellaneous or don't fit under "Physics", "Usability", and "Auxiliary Codes". The six categories here are: centering, faster interface routines, 1250 surface cells, code cleanup and commenting, shadowing (HIDCEL) improvements, and 'TYPE' conflict.

The new NASCAP centering scheme was a major improvement. It increased the stability and accuracy of the code, while at the same time greatly reducing running time! Faster execution time was also achieved by speeding up the subroutines that do calculations on the NASCAP grid interface regions.

The number of allowed surface cells was increased from 1024 to 1250. A comprehensive code cleanup made the Fortran coding easier to read and understand. Some improvements in the shadowing routines (HIDCEL) removed limitations on some unusual shadowing situations. Finally, we removed a small but annoying problem that resulted from conflicting flux type specifications.

### 4.1 CENTERING

The centering scheme used to update surface charges and potentials has been completely rewritten, a major task. Cell centered potentials and charges are now stored for each insulating cell and for each conductor. (These cell potentials are printed every timestep.) Potentials at nodal points bordering disparate materials are now fixed to area weighted averages. This scheme, exactly the reverse of the previous centering, results in much smoother potential

variations through transition regions. This scheme also allows the use of the capacitor model to fix surface potentials while space fields are converging, which significantly improves the rate and stability of the iterative convergence in POTENT.

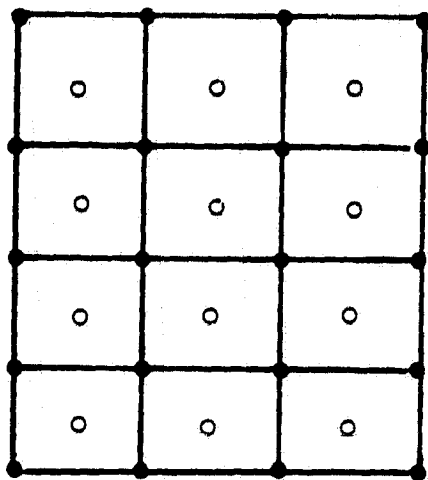


Figure 4.1. Centering scheme. Dark spots are nodal points - open circles are cell centers. Cell potentials and charges are now calculated at cell centers rather than at nodal points.

#### 4.2 FASTER INTERFACE ROUTINES

The interface routines called by COPROD have been revised to make use of fewer subroutine calls and to decrease the number of matrix operations required. As a result of this improvement and the recentering scheme, a full run of the four-grid SCATHA model to equilibrium in eclipse now requires approximately two hours UNIVAC 1100/81 CPU time, whereas nearly eight hours were required previously.

#### 4.3 1250 SURFACE CELLS

NASCAP is a large code. It always nudges the size limitations of its host computer. One result of this size problem is that NASCAP objects have always been limited to 1024 total surface cells.

This year, by using sophisticated mapping techniques and shaving space wherever possible, we have increased to 1250 the number of surface cells allowed. Because of extra arrays needed for insulating surface cells, not more than 1024 of the 1250 total are allowed to be insulators.

#### 4.4 CODE CLEANUP AND COMMENTS

Dr. M. J. Mandell went through the entire NASCAP code, subroutine by subroutine. He performed a major code cleanup and added comments. In detail:

1. The SUBROUTINE or FUNCTION statement was placed at the head of each symbolic element.
2. A comment was added stating the calling routine for each subprogram and the code module to which the subprogram belongs.
3. When appropriate, references were added to NASA CR's 159417, 135259, 159595, and 135256. In a few places references to open literature were added.
4. Excess lines of coding were deleted. Such lines included multiple spacer (blank comment) lines, debugging print statements, unused FORMAT statements, unnecessary COMMON statements, and old algorithms which have been superseded.
5. In a few places loops were replaced by S3MOVE or S3ZERO.

6. Obsolete subprograms were expunged.
7. Diverse sorting routines were replaced by a single, faster subroutine, SRTWDS.

#### 4.5 SHADOWING (HIDCEL) IMPROVEMENTS

Several improvements have been made in the operation of the HIDCEL shadowing routines. With the operation of the ROTATE and SPIN features of NASCAP in conjunction with the use of long thin booms, some difficulties were encountered in the shadowing algorithms, especially in the treatment of small boom "tips" in the SCATHA models. These operational problems have now all been corrected. Figure 4.2 illustrates one such shadowing case which caused the code to fail: it contains A2 (shadowing) surfaces which are entirely contained within A1 (shadowed) surfaces. The HIDCEL algorithm now recognizes the occurrence of such cases and calculates the correct shadowing fraction by simply subtracting the A2 area from the A1 area. Another improvement involved a new routine, POLYN, which eliminates redundant vertices from generated A1 polygons as necessary; previously HIDCEL could malfunction when polygons having over twelve vertices were generated.

#### 4.6 'TYPE' CONFLICT

In the original NASCAP, a conflict between the flux type in the flux file and the type chosen in the options (RDOPT) file would halt program execution. The user was required to supply information that was either redundant or incorrect.

Now, the flux type specified in the flux file is the one that counts. The options (RDOPT) file does not need to specify what flux type is being used.

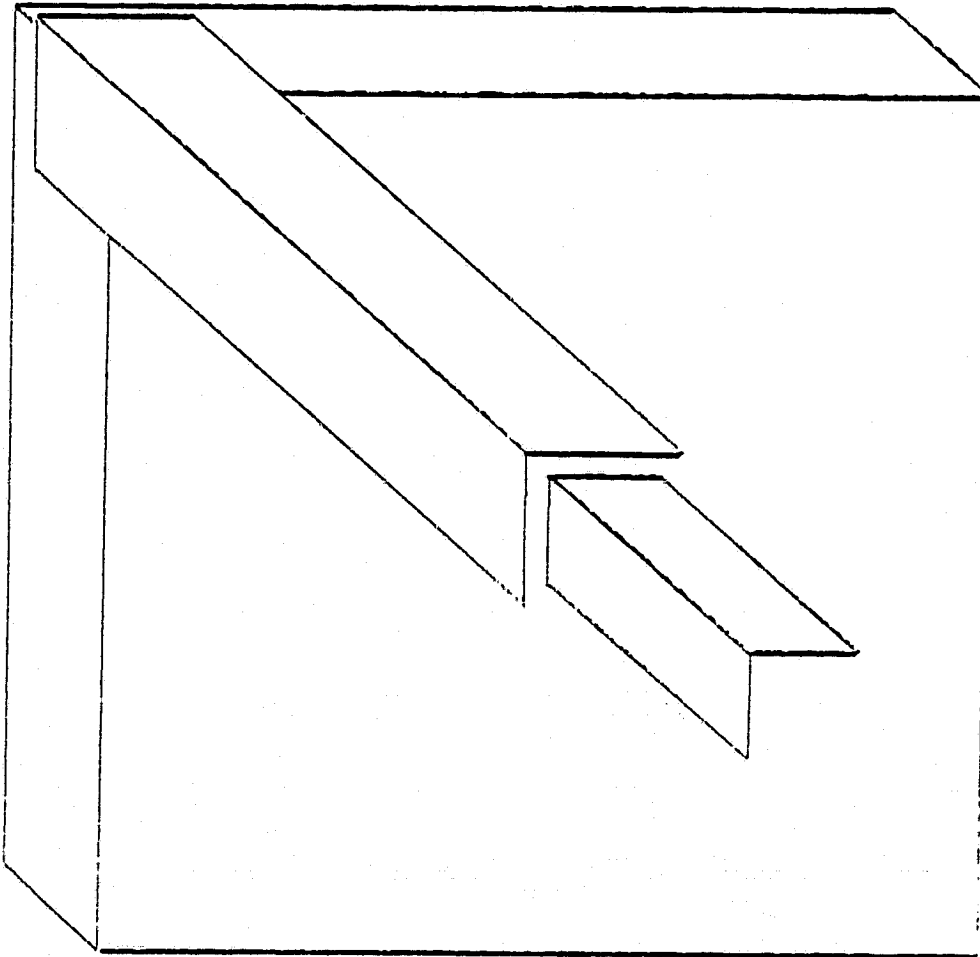


Figure 4.2. Illustration of a shadowing case in which A2 surfaces are contained entirely within A1 surfaces.

## 5. AUXILIARY CODES

NASCAP was designed as a stand-alone code. It requires no other programs for problem setup or interpretation. But now there is a small family of associated codes that make NASCAP use easier, and give the user a new degree of flexibility. The major auxiliary codes are TERMTALK, MATCHG, and the workshop codes (FILES, OBJCHECK, and POTPLT).

In original NASCAP, all output comes back as hard copy printout or graphics. If you want to see the evolution of electric charging on a particular surface cell, you have to page through a stack of output and read the potential at each timestep from a list. TERMTALK gets the computer to sort through NASCAP restart files to find the data you want.

MATCHG is a special code for investigating material properties. In effect, you take a little patch of any surface material, and subject it to a specified flux. You find out how that material will charge without the influences of geometry, other materials, and sunlight. This gives you a general idea of what will happen to a test object. MATCHG is very much faster and cheaper to run than NASCAP.

The workshop codes were designed to simplify things for new NASCAP users. They were used for the NASCAP workshops at NASA/LeRC. FILES does Univac file manipulation. OBJCHECK draws object illustration plots. POTPLT draws electric potential contours.

## 5.1 TERMTALK

TERMTALK is an interactive program for retrieving NASCAP data. It accesses NASCAP restart files to produce charging history tables and graphs and a variety of other information.

TERMTALK is a menu-style program - the user requests the desired information rather than answering a series of yes or no questions, "Do you want such and such? How about such and such? ..." As a result, the user can get any of the types of available output just by typing one or two commands, no matter what section of the program is currently operating.

There are four main program modules, named HISTORY, LATEST, SINGLE, and SPECIAL.

The HISTORY module outputs for any surface cell the time history of the user's choice of five quantities - potential, electric flux, external electric field, internal electric field (stress), or potential difference between an insulator surface and underlying conductor (delta). The output comes in the form of a printed table, and/or a rough plot of quantity versus time. The printed table will show up to seven surface cells across the page.

The LATEST module gives the user a complete list for all of the surface cells and conductors of any of the five quantities mentioned above. They may be printed in sequence or ordered by magnitude. Partial listings, including only some surface cells, are available.

Module SINGLE prints out information about a single surface cell. In addition to the five standard quantities, you can get the cell location, its surface material, its shape, its normal, and the number of its underlying conductor.

The SPECIAL module lets the user "turn off" all output coming to the terminal. This unseen output can be printed on a line printer at the end of the session. SPECIAL also allows the user to change the NASCAP cycle number.

#### PROGRAM STRUCTURE

TERMTALK is organized into four modules - LATEST, HISTORY, SINGLE, and SPECIAL. Each of the modules has its own set of commands. Each module also has access to a set of "aid" routines, named HELP, SUBSET, OUTLINE, LOCATION, and EXIT. A crude diagram of the program is shown in Figure 5.1.

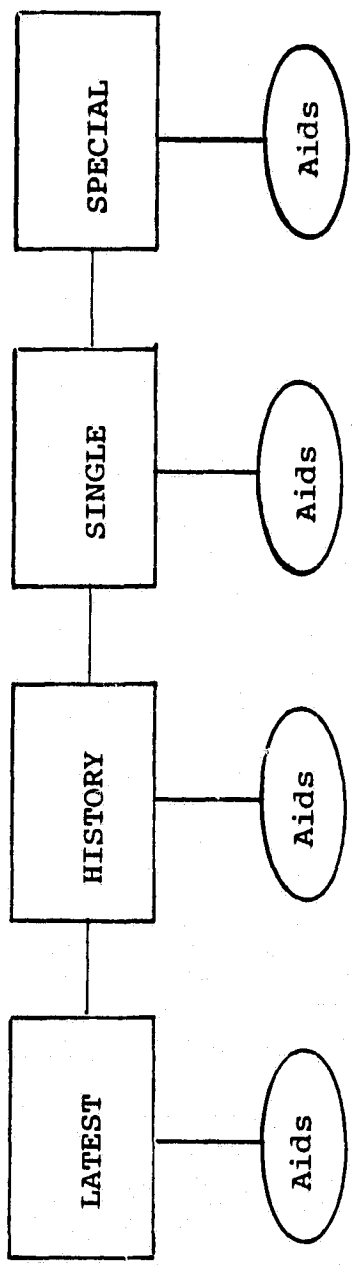
The user moves from any module to any other by typing the name of the new module. "Aid" routines always return to the module from which they were called.

#### CELL SPECIFICATIONS

NASCAP assigns a cell number to each surface cell. Each cell can also be identified with five basic geometrical attributes - location, material, surface normal, shape, and conductor number. TERMTALK provides a way for the user to go back and forth between cell numbers and geometrical attributes.

'SINGLE' takes a cell number and prints out attributes. It also prints out charging information.

'SUBSET' takes the user's geometrical specifications, and determines the set of cells that satisfy these. It is extremely general. You can easily determine the number of a particular cell, or you can define a complicated group of cells. For example, you could define the group of all non-boom cells that are either KAPTON or TEFLON and lie on conductor #1; or all cells between the planes of  $X = 1$  and  $X = 5$ .



Aids are: HELP  
OUTLINE  
SUBSET (optional group name)  
LOCATION #  
EXIT

Figure 5.1. Diagram of TERMTALK.

## CHARGING HISTORY

TERMTALK can plot surface cell potential as a function of time. It also prints cell histories in a tabular form. And it gives tables and plots of other quantities such as electric flux and electric fields.

If you are more interested in final equilibrium values than in histories, the module 'LATEST' gives only the most recent information.

## INSTRUCTIONS FOR USE

The most extensive documentation for TERMTALK is internal to the program. It is accessed by typing 'HELP' at any time. This gives the user a full-blown explanation of the commands and modes available for each module.

It is necessary to run NASCAP before using TERMTALK. A simple object definition will initialize enough files to use SUBSET. For instructions on NASCAP use, see the NASCAP User's Manual - 1978, NASA CR-159417, August 1978.

To use TERMTALK on a UNIVAC computer, type '@XQT TERMTALK.ABS'. The program will ask for the NASCAP file prefix and assign all necessary files.

On CDC machines, the user must attach NASCAP files 16, 17, and 21 before running. At the end of each run, file number 3 will contain a line printer image of the output.

## SAMPLE RUN

The following shows a simple TERMTALK example. Note that near the end, the mode 'NOTERM' is set. This suppresses terminal printing of output data. The user will rely on line printer output, without having to wait for terminal printout of the HISTORY graph.

QXQT TERMTALK.ABS  
WELCOME TO TERMTALK ...

PREFIX PLEASE ? >MM

THANK YOU

-- NOTICE -- THESE FILES WERE GENERATED UNDER 'OLD' NASCAP  
FIELD AND FLUX INFORMATION WILL NOT BE AVAILABLE

CHOOSE ANY MODULE  
HELP IS ALWAYS AVAILABLE - TYPE 'HELP'  
>SINGLE

SINGLE COMMAND OR MODE SET ?

>15  
CELL NUMBER 15  
CENTERED AT -5.5 -3.5 6.5  
MATERIAL IS SOLAR  
POTENTIAL = -5.389+03 VOLTS

SINGLE COMMAND OR MODE SET ?  
>ALSO STRESS  
MODE RESET

SINGLE COMMAND OR MODE SET ?  
>ALSO DELTA  
MODE RESET

SINGLE COMMAND OR MODE SET ?  
>155

CELL NUMBER 155  
CENTERED AT -5.5 -2.5 8.0  
MATERIAL IS GOLDDP  
POTENTIAL = -5.409+03 VOLTS  
DELTA V = 0.000 VOLTS  
INTERNAL FIELD STRESS = 0.000 VOLTS/METER

SINGLE COMMAND OR MODE SET ?  
>LATEST

LATEST COMMAND OR MODE SET ?

>LIST 1 45

POTL	IN VOLTS	FOR NASCAP	CYCLE	11 ...	TIME =	4.23+03	SEC		
1	-5.44+03	2	-5.39+03	3	-5.39+03	4	-5.39+03	5	-5.39+03
6	-5.39+03	7	-5.39+03	8	-5.41+03	9	-5.41+03	10	-5.41+03
11	-5.39+03	12	-5.39+03	13	-5.39+03	14	-5.39+03	15	-5.39+03
16	-5.41+03	17	-5.39+03	18	-5.44+03	19	-5.39+03	20	-5.39+03
21	-5.39+03	22	-5.39+03	23	-5.39+03	24	-5.39+03	25	-5.41+03
26	-5.41+03	27	-5.41+03	28	-5.39+03	29	-5.39+03	30	-5.39+03
31	-5.39+03	32	-5.39+03	33	-5.41+03	34	-5.39+03	35	-5.44+03
36	-5.39+03	37	-5.39+03	38	-5.39+03	39	-5.39+03	40	-5.39+03
41	-5.39+03	42	-5.41+03	43	-5.41+03	44	-5.41+03	45	-5.39+03

LATEST COMMAND OR MODE SET ?  
>HISTORY

HISTORY COMMAND OR MODE SET ?

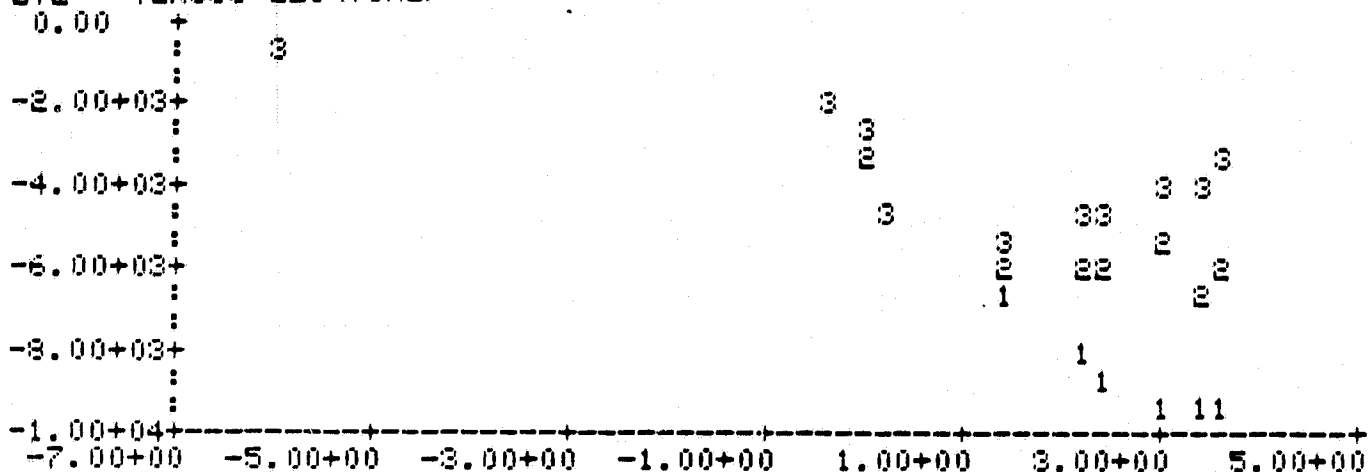
>-3 -4 -5

POTL IN VOLTS

TIME	-3	-4	-5	#4	#5	#6	#7
1.0-06:	-4.56+02	-5.00+02	-4.57+02				
4.0-01:	-1.77+03	-1.87+03	-1.75+03				
8.0-01:	-3.00+03	-3.17+03	-2.96+03				
1.0+00:	-4.51+03	-4.74+03	-4.42+03				
3.0+01:	-5.60+03	-5.30+03	-5.63+03				
1.0+02:	-5.83+03	-5.26+03	-4.96+03				
0.0+02:	-3.48+03	-5.17+03	-4.43+03				
1.0+03:	-3.23+03	-5.39+03	-4.03+03				
0.0+03:	-3.30+03	-5.50+03	-3.71+03				
3.0+03:	-3.00+03	-5.00+03	-3.46+03				
4.0+03:	-3.30+03	-5.12+03	-3.25+03				

... PRESS <CR> TO CONTINUE ...

POTL VERSUS LOG(TIME)



HISTORY COMMAND OR MODE SET ?

>CYCLES 6 TO 11

MODE RESET

HISTORY COMMAND OR MODE SET ?

>GRAPH

MODE RESET

HISTORY COMMAND OR MODE SET ?

>-3 -4 -5

POTL VERSUS LOG(TIME)

-3.00+03+	:	:	3	3	3
-4.00+03+	:	3	3		
-5.00+033	:		2		
-6.00+03+	:	2		2	2
-7.00+03+	2			2	
-8.00+031	:				
-9.00+03+	:	1	1	1	1
-1.00+04+	-----+-----+-----+-----+-----+				
2.10+00	2.50+00	2.90+00	3.30+00	3.70+00	

HISTORY COMMAND OR MODE SET ?  
 >SUBSET KAPTON  
 DEFINITION OF NEW SUBSET NAMED KAPTON  
 1267 REMAINING IN GROUP

SUBSET INSTRUCTION PLEASE ?  
 >MATL KAPTON  
 6 REMAINING IN GROUP

SUBSET INSTRUCTION PLEASE ?  
 >WHICH?  
 MEMBERS OF GROUP KAPTON  
 90 91 107 108 889 1120 0 0 0 0  
 6 REMAINING IN GROUP

SUBSET INSTRUCTION PLEASE ?  
 >DONE  
 GROUP KAPTON WITH 6 MEMBERS IS NOW DEFINED  
 RETURNING TO MODULE 'HISTOR'

HISTORY COMMAND OR MODE SET ?  
 >SPECIAL

SPECIAL COMMAND OR MODE SET ?  
 >NOTERM  
 MODE RESET

SPECIAL COMMAND OR MODE SET ?  
 >HISTORY

HISTORY COMMAND OR MODE SET ?  
 >GROUP KAPTON

HISTORY COMMAND OR MODE SET ?  
 >EXIT

WOULD YOU LIKE A LINE PRINTER COPY OF THIS  
 TERMTALK SESSION ?>YES  
 -EXIT TERMTALK-  
 FURPUR 27R3A E35 73R1-2 08/22/79 16:24:52  
 3 BLOCKS COPIED.

READY  
 >

## INTERNAL DOCUMENTATION

This is a computer printout of the actual on-line documentation available in TERMTALK. First is the complete output of the OUTLINE aid. Second is a listing of all available HELP sequences.





WHICHEVER MODULE YOU ARE IN, YOU HAVE AVAILABLE A SET OF COMMANDS AND A SET OF MODES. COMMANDS INITIATE OUTPUT. MODES ALTER THE FORM OF SUCCEEDING OUTPUT.

AT ANY TIME INSTEAD OF TYPING A COMMAND OR MODE, YOU MAY CHANGE MODULES OR CALL FOR AID. ALTOGETHER YOU HAVE FOUR CHOICES - TYPE A COMMAND, A MODE, THE NAME OF A DIFFERENT MODULES, OR THE NAME OF AN AID.

AS AN EXAMPLE, YOU ARE IN MODULE SINGLE. YOU TYPE THE NUMBER 317. THIS IS A COMMAND. THE TERMINAL PRINTS OUT THE POTENTIAL AND THE SURFACE NORMAL OF CELL #317. YOU WANT MORE. YOU TYPE 'EVERYTHING' (A MODE) AND ON THE NEXT LINE TYPE '317' AGAIN. MORE INFORMATION COMES OUT. TO CHANGE MODULES, YOU TYPE 'HISTORY'. NOW YOU DON'T KNOW WHAT TO DO, SO YOU TYPE 'HELP'. AND YOU GET THIS MESSAGE.

FOR ANY COMMAND, MODE, MODULE, OR AID, TERMTALK RECOGNIZES AN ENTIRE WORD BASED ON THE FIRST THREE LETTERS.

... PICK ANOTHER NUMBER -OR- TYPE 'MENU' TO SEE YOUR CHOICES  
-OR- <CR> TO RETURN TO MAIN

2

-- MAIN --

IF YOU ARE IN MODULE MAIN, YOU HAVE JUST ENTERED TERMTALK. I AM WAITING FOR YOU TO CHOOSE A MODULE. ALL OF THE AIDS ARE AVAILABLE AS WELL. HERE IS A LIST:

CHOOSE ANY MODULE NAME ...  
ANY AID MAY BE CALLED FROM ANY MODULE

MODULES	AIDS
HISTORY	AGAIN
LATEST	HELP
SINGLE	LOCATION #
SPECIAL	OUTLINE
	SUBSET
	EXIT
	SUBSET [GROUP NAME]

... PICK ANOTHER NUMBER -OR- TYPE 'MENU' TO SEE YOUR CHOICES  
-OR- <CR> TO RETURN TO MAIN

3

-- NUMBERING CONVENTIONS --

TERMTALK HAS PARTICULAR NUMBERING CONVENTIONS FOR SURFACE CELLS AND CONDUCTORS. A NASCAP OBJECT IS COMPOSED OF N FLAT SURFACE CELLS, M BOOM CELLS, AND L CONDUCTORS. N OR M MAY EQUAL ZERO.

NEGATIVE NUMBERS ( -L THROUGH THROUGH -1 ) REFER TO CONDUCTORS. THE POSITIVE NUMBERS 1 THROUGH N REFER TO FLAT SURFACE CELLS. THESE ARE THE SMALL RECTANGLES AND TRIANGLES COVERING THE SPACECRAFT. BOOM CELLS ARE SKINNY CYLINDERS. THEY ARE NUMBERED N+1 THROUGH N+M.

... PICK ANOTHER NUMBER -OR- TYPE 'MENU' TO SEE YOUR CHOICES  
-OR- <CR> TO RETURN TO MAIN

4

-- FLUX FIELD POTL DELTA STRESS --

THESE ARE THE FIVE DYNAMIC PIECES OF INFORMATION PERTAINING TO ANY SURFACE CELL. THEY CHANGE EACH TIME CYCLE. ONLY FLUX AND POTL PERTAIN TO CONDUCTORS. IF YOU ARE ANALYZING "OLD" NASCAP RUNS, FLUX AND FIELD WILL NOT BE AVAILABLE.

FLUX - TOTAL ELECTRIC FLUX TO A CELL OR CONDUCTOR - DUE TO INCIDENT PARTICLES, SECONDARIES, ELECTRON BACKSCATTER, AND PHOTOEMISSION. UNITS ARE AMPS PER SQUARE METER.

FIELD - THE EXTERNAL ELECTRIC FIELD IN THE VOLUME IMMEDIATELY ABOVE A SURFACE CELL. UNITS OF VOLTS PER METER.

POTL - ELECTRIC POTENTIAL ON THE EXTERNAL SURFACE OF A CELL OR A CONDUCTOR. UNITS ARE VOLTS.

DELTA - DIFFERENCE BETWEEN SURFACE POTENTIAL OF A DIELECTRIC CELL AND POTENTIAL OF THE UNDERLYING CONDUCTOR. IN VOLTS.

STRESS - INTERNAL ELECTRIC FIELD STRESS FOR DIELECTRIC CELLS. PROPORTIONAL TO DELTA. INVERSELY PROPORTIONAL TO MATERIAL THICKNESS. UNITS OF VOLTS PER METER.

... PICK ANOTHER NUMBER -OR- TYPE 'MENU' TO SEE YOUR CHOICES  
-OR- <CR> TO RETURN TO MAIN

5

-- SUBSET AND GROUPS --

YOU CAN USE SUBSET TO DEFINE A GROUP OF CELLS THAT ARE OF SPECIAL INTEREST TO YOU. FOR INSTANCE, YOU MIGHT WANT ALL KAPTON COATED SURFACE CELLS. OR ALL THE CELLS OVER CONDUCTOR #2. OR THE INTERSECTION OF BOTH SETS.

YOU ENTER SUBSET BY TYPING 'SUBSET', OR 'SUBSET' FOLLOWED BY A GROUP NAME. GROUP NAMES MUST BE TYPED OUT CORRECTLY, NOT JUST THE FIRST THREE LETTERS. YOU MAY DEFINE UP TO 34 DIFFERENT GROUPS, IN ADDITION TO THE 2 DEFAULT GROUPS 'ALL' AND 'NULL', WHICH REPRESENT THE COMPLETE SET AND THE EMPTY SET.

THE SUBSET SPECS CAN BE CLASSIFIED INTO NARROW DOWN TYPES, SET OPERATIONS, INFORMATION REQUESTS, AND OTHERS.

◆◆◆◆ NARROW DOWN ◆◆◆◆

A NEW SUBSET CONSISTS OF ALL CELLS AND CONDUCTORS. THE NARROW DOWN SPECIFICATIONS ELIMINATE ANY CELLS THAT DON'T FIT. ALL OF THE NARROW DOWN SPECIFICATIONS, EXCEPT 'NUMBERS', ELIMINATE ALL CONDUCTORS, -1 THROUGH -7.

XLIM # TO # - EXCLUDE CELLS WITH CENTERS OUTSIDE OF GIVEN LIMITS IN THE X DIRECTION

YLIM # TO # - LIKE XLIM

ZLIM # TO # - LIKE XLIM

INSULATOR - EXCLUDE CONDUCTING CELLS



MATL [MATERIAL NAME]  
SHAPE [SQUARE, RECTAN, RIGHT, EQUIL, OR BOOM]  
OR [GROUP NAME]  
AND [GROUP NAME]  
COMPL [GROUP NAME]  
NAME [ANY WORD]  
... PICK ANOTHER NUMBER -OR- TYPE 'MENU' TO SEE YOUR CHOICES  
-OR- <CR> TO RETURN TO MAIN

6

-- AIDS --

AIDS ARE AVAILABLE FROM ANY MODULE. YOU CANNOT  
GENERALLY CALL ONE AID WHILE YOU ARE USING ANOTHER.  
YOU CANNOT CALL 'EXIT' WHILE USING 'HELP', FOR  
EXAMPLE. THE AIDS ARE :

AGAIN - CAUSES TERMTALK TO REPEAT THE MOST RECENT PROMPT

HELP - PRINTS VARIOUS INFORMATIVE MESSAGES

LOCATION # - 'LOC' OR 'LOCATION' FOLLOWED BY A  
CELL NUMBER WILL GIVE THE COORDINATES OF THE  
CENTER OF THAT SURFACE CELL.

OUTLINE - PRINTS A MENU, A LIST OF AVAILABLE  
MODULES, COMMANDS, MODES, AND AIDS.

SUBSET - ALLOWS USER TO DEFINE A GROUP OF CELLS AND  
CONDUCTORS THAT ARE OF PARTICULAR INTEREST.  
THE ENTIRE SET OF CELLS IS NARROWED DOWN TO  
A DESIRED SUBSET.

SUBSET [GROUP NAME] - IF THE GROUP NAME HAS BEEN  
PREVIOUSLY DEFINED, PERMITS ALTERATION OF  
THE MEMBERS. IF NOT, A NEW GROUP WITH THAT  
NAME IS DEFINED.

EXIT - ENDS TERMTALK USE.

... PICK ANOTHER NUMBER -OR- TYPE 'MENU' TO SEE YOUR CHOICES  
-OR- <CR> TO RETURN TO MAIN

7

-- ERROR MESSAGES --

LET'S SAY YOU DID SOMETHING I DIDN'T EXPECT. OR  
LET'S SAY I JUST GOT CONFUSED. I WILL PRINT OUT AN  
ERROR MESSAGE. THE FIRST WORD OF AN ERROR MESSAGE HAS  
ASTERISKS AROUND IT, AND IDENTIFIES THE SUBROUTINE WHERE  
THE PROBLEM OCCURED, FOR EXAMPLE '◆◆◆ SINGLE ◆◆◆'.

WHAT DO YOU DO THEN? TRY IT AGAIN, OR TRY SOMETHING  
ELSE. YOU CAN'T DAMAGE THE PROGRAM. OR CALL FOR THE  
'OUTLINE' OR 'HELP'.

... PICK ANOTHER NUMBER -OR- TYPE 'MENU' TO SEE YOUR CHOICES  
-OR- <CR> TO RETURN TO MAIN

8

-- COORDINATE SYSTEM --

THE COORDINATE SYSTEM USED BY TERMTALK HAS THE ORIGIN IN THE CENTER OF THE INNERMOST GRID. LOCATIONS IN ALL GRIDS ARE IN TERMS OF INNER GRID UNITS.

IN OTHER WORDS, PERMITTED VALUES FOR X OR Y IN THE INNER GRID ARE FROM -8 TO +8. IN GRID #2 VALUES ARE FROM -10 TO +16 IN STEPS OF TWO, OR FROM +10 TO +16 BY TWOS. Z GOES FROM -16 TO +16 IN THE INNER GRID, AND FROM -32 TO +32 IN GRID #2.

... PICK ANOTHER NUMBER -OR- TYPE 'MENU' TO SEE YOUR CHOICES  
-OR- <CR> TO RETURN TO MAIN

9

-- LINE PRINTER FILE --

TERMTALK CREATES A LINE PRINTER FILE. AT THE END OF A RUN, YOU CAN SEND THIS FILE TO THE PRINTER TO MAKE A HARD COPY. IF YOU ARE USING A SLOW TERMINAL, YOU CAN ASK FOR MODE 'NOTERM' IN MODULE 'SPECIAL'. IN THIS MODE, ALL THE OUTPUT GOES TO THE LINE PRINTER FILE, AND NONE OF IT GOES TO YOUR TERMINAL. YOU CAN STILL GET A COMPLETE HARD COPY AT THE END OF THE RUN.

... PICK ANOTHER NUMBER -OR- TYPE 'MENU' TO SEE YOUR CHOICES  
-OR- <CR> TO RETURN TO MAIN

10

-- DEFAULTS --

AT THE BEGINNING OF TERMTALK ALL MODES ARE SET TO A DEFAULT VALUE. THE DEFAULT MODES FOR EACH MODULE ARE

HISTORY: POTL, ALL CYCLES, BOTH, LOG

LATEST: POTL, SEQUENTIAL

SINGLE: ALSO NUMBER, CENTER, MATL, POTL  
NOT ( EVERYTHING ELSE )

SPECIAL: TERMP

... PICK ANOTHER NUMBER -OR- TYPE 'MENU' TO SEE YOUR CHOICES  
-OR- <CR> TO RETURN TO MAIN

11

-- OLD NASCAP --

TERMTALK CAN BE USED ON NASCAP FILES THAT WERE GENERATED BEFORE TERMTALK WAS WRITTEN. BUT IN THE OLD DAYS, NASCAP DIDN'T SAVE FLUX OR FIELD INFORMATION ON THE RESTART FILES. SO THOSE NUMBERS AREN'T AVAILABLE FROM OLD NASCAP RUNS.

... PICK ANOTHER NUMBER -OR- TYPE 'MENU' TO SEE YOUR CHOICES  
-OR- <CR> TO RETURN TO MAIN

12

-- COMPLAINTS --

TERMTALK WAS WRITTEN TO BE A CONVENIENT, USER-ORIENTED DATA REDUCTION TOOL.

IF YOU DON'T LIKE IT, OR WOULD LIKE TO SEE SOME CHANGES, YOU CAN WRITE TO SYSTEMS, SCIENCE, AND SOFTWARE, PO BOX 1620, LA JOLLA, CALIFORNIA 92038. MARK IT 'ATTENTION: JACK CASSIDY'

... PICK ANOTHER NUMBER -OR- TYPE 'MENU' TO SEE YOUR CHOICES  
-OR- <CR> TO RETURN TO MAIN

13

CHOOSE ANY MODULE  
HELP IS ALWAYS AVAILABLE - TYPE 'HELP'  
>HISTORY  
HISTORY COMMAND OR MODE SET ?  
>HELP

- HELP IS AT HAND - PICK A NUMBER,
- |                                      |                       |
|--------------------------------------|-----------------------|
| (1) BASIC USE                        | (7) ERROR MESSAGES    |
| (2) CURRENT MODULE                   | (8) COORDINATE SYSTEM |
| (3) NUMBERING CONVENTIONS            | (9) LINE PRINTER FILE |
| (4) FLUX, FIELD, POTL, DELTA, STRESS | (10) DEFAULT MODES    |
| (5) SUBSET AND GROUPS                | (11) OLD NASCAP       |
| (6) AIDS                             | (12) COMPLAINTS       |
- (13) RETURN TO HISTOR

2

THE COMMANDS FOR MODULE 'HISTORY' ARE CELL NUMBERS. YOU CAN TYPE ONE CELL NUMBER, OR A STRING OF UP TO FIFTEEN NUMBERS ON THE SAME LINE. CONDUCTOR NUMBERS (NEGATIVE) ARE ALSO VALID. IF YOU HAVE A SET OF NUMBERS YOU PLAN TO USE MORE THAN ONCE, YOU CAN DEFINE THEM AS A GROUP USING 'SUBSET'.

YOUR OUTPUT WILL BE A TABLE AND/OR A GRAPH OF WHICHEVER ONE OF THE 5 QUANTITIES IS THE CURRENT MODE. NOTICE THAT THE 'HISTORY' MODES ARE DISTINCT FROM THE 'LATEST' MODES. IF YOU SPECIFY A RANGE OF CYCLES OR A RANGE OF TIMES, ONLY THOSE ONES WILL BE INCLUDED IN THE TABLE AND GRAPH. THE X AXIS OF THE GRAPH WILL BE THE TIME, THE LOG BASE 10 OF THE TIME, OR THE CYCLE NUMBER - DEPENDING ON WHETHER THE MODE IS 'LINEAR', 'LOG', OR 'NUMCYC'.

### HISTORY MODULE

MODES	COMMANDS
FLUX - FIELD - POTL	#
- DELTA - STRESS	#, #, #, ...
CYCLE # TO #	GROUP [GROUP NAME]
TIME # TO #	
TABLE - GRAPH - BOTH	
LINEAR - LOG - NUMCYCLE	

... PICK ANOTHER NUMBER -OR- TYPE 'MENU' TO SEE YOUR CHOICES  
-OR- <CR> TO RETURN TO HISTOR

HISTORY COMMAND OR MODE SET ?  
>LATEST  
LATEST COMMAND OR MODE SET ?  
>HELP

- HELP IS AT HAND - PICK A NUMBER,
- |                                      |                       |
|--------------------------------------|-----------------------|
| (1) BASIC USE                        | (7) ERROR MESSAGES    |
| (2) CURRENT MODULE                   | (8) COORDINATE SYSTEM |
| (3) NUMBERING CONVENTIONS            | (9) LINE PRINTER FILE |
| (4) FLUX, FIELD, POTL, DELTA, STRESS | (10) DEFAULT MODES    |
| (5) SUBSET AND GROUPS                | (11) OLD NASCAP       |
| (6) AIDS                             | (12) COMPLAINTS       |
- (13) RETURN TO LATEST

2

LATEST PRINTS INFORMATION ABOUT A GROUP OF CELLS AND CONDUCTORS. THE THREE COMMANDS ARE THREE WAYS TO SPECIFY A GROUP. 'ALL' WILL INCLUDE THE FULL SET OF CELLS AND CONDUCTORS. 'GROUP' FOLLOWED BY A GROUP NAME PRINTS ONLY THOSE IN THE USER-DEFINED GROUP. 'LIST' FOLLOWED BY TWO NUMBERS WILL LIST THE INTERVENING CELLS.

THE INFORMATION PRINTED CAN BE FLUX, FIELD, POTL, DELTA, OR STRESS.

IF THE MODE IS 'SEQUENTIAL' THE INFORMATION WILL BE ORDERED BY CELL NUMBER. IF 'MAGNITUDE', IT WILL BE ORDERED BY THE VALUES THAT ARE BEING PRINTED. FOR MODE 'ABSMAG', ORDERING IS BY ABSOLUTE VALUES.

### LATEST MODULE



----- MODES -----	----- COMMANDS -----
FLUX - FIELD - POTL	GROUP [GROUP NAME]
- DELTA - STRESS	LIST # TO #
SEQUENTIAL - MAGNITUDE	ALL
- ABSMAG	

... PICK ANOTHER NUMBER -OR- TYPE 'MENU' TO SEE YOUR CHOICES  
-OR- <CR> TO RETURN TO LATEST

LATEST COMMAND OR MODE SET ?  
>SINGLE  
SINGLE COMMAND OR MODE SET ?  
>HELP  
HELP IS AT HAND - PICK A NUMBER.

- |                                      |                       |
|--------------------------------------|-----------------------|
| (1) BASIC USE                        | (7) ERROR MESSAGES    |
| (2) CURRENT MODULE                   | (8) COORDINATE SYSTEM |
| (3) NUMBERING CONVENTIONS            | (9) LINE PRINTER FILE |
| (4) FLUX, FIELD, POTL, DELTA, STRESS | (10) DEFAULT MODES    |
| (5) SUBSET AND GROUPS                | (11) OLD NASCAP       |
| (6) AIDS                             | (12) COMPLAINTS       |
|                                      | (13) RETURN TO SINGLE |

2

-- SINGLE--

THIS MODULE GIVES VARIOUS INFORMATION ABOUT A SINGLE FLAT CELL OR BOOM CELL. THE ONLY COMMAND IS THE NUMBER OF A CELL.

MODES SPECIFY WHICH CELL PROPERTIES ARE TO BE PRINTED. IF YOU WANT ALL OF THEM, SET 'EVERYTHING'. TO WIPE THE SLATE CLEAN, TYPE 'NOTHING'. IF YOU WANT TO INCLUDE A CELL PROPERTY, TYPE 'ALSO' FOLLOWED ON THE SAME LINE BY THE PROPERTY NAME - FOR EXAMPLE 'ALSO POTL'. TO EXCLUDE A PROPERTY, TYPE 'NOT' AND THE PROPERTY NAME.

THE DYNAMIC PROPERTIES, WHICH CHANGE FROM ONE CYCLE TO THE NEXT, ARE 'FLUX', 'FIELD', 'POTL', 'DELTA', AND 'STRESS'.



2

-- SPECIAL --

THIS COULD BE CALLED MODULE MISCELLANEOUS.  
PRESENTLY, IT HAS ONLY TWO FUNCTIONS - PRINT  
CONTROL AND CYCLE RESETTING.

ALL PRINTOUT GOES BOTH TO THE TERMINAL AND TO FILE  
3. IF YOU ARE GENERATING A LOT OF PRINTOUT AND DON'T  
WANT TO WAIT FOR IT AT THE TERMINAL, USE MODE 'NOTERM'.  
THEN YOUR PRINTOUT WILL GO ONLY TO FILE 3, WHICH CAN BE  
SENT TO THE LINE PRINTER AT THE END OF TERMTALK.

YOU USE CYCLE RESET IF YOU ARE GOING TO MAKE  
FURTHER NASCAP RESTART RUNS, BUT HAVE NO FURTHER USE  
FOR THE DATA ALREADY GENERATED. IN 'SPECIAL' IF  
YOU TYPE 'CYCSET 0' ALL OLD DATA WILL BE DISCARDED  
FROM THE 'HISTORY' FILES. 'LATEST' AND 'SINGLE'  
WILL REMAIN UNCHANGED.

#### SPECIAL MODULE



---- MODES ----

---- COMMANDS ----

TERMT - NOTERM

CYCSET #

... PICK ANOTHER NUMBER -OR- TYPE 'MENU' TO SEE YOUR CHOICES  
-OR- <CR> TO RETURN TO SPECIA

SPECIAL COMMAND OR MODE SET ?  
>EXIT

## 5.2 MATCHG

Bulk conductivity currents and a facility to specify completely aligned fluxes have been added to MATCHG. Also, MATCHG now handles multiple maxwellian plasmas. These changes and two minor input-output changes are described here.

### 5.2.1 Bulk Conductivity

For insulating materials, MATCHG now includes the bulk conductivity current,  $J_{\text{con}}$ , in the calculation of the net flux:

$$J_{\text{con}} = - \left( \frac{\sigma}{d} \right) (V - V_0) = \sigma E \quad (5.1)$$

where  $\sigma$  is the bulk conductivity,  $d$  the material thickness,  $V$  the surface potential, and  $V_0$  the fixed potential of the conducting back plate underlying the insulator. MATCHG will now request the user to specify  $V_0$  for runs with insulating materials. The bulk conductivity current will be significant whenever  $(\sigma/d)$  is of comparable magnitude to  $(\partial J_{\text{net}}/\partial V)$ , where  $J_{\text{net}}$  is the net incident flux from the plasma or gun. Note that equilibrium potentials in MATCHG can now vary as the material thicknesses are changed. This new feature of MATCHG will allow a crude prediction of insulating surface potentials as a function of satellite ground potential.

### 5.2.2 Aligned Fluxes

MATCHG will now allow simulation of either an isotropic or a completely aligned incident particle distribution. For the isotropic case, the material collects current as would a part of a spherical probe. For the completely aligned case, the user will be asked to specify  $\theta$ , the angle of incidence with respect to the material surface normal ( $0^\circ \leq \theta < 90^\circ$ ;

default is  $\theta = 0^\circ$ ). The material will then collect current as could part of an infinite plane, i.e., for attracted particles,

$$J_{inc} = Ne \sqrt{\frac{kT}{2\pi m}} \cos\theta \quad (5.2)$$

where  $J_{inc}$  is the incident proton or electron flux,  $T$  the temperature, and  $N$ ,  $e$ , and  $m$  the particle density, charge, and mass respectively. Unlike the isotropic case, the planar collection model has no dependence on the surface potential for attracted particles. For repelled particles,  $J_{inc}$  is reduced by a factor  $e^{-|V|/kT}$ , as in the spherical case.

In the tank charging case, the flux is assumed completely aligned, and MATCHG will now always request the user to specify the angle of incidence,  $\theta$ . The incident flux will then be  $J_{inc} = J_0 \cos\theta$ , where  $J_0$  is the flux from the gun at normal incidence.

The formulation used to calculate electron backscatter in MATCHG is chosen to be consistent with the incident flux direction: an average over a  $\cos\theta$  distribution is used for isotropic fluxes, and the yield at a fixed angle  $\theta$  is calculated for aligned fluxes. If the 'ANGLE' secondary formulation is used, the above statement applies to proton and electron secondary yields as well. Use of the 'NORMAL' secondary formulation overrides these implicit choices and forces the secondary yield at normal incidence to be used irrespective of the incident flux direction. Note that the use of 'NORMAL' is somewhat inconsistent with an aligned flux at  $\theta \neq 0^\circ$ ; MATCHG will print a warning when this choice is made.

In summary, specification of the MATCHG flux formulation requires choice of incident flux type, incident flux direction, and secondary emission formulation, as indicated here:

A. INCIDENT FLUX TYPE	B. INCIDENT FLUX DIRECTION	C. SECONDARY EMISSION FORMULATION
TANK	ISOTROPIC	ANGLE
MAX (single Maxwellian)	ALIGNED	NORMAL
DBLMAX (double Maxwellian)		

All combinations of the descriptors in columns A, B, and C are allowed except that the TANK flux type is assumed to be aligned.

### 5.2.3 Emission Table

The table of selected emission values produced by MATCHG is now consistent with the emission formulations used in charging. For a given energy in the table, MATCHG calculates the yield at a fixed angle or averaged over a  $\cos\theta$  distribution, as described above. Previously, the yield at normal incidence had been given in the table irrespective of the formulation used during charging.

### 5.2.4 Initial Voltage

The latest version of MATCHG requests both the initial surface potential and the backing plate potential in keV, not eV.

### 5.2.5 Multiple Maxwellian Plasmas

MATCHG has been revised to accept ambient Maxwellian plasmas with up to five distinct electron and ion components. The new mode is activated by the keyword 'MLTMAX' during flux specification; MATCHG will then prompt the user for the number of components. Using 'MLTMAX' with one or two components is equivalent to the old 'MAX' or 'DBLMAX',

respectively. (The old keywords 'MAX' and 'DELMAX' have been retained, however.)

There are no default values for the third through fifth components of the Maxwellian description. The defaults for the first two components are now  $n_e = n_i = 1 \text{ cm}^{-3}$ ,  $T_{e1} = T_{i1} = 1 \text{ keV}$ ,  $T_{e2} = T_{i2} = 10 \text{ keV}$ .

### 5.3 WORKSHOP CODES

In preparation for the NASCAP workshops held at NASA/LERC, some special new codes were developed. These make use of some Univac features to simplify NASCAP running for the new user. The three codes are called FILES, OBJCHECK, and POTPLT.

To run NASCAP on a Univac, a user needs three input files (OPTIONS, OBJECT, and FLUX), as well as six scratch and restart files numbered 10, 15, 16, 17, 21, and 27. FILES will generate executive commands to assign, delete, or copy a complete set of these files.

OBJCHECK generates a three-dimensional picture of a satellite or test object. It uses the NASCAP shadowing routines, without invoking the rest of NASCAP. It is a diagnostic tool at object definition time.

POTPLT is a NASCAP post processor that produces potential contour plots. The user specifies for each plot the number of grids desired and the location of the plane where the contours are drawn.

#### 5.3.1 FILES

FILES will create or destroy a set of NASCAP files, or copy from one set into another set. A set of files is identified by a file prefix, from one to nine characters long. For example, if the user chose 'SCATHA' as a prefix,

the files would be named 'SCATHA10', 'SCATHA15', 'SCATHA21', and so on.

FILES is actually a set of three programs - FILES.ASSIGN (creation), FILES.DELETE (destruction), and FILES.COPY (copying).

The program asks for the prefix name, and it asks whether the files are to be public, private, or temporary. Public files are default. A private file can be referenced only by the person who created it. Temporary files disappear when you sign off the computer.

```
WELCOME TO ASSIGN ... THIS PROGRAM WILL ASSIGN
A SET OF NEW RESTART FILES FOR NASCAP
I NEED A FILE PREFIX, 1-9 CHARACTERS LONG, NO BLANKS
```

```
PREFIX PLEASE ?
JJC
```

```
THANK YOU
```

```
PUBLIC OR PRIVATE OR TEMPORARY?
```

```
Public
@ASG,PU JJC10 .
@ASG,PU JJC15 .
@ASG,PU JJC16,///1000 .
@ASG,PU JJC17 .
@ASG,PU JJC21 .
@ASG,PU JJC27 .
@ASG,PU JJC0BJ .
@ASG,PU JJCFLX .
@ASG,PU JJC0PT .
```

```
ALL 9 FILES SUCCESSFULLY ASSIGNED
```

Figure 5.2. An example of use of the FILES.ASSIGN program.

### 5.3.2 OBJCHECK

OBJCHECK allows the user to create an object and look at a 3-D picture of it, before worrying about running NASCAP itself. OBJCHECK produces material plots, building block plots, and hidden line surface cell plots.

Before defining the object, OBJCHECK asks for NZ, NG, XMESH, and the file prefix. NZ is the number of grid units in the Z direction. 33 is standard, but for a smaller grid, 29, 25, 21, or 17 are allowable inputs. NG is the number of nested grids necessary to hold the object, including booms. XMESH is the NASCAP zone size.

OBJCHECK then reads the '-OBJ.' file, where '-' represents the user supplied prefix. It echoes all input.

Finally it asks whether object illustration plots are desired. If so, it asks if you want material plots. Material plots are fairly time consuming, and are not needed in the early stages of object definition. The last input is the direction-of-view for the 3-D object illustration plots.

The directions-of-view are input as (X,Y,Z) vectors, not necessarily normalized. Permutations of plus or minus 1, 2, and 3 usually give good pictures. After you have as many views as you want, a carriage return will end the program. As a final task, OBJCHECK runs a few more tests on the object, having to do with cell connectivity.

@xqt objcheck.

ASGFIL: FILE 21

ISTAT= 100000000000

ASGFIL: FILE 17

ISTAT= 100000000000

ASGFIL: FILE 3

ISTAT= 100000000000

NZ>

33

NG>

2

XMESH>

.1

PREFIX PLEASE ?

jje

THANK YOU

ADDITIONAL OUTPUT WILL BE ON UNIT 3.

Input echoing omitted from figure.

Figure 5.3. Example of OBJCHECK use. Some printout has been omitted for brevity. Object definition read from JJCOBJ file.

```
403 VOLUME CELLS NUMBERED BY NUMLTB.  
GENERATE PLOT FILE?>  
yes  
MATERIAL PLOTS?>  
no
```

```
PERSPECTIVE PLOTS -- <CR> TO EXIT  
X>  
3  
Y>  
1  
Z>  
-2
```

```
FINAL NA1 = 199
```

```
PERSPECTIVE PLOTS -- <CR> TO EXIT  
X>  
-1  
Y>  
-2  
Z>  
3
```

```
FINAL NA1 = 186
```

```
PERSPECTIVE PLOTS -- <CR> TO EXIT  
X>
```

Figure 5.3. Continued. User selects directions-of-view.

CALLING GENMTL

INSLST -- 219 INSULATING SURFACE CELLS FOUND  
234 INCLUDING BOOM CELLS

SOLAR	HAS SURFACE RESISTIVITY OF	1.0+19 OHMS
WHITEN	HAS SURFACE RESISTIVITY OF	1.0+13 OHMS
KAPTON	HAS SURFACE RESISTIVITY OF	1.0+16 OHMS
ASTROD	HAS SURFACE RESISTIVITY OF	1.0+11 OHMS
TEFLON	HAS SURFACE RESISTIVITY OF	1.0+16 OHMS
BOOMAT	HAS SURFACE RESISTIVITY OF	1.0+11 OHMS

FNDSCE -- 493 SURFACE CONDUCTING EDGES FOUND

BOOMEJ -- 526 EDGES FOUND

1116 ENTRIES IN REVISED VTXL

NC DETERMINED BY GETNC TO BE 4  
END GENMTL

[EXIT]

Figure 5.3. Concluded. Checking cell connectivity.

### 5.3.3 POTPLT

POTPLT produces the same type of potential contour as NASCAP. The difference is that with NASCAP, you have to decide before each timestep which contour views you want to see. With POTPLT, you can choose a view, look at it, then go back and produce some more views, without running NASCAP again.

The user can have the plane of view perpendicular to the X, Y, or Z axis, located at any node point. Each picture can include anywhere from one grid up to the complete computational space.

POTPLT first asks for the file prefix. It then gives the options of smoothed contour lines (as opposed to quick, rougher lines) and of absolute, 1 to 33, coordinates (as opposed to centered, -16 to +16 coordinates). A carriage return will bypass these.

For each picture the user specifies number of grids, view direction, cut value, and number of contours. The number of grids can be from 1 to NG, the total number of computational grids. The view direction is X, Y, or Z, and is perpendicular to the contour plane. So if Y is the view direction, contours are drawn in the X-Z plane. The cut value determines where the contour plane will cut through computational space. The number of contours is set to a default of approximately 20. You may choose more or less.

After all desired views are generated, respond to the 'GRIDS TO PLOT <EXIT>' question with a carriage return to end the program.

PREFIX PLEASE ?  
JJc

THANK YOU

TYPE 'SMOOTH' FOR SLOW DRAWING, SMOOTH CONTOURS  
TYPE 'POSITIVE' FOR POSITIVE COORDINATES (1-33)  
<CR> FOR DEFAULT - ROUGH AND CENTERED

FAST CONTOURS WILL BE DRAWN  
CENTERED COORDINATES (-16 TO +16)  
GRIDS TO PLOT [EXIT]>

1  
DIRECTION>  
Z  
CUT VALUE [0] >  
3  
HOW MANY CONTOURS? [20] >

GRIDS TO PLOT [EXIT]>  
2  
DIRECTION>  
X  
CUT VALUE [0] >  
-4  
HOW MANY CONTOURS? [20] >  
10  
GRIDS TO PLOT [EXIT]>

YOU HAVE CREATED 4 FRAMES OF MICROFILM  
[EXIT]

Figure 5.4. Example of FOTPLT use. User generated two contour planes, at  $Z = 3$  and at  $X = -4$ .

## 6. PRELIMINARY LOW EARTH ORBIT (LEO) MODEL

This section describes development of a preliminary version of NASCAP designed to simulate charging response of high voltage satellites in low earth orbit. During magnetospheric substorms at GEO, typical plasma densities and temperatures are  $1 \text{ cm}^{-3}$  and 10 keV, respectively, so that the plasma Debye length is on the order of several hundred meters. For satellites whose characteristic dimensions are a few meters, current collection is orbit limited, and spherical probe formulations can be used. Furthermore, the charge stored on the satellite surface is much larger than the ambient space charge, so that plasma screening can be neglected or approximated by linear screening expressions. The original NASCAP code made use of these approximations to simulate charging response at GEO. In LEO, the plasma is much denser, typically  $10^5 \text{ cm}^{-3}$ , and characterized by a lower temperature, say 1 eV. Debye lengths are on the order of 1 cm, and the orbit limited current collection approximations and linear screening expressions are invalid. Therefore, the NASCAP/LEO code required the development of sheath limited current collection algorithms as well as solutions to the Poisson problem for the case of highly nonlinear ambient screening.

A detailed description of the physical models and computational techniques of the NASCAP/LEO code is contained in a paper presented at the AIAA Aerospace Sciences Meeting, January 1980, included in this report as Section 6.4. This paper includes a simulation of the experiments performed by Konradi and McCoy at the Johnson Space Center. [6] The results indicate that ion focusing observed in the laboratory during high voltage collection experiments is probably due to voltage gradients on the collecting surfaces.

Very large ( $\sim 100$ - $1000$  m) spacecraft which have high voltage solar arrays are now in the design phase. NASCAP/LEO includes a fine resolution mode which allows the current collection on a periodically continued voltage pattern for a large object to be treated with high resolution. This mode has been used to study the effects of solar voltage array patterns on plasma power losses; our preliminary calculations suggest that plasma power loss should not be a primary consideration in designing the physical arrangement of high voltage arrays. These results have been published in IEEE Transactions on Nuclear Science, Volume NS-27, No. 6, December 1980, and the paper is reprinted in Section 6.3.

Section 6.1 describes calculations comparing NASCAP/LEO results to Langmuir probe theory as a simple validation of the code. NASCAP/LEO is currently in a very preliminary form, and many of the features available in the original NASCAP code have yet to be implemented. Section 6.2 assesses the status of the code by describing the principle restrictions.

#### 6.1 LANGMUIR PROBE THEORY COMPARISON

As a validation of the NASCAP/LEO code, current collection to a simple object has been calculated for various values of the object potential and plasma Debye length. The results are compared to the exact numerical calculations for a spherical probe as given by Laframboise.<sup>[7]</sup>

The object used in the calculations was a cube with 1.8 m edges; the zone size was 0.3 m. Plasma temperature was 1 eV in all cases, and the sheath boundary was defined to be at a potential of 0.1 volt. The object voltage was 10 or 20 volts, and the Debye length was varied from 1 to 100 cm. The results are given in Table 6.1.

TABLE 6.1. LANGMUIR PROBE THEORY COMPARISON

$\lambda_D$ (cm)	$V = 10$ Volts		$V = 20$ Volts	
100	15.7	(9.6)	19.7	(17.1)
10	3.1	(3.8)	3.8	(4.9)
1	2.7	(1.9)	3.1	(2.0)

Ratio of collected current to thermal current calculated using NASCAP/LEO for various values of  $\lambda_D$  (Debye length) and probe voltage. Numbers in parentheses are for a spherical probe as calculated in Reference 7.

The agreement between NASCAP/LEO calculated values and the spherical probe results is good. The effective radius of the cubical object employed in the calculations is 1.24 m. The ratio of object radius to electron Debye length therefore ranges from 1.24 to 124 in these calculations, covering the entire range explored by Laframboise. The results are somewhat sensitive to the potential value used to define the sheath boundary. Collected current varies logarithmically with the sheath boundary potential; a decade change in the boundary potential changes the current by  $\pm 50$  percent. The agreement with the probe theory results is within 50 percent in all cases, even though the code resolution is three times the Debye length in the  $\lambda_D = 10$  cm case. The cases considered for comparison here were chosen to match the parameter ranges reported by Laframboise.<sup>[7]</sup> The agreement would certainly be better if the comparison had been made for a higher object potential, where the physical models in NASCAP/LEO are more nearly exact. Given the uncertainty associated with comparison of calculations for a cubical object to a perfect sphere, and considering the large zone size, these results provide an excellent validation of the nonlinear screening and current collection algorithms in NASCAP/LEO.

## 6.2 NASCAP/LEO LIMITATIONS

The present version of the NASCAP/LEO code is intended as a preliminary version only. Considerable development will be required to bring the code to a state of development similar to that of the present NASCAP code itself. The calculations described represent the full range of capabilities of the NASCAP/LEO code.

The limitations and restrictions on the preliminary NASCAP/LEO model include the following:

Object Definition. Only objects composed of complete cubes are allowed. Booms, flat plates, wedges, tetrahedra, and truncated cubes are not provided for.

Material Properties: Provision for material parameters has not yet been included. Secondary emission, photoemission, conductivity effects, etc. are therefore not implemented. This restriction effectively limits objects to those consisting of surfaces at fixed potentials.

Time Dependence: Only the equilibrium solution is calculated. Time dependent charging effects are not simulated.

Object Potentials: Floating potentials are not implemented.

Code Flexibility: The preliminary version of NASCAP/LEO is not yet a user-oriented code in the style of NASCAP. The code presently exists in three distinct sections: object definition, potential solution, and current collection. These sections are executed sequentially, and the user must monitor the progress of the results to be sure that proper convergence is attained.

6.3 THE EFFECT OF SOLAR ARRAY VOLTAGE PATTERNS ON  
PLASMA POWER LOSSES

This is the paper published in IEEE Transactions on  
Nuclear Science, Volume NS-27, No. 6, December 1980.

THE EFFECT OF SOLAR ARRAY VOLTAGE PATTERNS  
ON PLASMA POWER LOSSES\*M. J. Mandell, I. Katz, P. G. Steen, G. W. Schnuelle  
Systems, Science and Software  
P. O. Box 1620, La Jolla, CA 92038Introduction

There has been considerable interest recently in using high voltage solar arrays in space. The primary reason is that as power requirements increase, cables and DC to DC converters become significant weight factors in satellite design. A principal difficulty in using high voltages in Low Earth Orbit (LEO), or with a Solar Electric Propulsion Stage (SEPS), is the draining of array power by currents flowing between exposed surfaces through the surrounding plasma. This plasma may be of natural origin (as in LEO), or generated by the spacecraft (for SEPS). Early studies by Kennerud<sup>1</sup> have shown that small pinholes in insulation can make almost perfectly insulated solar arrays collect current from the surrounding plasma as effectively as bare metal plates. Therefore, simply insulating exposed high voltage areas may not prevent substantial power losses.

Experimental<sup>2</sup> and theoretical<sup>3</sup> studies have analyzed plasma-array interactions for cases in which the potential variation was on the scale of the dimensions of the test object. For some cases, the magnitude of the power loss would prohibit the system from functioning. It has been suggested, however, that the power loss might be reduced by arranging solar cell strings in repeated small-area modules to eliminate any large areas at high potentials. Since the sheath height and area increase with the surface potential, smaller sheath voltages might reduce total power losses. In this paper, the effect of this suggestion is examined both analytically and with the use of a new, nonlinear plasma sheath simulation code. The results indicate that small repeated voltage patterns are of marginal utility in reducing power loss to the surrounding plasma.

Theory

The analysis presented is valid for plasma current collection by surfaces at high voltages. We define high voltages,  $\phi$ , to be voltages such that the associated electron potentials,  $e\phi$ , are much greater than their thermal kinetic energy,  $k\theta$ :

$$e\phi \gg k\theta \quad (1)$$

There are three length scales of concern: the object size,  $L$ , the characteristic length for potential variation,  $\ell$ , and the plasma Debye length,  $\lambda$ . We require that  $\lambda$  be less than the typical object size,  $L$ :

$$\lambda < L \quad (2)$$

This clearly places us in the space-charge-limited regime.

\* This work supported by NASA/Lewis Research Center, Cleveland, OH, and Air Force Geophysics Laboratory, Hanscom AFB, MA, under Contract NAS3-21762.

In the limit of very small Debye length and very high voltages, a quasi-one-dimensional sheath forms in front of the collecting surface. The current through this sheath is the one-sided thermal current,  $J$ :

$$J = n_0 e \left( \frac{k\theta}{2\pi m} \right)^{1/2} \quad (3)$$

To find the current structure within the sheath requires calculating particle trajectories and solving Poisson's equation in a mutually consistent fashion. It is far more convenient to approximate the space charge density,  $\rho$ , as a function of potential,  $\phi$ , only. The most common such approximation (linear, Debye screening), valid for  $\phi < \theta$ , is

$$\rho(\phi) = -\epsilon_0 \phi / \lambda^2; \quad \lambda^2 = \frac{\epsilon_0 k\theta}{ne^2} \quad (4)$$

Another useful expression (thin sheath approximation) is valid for  $\phi \gg \theta$  and locally one-dimensional geometry. Requiring the current to remain constant at the value given by Equation (3) yields

$$\rho(\phi) = J/v = -n_0 e \left( \frac{k\theta}{4\pi e\phi} \right)^{1/2} \quad (5)$$

This expression leads to a nonlinear Poisson equation, as discussed below.

The power loss for an object whose potential varies from 0 to  $V_{\max}$  is given by

$$P = (\eta JA) (vV_{\max}) \quad (6)$$

where  $A$  is the area of the sheath boundary,  $\eta$  is the fraction of charged particles entering the sheath that strike the object, and  $vV_{\max}$  is the mean potential at which they strike. We would expect  $v$  to depend primarily on  $\ell$  and  $\lambda$ , while  $A$  and  $\eta$  depend primarily on  $L$  and  $\lambda$ . If the screening is nonlinear,  $A$  and  $v$  will both depend on  $V_{\max}/\theta$ . The parameter  $\eta$  will usually be near unity.

Calculations

The complete self-consistent set of electron kinetic equations and Poisson's equation are formidable to solve in all but the simplest cases. Instead we examine here two different simplifications which enable us to analyze the dependence of the mean collection potential on system parameters.

Harmonic Potential with Linear Screening

A readily solved case is a large plane with potential

$$V(x,0) = \frac{1}{2} V_{\max} (1 + \sin \kappa x) \quad (7)$$

where  $\kappa L \gg 1$ . If we replace Poisson's equation with a Helmholtz equation

$$(\nabla^2 - \lambda^{-2}) V(x,z) = 0 \quad (8)$$

we find

$$V(x,z) = \frac{1}{2} V_{\max} \left( \sin \kappa x e^{-\kappa_1 z} + e^{-z/\lambda} \right) \quad (9)$$

where  $\kappa_1^2 = \kappa^2 + \lambda^{-2}$ . The function  $v(\kappa\lambda)$ , obtained by numerically calculating particle trajectories, is shown in Figure 1. This function has a maximum for  $\kappa\lambda \sim 1$ . The total variation in  $v$  is from  $\sim 0.50$  for small  $\lambda$  to  $\sim 0.65$  at maximum. This would indicate that variations in panel design result in at most a 30 percent variation in power loss. For  $\kappa\lambda \gg 1$ , particle deflections are small because the transverse fields are encountered at high energy. For  $\kappa\lambda \ll 1$ , particle deflections vanish with the sheath thickness.

### Three-Dimensional Array with Nonlinear Screening

To make a more realistic estimate of the plasma loss, a better formulation of the plasma screening is necessary as well as a three-dimensional treatment of the problem. For cases in which  $V_{\max} \gg \theta$ , a better approximation for Poisson's equation than the Helmholtz equation (8) is<sup>3</sup>

$$\nabla^2 \phi = \frac{\phi}{\lambda^2} \left[ 1 + \sqrt{4\pi} (e\phi/\kappa\theta)^{3/2} \right]^{-1} \quad (10)$$

This formulation reduces to Equation (4) for low potentials and to Equation (5) for high potentials. The Low Earth Orbit (LEO) code<sup>3</sup> is designed to calculate current collection using space potentials obtained by solving Equation (10).

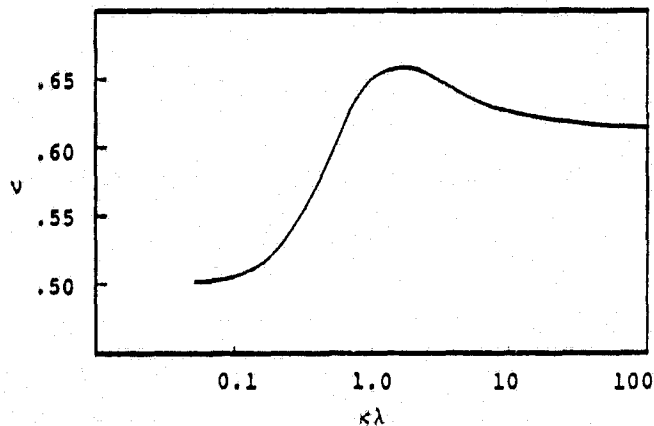


Figure 1. Effective voltage factor,  $v$ , for sine wave potential [Equation 7] as a function of screening length.

The LEO code also has an expanded resolution mode which may be used to calculate  $v$  for a finally-resolved periodic surface region.

In our previous work<sup>3</sup> we calculated the sheath structure and power loss for a simulated solar array intended to represent the experiments of McCoy and Konradi.<sup>3</sup> The model (Figure 2) consisted of a panel 8.7 m long and 1.8 m wide, with a 1.2 m wide high voltage current collecting strip along its length. Of the several cases previously considered, we will focus on the "linear," high-voltage case, in which the strip was linearly biased 4800 volts from end to end, and on the comparable "uniform" case in which the strip was uniformly 2400 volts. The results are shown in Table I for plasma temperature  $\theta = 1$  eV and Debye length  $\lambda = 10^{-2}$  or  $10^{-3}$  meters. (The power loss has been normalized to the plasma thermal current ( $\sim 10^{-4}$  or  $10^{-2}$  A/m<sup>2</sup> for an oxygen plasma with the respective Debye lengths).

We wish to compare the power loss from the "linear" array with that from a "modular" array in which the 0 - 4800 volt potentials are contained in 30-cm-square modules (Figure 3). It is assumed that the gross structure of the sheath is the same as that for the "uniform" array at the average potential. To determine the change in sheath structure near the surface, we used the expanded resolution (.01875 m zones) periodic version of the LEO code. This was done for two different module patterns (Figure 3). The results are given in Table II. The power losses are calculated by first doubling the results of cases III and IV of Table I (since  $V_{\max}$  increases from 2400 volts to 4800 volts), and then multiplying by  $v_{\text{expanded}}$ . The resultant losses are virtually identical to the linear cases. Note that, when the bracketed factor of Equation (10) is taken into account, we are, for these parameters, in the region  $\kappa\lambda > 1$  of Figure 1. Thus making the pattern finer will reduce  $v_{\text{expanded}}$  to a limit of about 0.6.

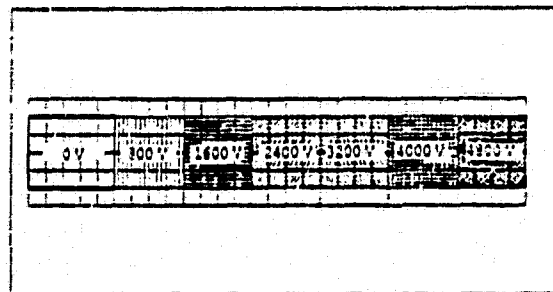


Figure 2. "Linear" array test object, indicating bias potentials. The labeled portions represent a conductive strip, while the border, sides, and back are insulating plastic. For the "uniform" test object, the entire conductive strip is at 2400 volts.

Table I. Power Loss Parameters

Case	Potential	$\lambda$ (m)	$n$	A(m <sup>2</sup> )	$v$	P/J kw-m <sup>2</sup> /amp
I	0-4800V (linear)	0.01	1.0	80.7	.6935	269
II	0-4800V (linear)	0.001	1.0	44.4	.6675	142
III	2400V (uniform)	0.01	1.0	92.1	.9758	216
IV	2400V (uniform)	0.001	1.0	48.3	.9739	113

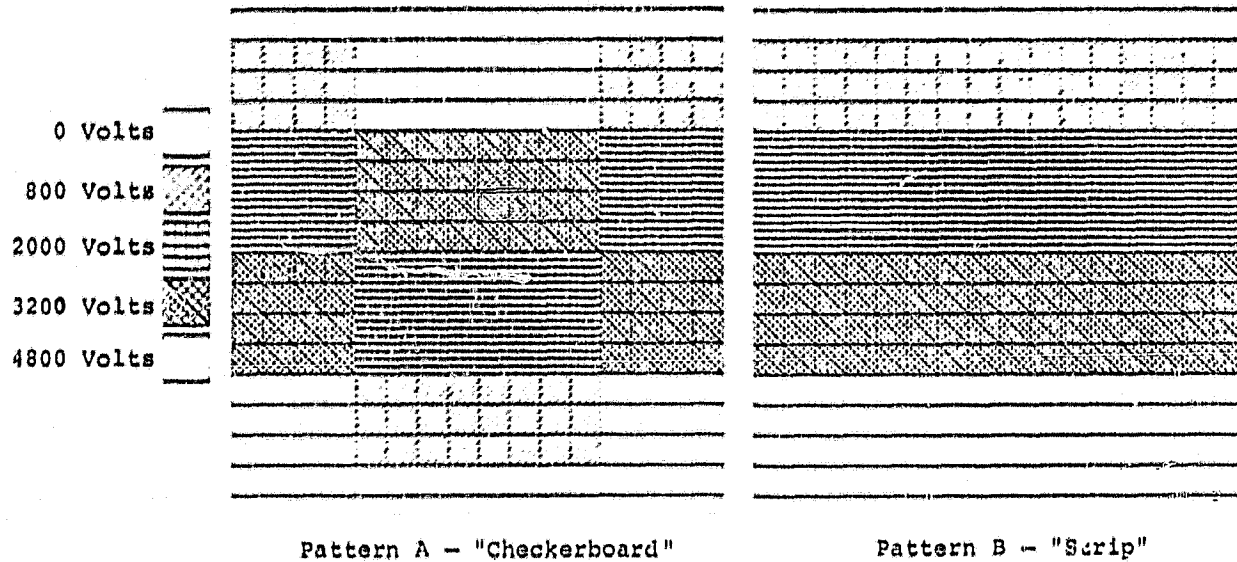


Figure 3. Voltage patterns for module high voltage array power loss calculations. Each pattern represents a 30-cm square module.

Table II. Power Loss Parameters - Expanded Resolution for Modular Cases

Pattern	$\lambda$ (m)	$v_{expanded}$	P/J (kw-m <sup>2</sup> /amp) <sup>+</sup>
A (Checkerboard)	0.01	.6210	268
A (Checkerboard)	0.001	.6278	142
B (Strip)	0.01	.6052	261
B (Strip)	0.001	.6464	146

<sup>+</sup> Calculated from Equation (6) with  $v$  given by  $v$  from Table I times  $v_{expanded}$  from this Table.

### Conclusions

These calculations indicate that the difference in power loss between modular and linear patterned high-voltage arrays is fairly small. While the use of modular patterns can reduce the effective mean potential by 10 percent, for the type of configuration considered here we also have a 10 percent increase in sheath area, leading to only a few percent change in total power loss. Correct comparison of the relative power losses in the linear and modular cases requires use of the expanded resolution code. Comparison based on Table I alone incorrectly predicts a reduced power loss for the modular arrangement.

These preliminary calculations suggest that plasma power loss should not be a primary consideration in designing the physical arrangement of high voltage arrays.

### References

1. Kennerud, K. L., "High Voltage Solar Array Experiments," NASA CR-12180 (1974).
2. McCoy, James E., and A. Konradi, "Sheath Effects Observed on a 10 Meter High Voltage Panel in Simulated Low Earth Orbit Plasma," Spacecraft Charging Technology-1978, p. 315, NASA Conference Publication 2071, AFGL-TR-78-0082 (1979).
3. Katz, I., M. J. Mandell, G. W. Schnuelle, D. E. Parks, and P. G. Steen, "Plasma Collection by High Voltage Spacecraft at Low Earth Orbit," AIAA 18th Aerospace Sciences Meeting, AIAA-80-0042 (1980).

**6.4 PLASMA COLLECTION BY HIGH VOLTAGE SPACECRAFT AT LOW EARTH ORBIT**

This is a reproduction of a paper presented at the AIAA 18th Aerospace Sciences Meeting, Pasadena, CA, July 14-16, 1980.

# PLASMA COLLECTION BY HIGH VOLTAGE SPACECRAFT AT LOW EARTH ORBIT

I. Katz,\* M. J. Mandell,\*\* G. W. Schnuelle,\*\* D. E. Parks,† P. G. Steent‡  
Systems, Science and Software  
La Jolla, California 92038

## Abstract

A computer model of the three-dimensional sheath formation and plasma current collection by high voltage spacecraft has been developed. By using new space charge density and plasma collection algorithms, it is practical to perform calculations for large, complex spacecraft. The model uses NASCAP compatible objects and geometries. Results indicate that ion focusing observed in the laboratory during high voltage collection experiments is probably due to voltage gradients on the collecting surfaces.

## Nomenclature

D	Renormalized screening length
e	Electron charge
I	Total collection current
$j_0$	One-sided electron (ion) thermal current
k	Boltzmann constant
L	Object dimension; computational mesh constant
$\mathcal{Z}_I$	Variational function for $\phi_I$
m	Electron (ion) mass
$n_0$	Ambient plasma density
r	General space point
$\bar{T}$	Renormalized plasma temperature
V	Particle velocity
$V_0$	Particle thermal velocity
x	Distance from sheath edge
$\hat{c}$	Functional derivative operator
$\epsilon_0$	Permittivity of free space
$\theta$	Plasma temperature
$\lambda_D$	Debye (screening) length
$\rho$	Space charge density
$\rho'$	Derivative of space charge function with respect to potential
$\phi$	Electrostatic potential
$\phi_I$	Solution to Ith linearized Poisson equation
$\phi_{Ij}$	jth iterate of solution for $\phi_I$

## I. Introduction

As satellite electrical power requirements increase, there is constant effort to increase operating voltages on solar arrays. The prime driver is weight reduction in both power cables and elimination of DC to DC converters used to supply high voltages to high power microwave tubes or ion thrusters. One of the primary difficulties associated with high voltages on satellites in low earth orbit is the power drain due to leakage currents flowing between exposed surfaces through the ambient

plasma. Early studies by Kennerud<sup>1</sup> have shown that small pinholes in insulation can make almost perfectly insulated solar arrays couple to an ambient plasma as effectively as bare metal plates. Thus just covering exposed high voltages may not be an adequate solution.

In order to predict parasitic losses due to surrounding plasma, some simple models of plasma collection have been devised. These include models for current collection from other plasmas, such as ion engine efflux<sup>2,3</sup> and simple models designed for LEO.<sup>4,5</sup> Recently large scale experiments have been performed in the thermal vacuum test chamber at NASA Johnson Space Center to simulate collection in LEO by a large (1 m x 10 m) solar array.<sup>4</sup>

The purpose of this paper is to introduce a new three-dimensional computer model, NASCAP/LEO, which is designed to calculate plasma leakage currents. We will present the physical arguments that led to the model followed by a brief description of the numerical techniques employed. We will then show results of applying this model to the NASA/JSC experiments of McCoy and Konradi.<sup>4</sup> These simulations reproduced the observed ion focusing phenomenon.

## II. Theory

We develop here a simplified nonlinear screening model for electric potentials and plasma structure surrounding an object with exposed high voltage surfaces. We define high voltages,  $\phi$ , by requiring that the potential energy associated with the voltage,  $e\phi$ , be much larger than the plasma thermal energy,  $\theta$ :

$$e\phi \gg k\theta.$$

We also require that the Debye length,  $\lambda_D$ , of the plasma be less than, or at most comparable to, typical object dimensions, L:

$$\lambda_D \lesssim L.$$

This clearly places us in the space charge limited collection regime.

In the limit of very small Debye length and very high voltages a quasi-one-dimensional sheath forms in front of the collecting surface. The current in the sheath is the one-sided random thermal current:

$$j_0 = n_0 e (k\theta/2\pi m)^{1/2}. \quad (1)$$

\*Program Manager, \*\*Research Scientist, †Senior Research Scientist, ‡Junior Research Scientist.

The velocity within the sheath is

$$\frac{1}{2} m v^2 = \frac{1}{2} m v_0^2 + e\phi(z) \quad (2)$$

where

$$v_0 = (k\theta/2\pi m)^{1/2} \quad (3)$$

and the charge density is

$$\rho = -\frac{j_0}{v} \quad (4)$$

For  $e\phi \gg k\theta$  this reduces to

$$\rho \rightarrow -n_0 e (k\theta/4\pi e\phi)^{1/2} \quad (e\phi \gg k\theta) \quad (5)$$

When the voltage drops down near the plasma potential the charge density is determined by the exclusion of oppositely charged particles and a Debye screening expression is valid:

$$\frac{\rho}{\epsilon_0} + \frac{-\phi}{\lambda_D^2}; \quad \lambda_D^2 = \frac{\epsilon_0 k\theta}{n_0 e^2} \quad (e\phi < k\theta) \quad (6)$$

Laframboise and Parker have shown that this expression is valid at very small potentials even for collisionless plasmas.<sup>6</sup> Since the space charge limited potentials have a  $x^{4/3}$  form and the electric field has an  $x^{1/3}$  dependence, then half the screening of the field is accomplished in the first one-eighth of the sheath. If object dimensions are large or comparable to sheath dimensions, then the one-dimensional charge density formulation can be used as an effective nonlinear screening to determine sheath potential contours.

Combining the low and high potential expressions we can construct a single analytical formula which is a function of only the local potential and depends parametrically on the neutral plasma temperature and density:

$$\frac{\rho(\phi)}{\epsilon_0} \approx -\frac{\phi}{\lambda_D^2} \left[ 1 + \sqrt{4\pi} (e\phi/k\theta)^{3/2} \right]^{-1} \quad (7)$$

This expression has the properties of going to the low potential Debye shielding limit (equation 6) when  $e\phi \ll k\theta$ , and to equation (5) for  $e\phi \gg k\theta$ . The advantages of this expression over a particle tracking formulation for obtaining charge densities are overwhelming. Statistical and numerical difficulties preclude the direct approach for all but the very simplest problems. Using the screening formulation presented here reduces the complex Poisson-Vlasov sheath problem to a nonlinear equation which for small potentials is Helmholtz in character:

$$\epsilon_0 \nabla^2 \phi + \rho(\phi) = 0 \quad (8)$$

We then use these potentials surrounding an object to define an approximate sheath boundary. Typically we define the sheath to be the equipotential surface  $\phi = k\theta/e$ .

The sheath current density at the sheath boundary is the plasma thermal current. Thus the total current collected is

$$I = \int_{\text{sheath boundary}} j_0 \, dS \\ = j_0 \times \text{Area}_{\text{sheath}} \quad (9)$$

The distribution of currents on the spacecraft is found by the forward pushing of representative particles from the sheath boundary until they impinge upon the satellite. The particles start out with thermal velocity normal to the local sheath surface and are accelerated by the sheath electric fields. By integrating the product of the collected current and the local surface potential the power drain can be computed.

The nonlinear screening model can be made more accurate by modifying the shielding due to focusing effects. The particle tracking algorithms can calculate local enhancement of charge density due to the convergence of sheath particles. These terms can be used to modify the screening iteratively to reach a self-consistent solution. The final results then would be accurate for all ratios of object dimensions to sheath lengths.

### III. Code Implementation

The implementation of the above ideas has been performed using the basic techniques developed for the standard NASCAP code.<sup>7-9</sup> Calculations proceed in four phases: (A) Object definition; (B) Solution of the nonlinear Poisson equation (equation 8); (C) Determination of the sheath boundary and its area; and (D) Particle tracking to determine the current distribution on the test object.

#### A. Object Definition

Objects for NASCAP/LEO are defined using the standard NASCAP code. This takes advantage of the simple input and powerful graphics developed for NASCAP. However, the preliminary version of NASCAP/LEO does not handle the full generality of NASCAP-defined objects.

#### B. Nonlinear Potential Solution

The nonlinear Poisson equation (equation 8) is solved iteratively by successive linearization (a multidimensional Newton-Raphson method). The linearized form of equation (8) is

$$-\epsilon_0 \nabla^2 \phi_I - \rho(\phi_{I-1}) - (\phi_I - \phi_{I-1}) \rho'(\phi_{I-1}) = 0 \quad (10a)$$

or

$$-\epsilon_0 \nabla^2 \phi_I - \phi_I \rho'(\phi_{I-1}) = \rho(\phi_{I-1}) - \phi_{I-1} \rho'(\phi_{I-1}) \quad (10b)$$

where  $\rho'$  denotes  $(\partial\rho/\partial\phi)$ , and  $\phi_I$  denotes the  $I$ th "major" iterate of the solution. The linear equation (10b) is solved iteratively (leading to a sequence of "minor" iterates  $\phi_{Ij}$ ) using (as in NASCAP) a finite element, scaled conjugate gradient method with provision for multiple nested grids with compatible boundary elements.

The finite element formulation for (10b) is derived from the variational principle

$$\frac{\delta}{\delta\phi_I} \int d^3r \mathcal{L}_I(\underline{r}) = 0 \quad (11a)$$

with

$$\mathcal{L}_I(\underline{r}) = \frac{\epsilon_0}{2} |\nabla\phi_I|^2 - \frac{1}{2} \rho'(\phi_{I-1}) \phi_I^2 - \phi_I [\rho(\phi_{I-1}) - \phi_{I-1} \rho'(\phi_{I-1})] \quad (11b)$$

Two points should be made concerning equations (11). First, since equation (7) is non-monotonic,  $\rho'$  can be positive, leading to a non-positive definite set of equations. We have found it satisfactory to circumvent this problem by making the replacement

$$\rho'(\phi_{I-1}) \rightarrow \max[0, \rho'(\phi_{I-1})] \quad (11c)$$

in (11b). Alternatively, a method<sup>10</sup> designed to handle non-positive-definite problems might be adopted.

Second, if  $\rho'$  is too far negative so that the second term of (11b) dominates the first, the solution of equations (11) is an unphysical oscillatory potential. This takes place for  $\lambda_D < 0.7 L$ , where  $L$  is the local mesh spacing. These oscillations are eliminated by replacing (7) by a formula which has the same values for large  $\phi$ , but no more screening than the code can resolve at small  $\phi$ :

$$\frac{\rho(\phi)}{\epsilon_0} = -\frac{\phi}{D^2} \left[ 1 + (\phi/T)^{3/2} \right]^{-1} \quad (12a)$$

where

$$D = \max(\lambda_D, 0.7 L) \quad (12b)$$

and

$$T = \left( \frac{k\theta}{e} \right) (4\pi)^{-1/3} \left( \frac{D}{\lambda_D} \right)^{4/3} \quad (12c)$$

For the typical case  $T \gg k\theta/e$ , the

modified screening should be compensated for by defining the sheath boundary to be at some potential intermediate between  $\theta$  and  $T$ .

For the sample calculations discussed below, approximately 3-5 minutes of UNIVAC 1100/81 time were required for solution to equation (8).

### C. Sheath Boundary Determination

The sheath boundary is determined by a set of routines which examine each finite element for the presence of a user-specified sheath boundary potential contour. The three-dimensional sheath contour is approximated in each selected element by a collection of contiguous triangles. The entire set of neighboring triangles defines the sheath boundary together with its area, and thus the net current collected.

### D. Particle Tracking

Particle trajectories are followed by forward tracking from the centroid of each sheath boundary triangle. Each particle is given an initial current which is proportional to the local ambient flux and to the area of the triangle, an initial kinetic energy equal to a user-specified value, and an initial direction antiparallel to the local E-field (for electrons). The particle tracking is performed using Boris' second-order leapfrog scheme<sup>11</sup> with a dynamically adjustable timestep. Provisions are included for magnetic field effects on particle motions. The actual particle tracking routines of NASCAP/LEO are straightforward adaptations of the NASCAP emitter particle tracking subroutines.

## IV. Sample Calculations

To illustrate the capabilities of NASCAP/LEO we studied a system similar to one used in experiments by McCoy and Konradi.<sup>4</sup> The system consisted of an object  $8.7 \times 1.8 \times 0.3$  meters with  $1.2 \times 1.2$  meter patches which can be biased on one surface (Fig. 1). This is intended

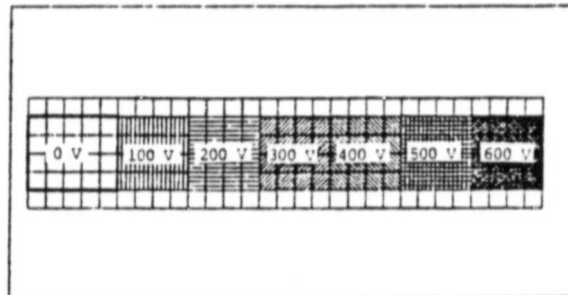


Fig. 1 Test object for sample calculations. The labeled portions represent a conductive strip, while the border, sides, and back are insulating plastic. Biasing indicated is for case (d).

to represent a plastic sheet with a conducting metal strip. The total area was  $37.6 \text{ m}^2$  and the metal area was  $10.4 \text{ m}^2$ . It was modeled with  $0.3 \text{ m}$  resolution in a volume  $9.6 \times 9.6 \times 19.2$  meters, filled with  $2.3 \text{ eV}$  plasma with density  $1.3 \times 10^6 \text{ cm}^{-3}$ , and thus a Debye length of  $1 \text{ cm}$  and one-sided electron thermal current of  $53 \text{ mA/m}^2$ .

All simulations were done in positive bias (electron-collecting) mode. Similar results would be obtained for negative (ion collecting) objects, with currents reduced by the square root of the mass ratio. Seven test cases are shown here:

- (a) entire object at  $+100 \text{ V}$ .
- (b) entire object at  $+2400 \text{ V}$ .
- (c) plastic at ground, metal at  $+2400 \text{ V}$ .
- (d) plastic at ground, metal biased as indicated in Fig. 1.
- (e) same as (d), but with potentials doubled ( $V_{\text{max}} = 1200 \text{ V}$ ).
- (f) same as (d), but with potentials quadrupled ( $V_{\text{max}} = 2400 \text{ V}$ ).
- (g) same as (d), but with potentials octupled ( $V_{\text{max}} = 4800 \text{ V}$ ).

The sheaths for cases (a) and (b) are illustrated in Fig. 2. For the  $100 \text{ V}$  case the sheath area was  $69 \text{ m}^2$ , and for the  $2400 \text{ V}$  case (b) the sheath area was  $258 \text{ m}^2$ , leading to collection currents of  $3.66$  and  $13.7$  amperes respectively.

In the actual experiment the object was not at uniform potential, but rather the insulating plastic collected sufficient current to remain near plasma ground. This was the motivation for cases (c)-(g), which provided more interesting potential contours and particle trajectories.

The sheath for case (c) is shown in Fig. 3. It is apparent that the sheath spills over the ends and sides to substantially enhance the current collection. The sheath area for this case was  $92 \text{ m}^2$ , giving a current of  $4.9$  amperes. Note also the electrostatic focusing indicated by the x-y cross-section of the particle trajectories, tending to concentrate the current near the center of the strip.

The sheaths for cases (d)-(g) are shown in Figs. 4-5. The sheath areas are  $27$ ,  $37$ ,  $61$ , and  $81 \text{ m}^2$  respectively. Electrostatic focusing effects similar to case (c) are observed. The current versus voltage is shown in Fig. 6. Except for the high-voltage end of each panel, the points are not far from a universal curve, indicating that a two-dimensional representation would be fairly good in this case. Area enhancement factors range from  $\sim 2$  at  $100 \text{ V}$  to  $\sim 10$  at  $3 \text{ kV}$ . The greatly enhanced current to the end

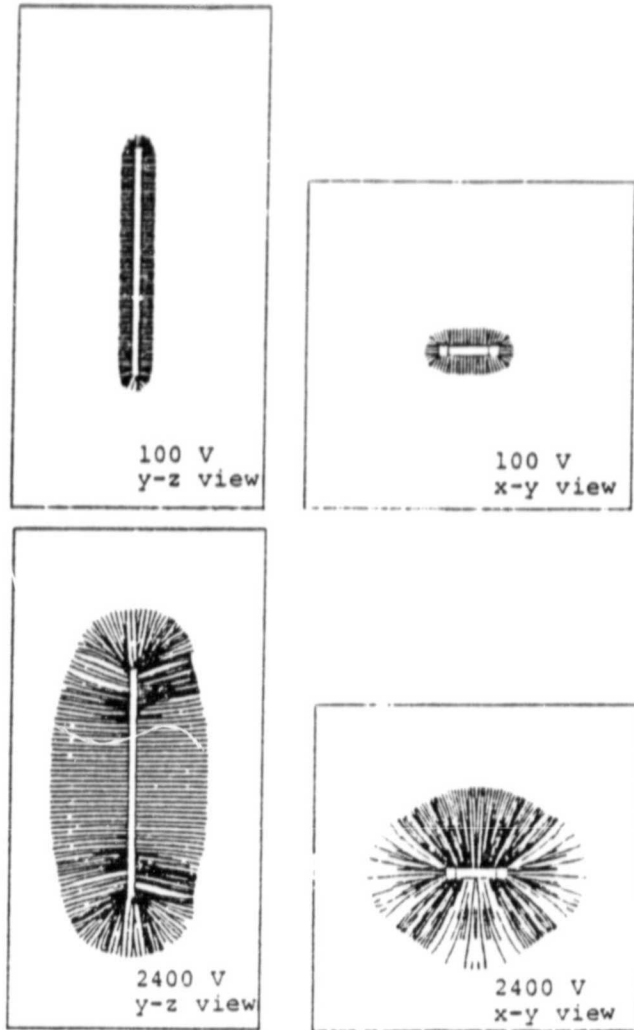


Fig. 2 Electron sheath particle trajectories for cases (a) and (b), with the test object at uniform potential.

section of each panel is a three-dimensional effect, and makes a substantial contribution to the power drain on the array.

A comparison of the results presented here with those of McCoy and Konradi must be approximate because the plasma in the experiment was far from homogeneous. The temperature and density we have chosen in our calculation correspond roughly to the estimated mean experimental values. The collection current per unit area from our calculation can be converted to Argon ion current by dividing by the square root of the mass ratio, yielding a one-sided plasma current of  $0.2 \text{ mA/m}^2$ . For the  $0-4800$  volt bias case, the predicted Argon ion current collected per unit area then is  $1.6 \text{ mA/m}^2$ . This is quite close to the experimentally observed current of  $2 \text{ mA/m}^2$ , far closer than one would expect due to the uncertainty in the experimental plasma parameters. That the calculation and experiment are in reasonable

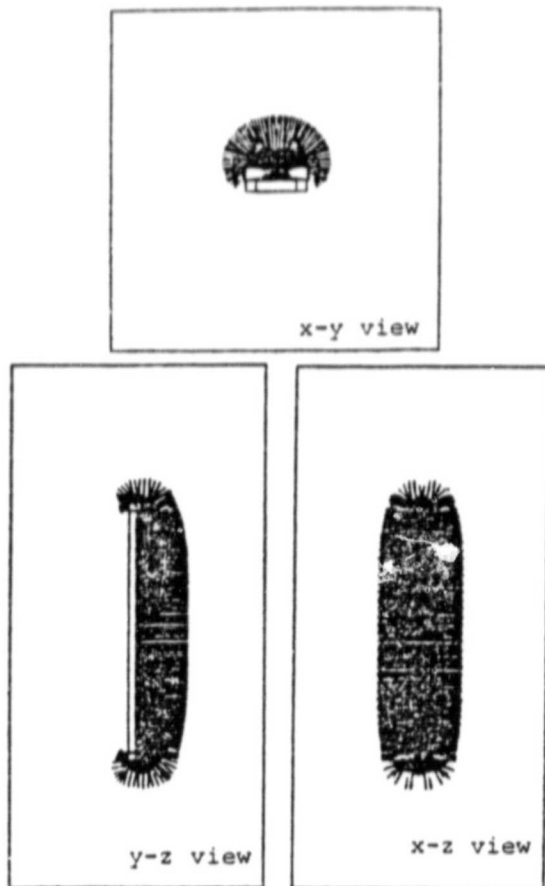


Fig. 3 Electron sheath particle trajectories for case (c). (Plastic at 0 V, metal strip at 2400 V.)

agreement, however, is certainly encouraging.

#### V. Summary

We have presented calculations using a preliminary version of NASCAP/LEO, a fully three-dimensional model for the study of current collection by large, high-voltage spacecraft. These calculations have reproduced both qualitative features such as ion focusing and quantitative ion collection currents observed in laboratory experiments. Extensions of NASCAP/LEO to include more complex geometries and materials as well as finer spatial resolution will increase the accuracy and applicability of the model. NASCAP/LEO should be a useful engineering tool for designing the spacecraft of the future.

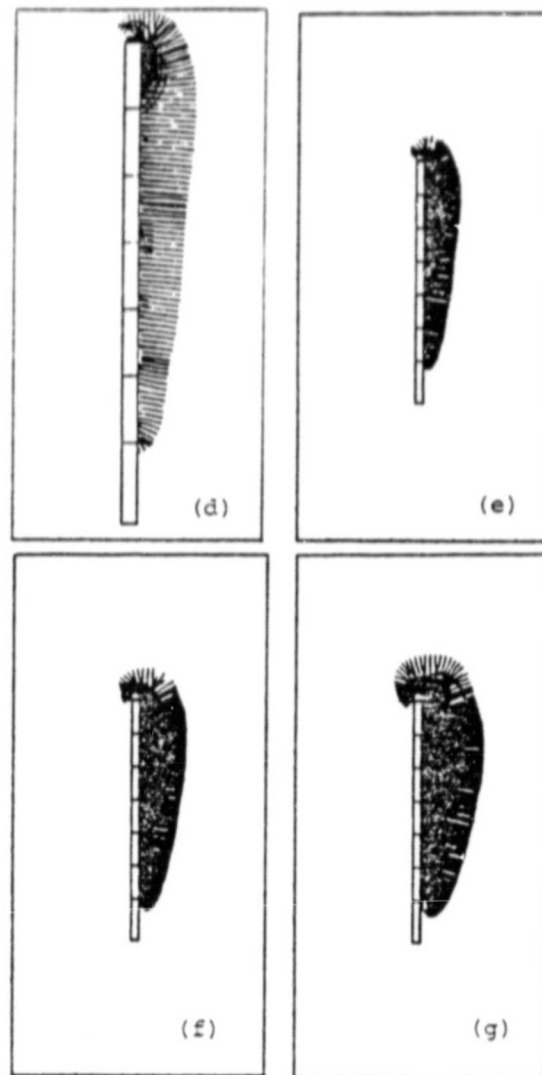


Fig. 4 y-z views of electron sheath particle trajectories for cases (d)-(g). Case (d) is shown twice scale.

#### References

1. Kennerud, K. L., "High Voltage Solar Array Experiments," NASA CR-12180 (1974).
2. Kaufman, H. R., "Interaction of a Solar Array with an Ion Thruster Due to the Charge-Exchange Plasma," NASA CR-135099 (1976).
3. Parks, D. E. and I. Katz, "Spacecraft-Generated Plasma Interaction with High-Voltage Solar Array," *J. Spacecraft and Rockets* 16, 259 (1979).
4. McCoy, James E. and Andrei Konradi, "Sheath Effects Observed on a 10 meter High Voltage Panel in Simulated Low Earth Orbit Plasma," *Spacecraft Charging Technology-1978*, p. 315, NASA Conference Publication 2071, AFGL-TR-79-0082 (1979).
5. Parker, Lee W., "Plasma Sheath Effects and Voltage Distributions of Large High-Power Satellite Solar Arrays," *ibid*, p. 341.

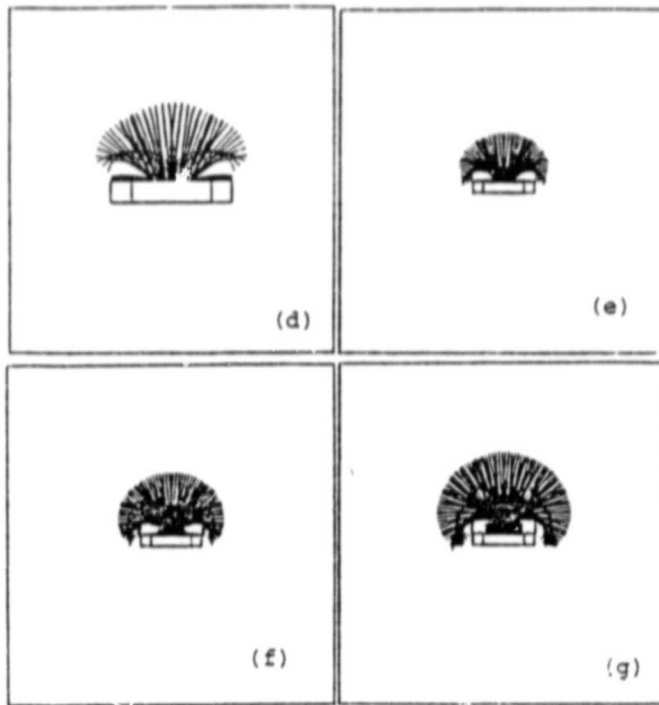


Fig. 5 x-y views of electron sheath particle trajectories for cases (d)-(g). Case (d) is shown twice scale.

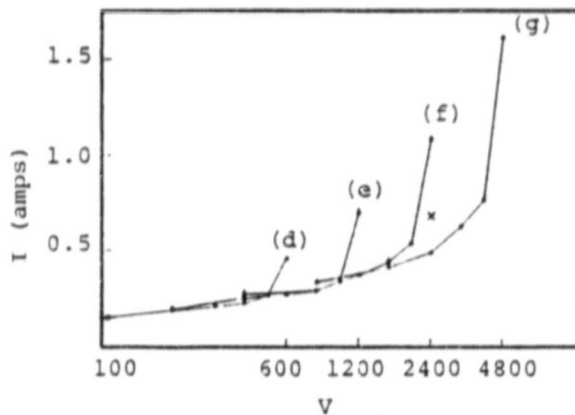


Fig. 6 Current per  $1.44 \text{ m}^2$  section of panel versus potential for the four cases (d)-(g). Note sharp increase in current to the end section, and the relative insensitivity of section current to other sections. The cross indicates the mean current to a similar area of a panel whose conducting strip is uniformly held at 2400 volts (case (c)).

6. Laframboise, J. G. and L. W. Parker, "Probe Design for Orbit Limited Current Collection," *Phys. Fluids* 16, 629 (1973).
7. Katz, I., et al., "A Three Dimensional Dynamic Study of Electrostatic Charging in Materials," NASA CR-135256 (1977).
8. Katz, I., et al., "Extension, Validation and Application of the NASCAP Code," NASA CR-159595 (1979).
9. Katz, I., et al., "The Capabilities of the NASA Charging Analyzer Program," presented at USAF/NASA Spacecraft Charging Technology Conference, U.S. Air Force Academy, 31 October-2 November 1978.
10. Luenberger, D. G., "Hyperbolic Pairs in the Method of Conjugate Gradients," *SIAM J. Appl. Math* 17, 1263 (1969).
11. Boris, J. P., Proc. 4th Conference on Numerical Simulation of Plasmas, pp. 3-67, NRL, Washington, D. C. (1970).

#### Acknowledgments

This work supported by NASA/Lewis Research Center, Cleveland, OH and Air Force Geophysics Laboratory, Hanscom AFB, MA, under Contract NAS3-21762.

**"Page missing from available version"**

APPENDIX A  
REPLACEMENT OF SECTION 7.3  
OF  
NASCAP USER'S MANUAL  
NASA CR-159417

### 7.3 FLUX DEFINITION FILE

There are four basic NASCAP flux types - test tank beam, maxwellian, particle pushing, and double maxwellian. The first card in the flux file identifies which of these types you are using. It must have the word 'TYPE' followed by an integer from 1 to 4.

This section describes the input for each flux type. The most complicated case is TYPE 1, the test tank electron beam. You may skip over that subsection if you don't intend to use it.

Free format input is used throughout NASCAP. The test tank beam relative intensity cards for polar coordinates are the exception. This one set of cards requires a specific format (see below). All other data can be placed anywhere in the first 80 columns of a data card image.

#### 7.3.1 Test Tank Electron Beam - Type 1

Type 1 flux is for a test tank with an electron beam source. There are actually two input forms, depending on whether the user specifies the beam pattern in polar or Cartesian coordinates. But these two types of input are almost identical, differing in cards number 2, number 10, and the pattern specification.

<u>Card Number</u>	<u>Contents</u>
1	"TYPE 1"
2	Beam pattern option (see below)
3	Position of calibration plane on NASCAP grid - constant Z value[1-33]
4	Beam dimensions (X, Y) in meters
5	Beam energy (eV)
6	Tracking timestep velocity (grid units/timestep)
7	Gun location on NASCAP grid (X, Y, Z)[outer grid units]

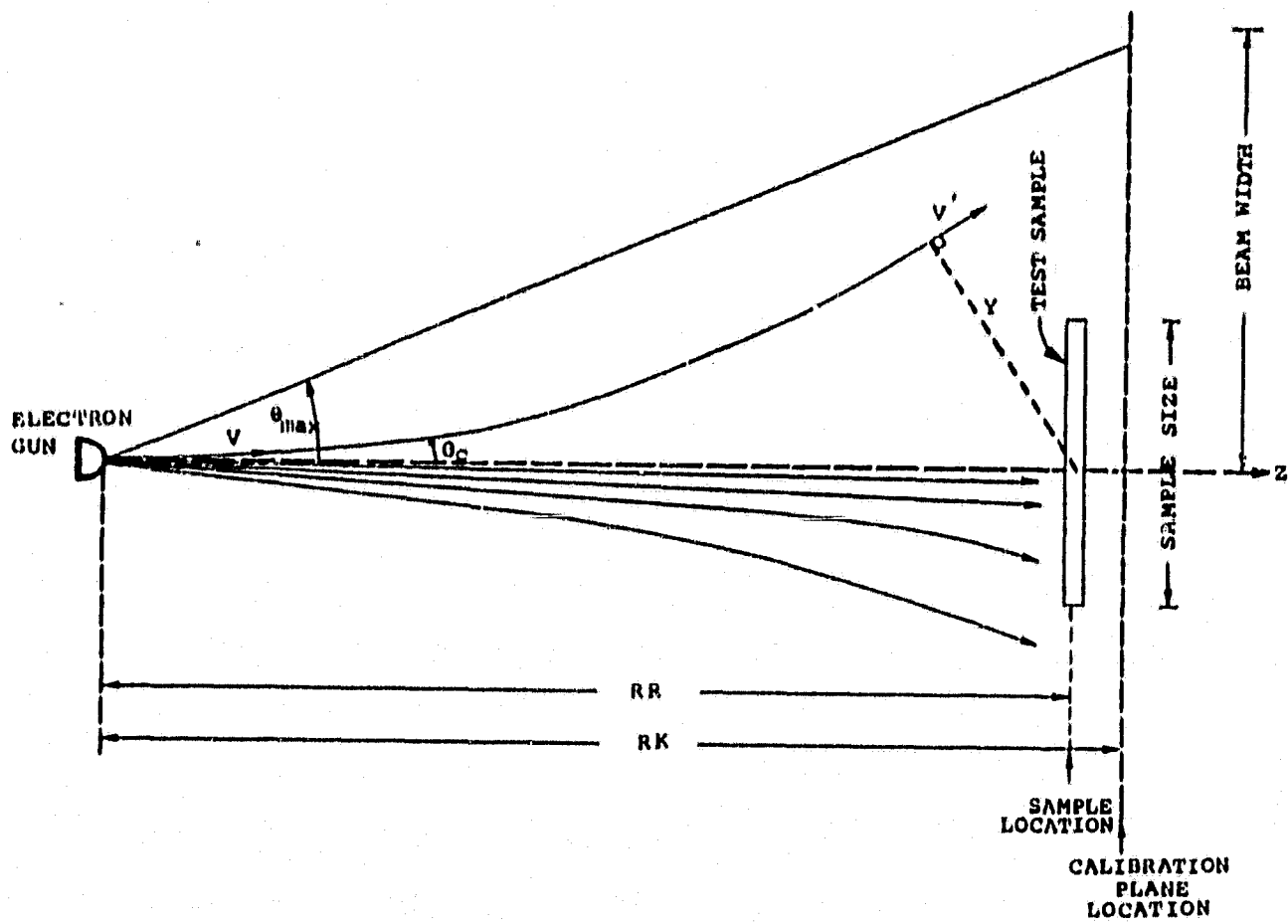


Figure 7.3. Geometry of the test tank configuration.

<u>Card Number</u>	<u>Contents</u>
8	Position of sample plane on NASCAP grid - constant Z value [1-33, inner grid units]
9	Total beam current (amperes)
10	(Cartesian input only) number of points (NX, NY) in calibration input grid (2 integers between 2 and 33)
-END	Specify beam pattern: Polar - 36 formatted cards. Cartesian - any number of free format cards NX.NY

The four things that NASCAP needs to know are (1) Beginning and end of the beam, (2) Beam intensity and energy, (3) Timestep for tracking beam particles, and (4) Beam pattern. NASCAP also finds out here if you just want to run a beam calibration or want to continue with one or more TRILIN iterations. The user does not specify beam direction - it is assumed to be parallel to the Z axis.

#### Beginning and End of Beam

Cards 7, 3, and 8 are used to specify the beam limits. Card 7 gives the electron gun location. The location is given in off-center (1-17, 1-33 style) NASCAP grid units, and it must be in terms of the outermost grid.

For the end of the beam you must specify a calibration plane and a sample plane. The calibration plane is the plane at which the beam pattern was measured. The sample plane is the point at which particle tracking is discontinued. Therefore, the NASCAP object should be located between the electron gun and the sample plane.

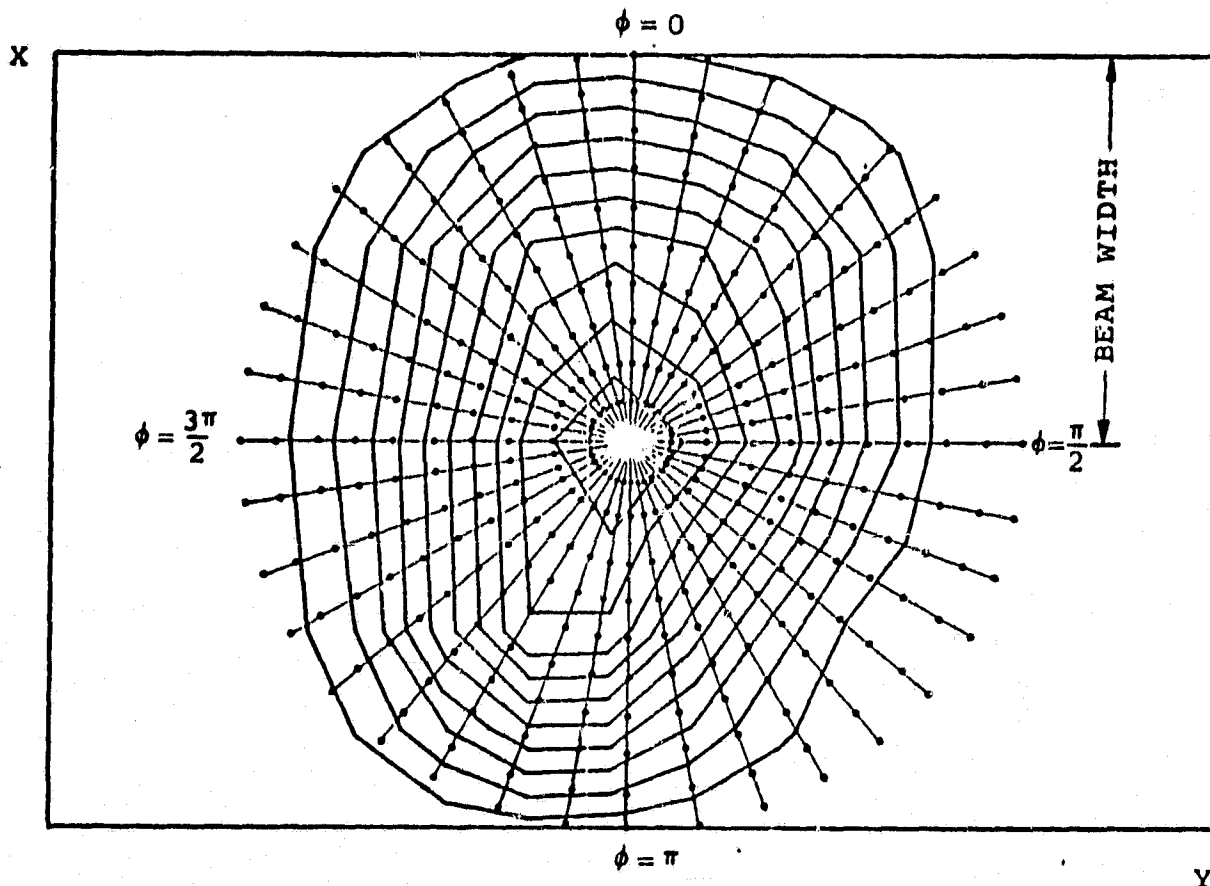


Figure 7.4. Specification of electron gun characteristics for the polar coordinate test tank case. Electron fluxes at the sample plane for an uncharged environment are to be specified at the solid points. Notice that the Z axis is pointing into the figure. We are looking at the calibration plane from the point of view of the electron gun.

For both the calibration plane and sample plane, the location is specified by a single Z value. This is the plane position in inner grid units.

#### Beam Intensity and Energy

Card 9 gives the beam intensity. This is the total beam current in amperes.

Card 5 gives the beam energy in eV. It is a mono-energetic beam.

#### Timestep for Tracking

The user supplies the tracking timestep indirectly, by specifying how far an electron, having the given beam energy, will travel in one timestep. For instance, if the tracking velocity is given as .3 grid units/timestep, the timestep will be chosen so an electron just leaving the gun will travel .3 inner grid units before its velocity is recomputed for the second timestep. This number goes on card 6.

#### Beam Pattern

The various aspects of beam pattern that the user must specify are: choice of polar or Cartesian input, calibration pattern size, number of calibration points (Cartesian input only), and relative beam intensity matrix (many cards).

Card 2 indicates the coordinate system, and tells NASCAP whether to stop after calibration or continue with the TRILIN cycle. Permitted options are:

POLAR RUN  
or POLAR CALIBRate  
or CARTESian RUN  
or CARTESian CALIBRate.

Any first literal other than CARTES will default to POLAR.  
Any second literal other than CALIBR will default to RUN.

Specification of the CALIBR option will result in cleanly exiting NASCAP as soon as test tank particle tracking is completed.

Card 4 gives the dimensions of the calibration pattern in meters in the X and Y directions. If you are using Cartesian coordinates, this is the distance from the first to the last grid point in either direction on your rectangular mesh. If you use polar coordinates, the beam radius will be the larger of the two values.

Card 10 gives the number of calibration points. For polar coordinates you must use an 11 x 36 mesh, so this card is omitted. For Cartesian coordinates, the lower bound in either direction is 2. The upper bound is 33. If your calibration plane dimensions from card 4 are (X, Y) and your number of points is NX by NY, then the distance between points in the X direction is  $X/(NX-1)$ . In the Y direction, it is  $Y/(NY-1)$ . The two numbers on card 10 must be integers - no decimal point.

Cards 10-45 (polar) or 11-END (Cartesian) give the relative intensities of the calibration points. These can be in arbitrary units, since NASCAP will normalize the relative intensities to correspond with the total beam current given on card 9. NASCAP internally stores the beam using polar coordinates, so after reading the relative intensities, either polar or Cartesian, it will print out the (R,  $\theta$ ) values of an equivalent polar grid.

If you are using polar coordinates, you must format the relative intensity input (11F4.1). You must supply 36 cards for 36 angles in 10° increments, and each card must have 11 values for the 11 radial positions along a single angle. The first value on each card corresponds to

the exact center of the pattern, so it must be the same on every card. A particular (i, j) value will be the i<sup>th</sup> value on the j<sup>th</sup> card, and it corresponds to the (R,  $\theta$ ) location

$$R = \frac{(i - 1)}{10} \times \text{maximum radius (card 4)}$$

$$\theta = \frac{(i - 1)}{36} \times 2\pi$$

where the angle  $\theta = 0$  lies along the positive X axis in a right-handed coordinate system.

If you are using Cartesian coordinates, the relative intensities are free format - like everything else in NASCAP. You can have from one to fifteen values on each card.

The values are read with X as the running index. That is, the first NGX values read will correspond to locations (1, 1) to (NGX, 1). You do not have to group the input on the cards in any particular way. For clarity, you might want to start a new card for each new group of NGX values.

### 7.3.2 Maxwellian Probe Approximation - Type 2

For a maxwellian distribution, the user specifies the plasma density for electrons and protons, and the plasma temperature for electrons and protons.

Density is in units of particles per cubic centimeter or per cubic meter, depending on whether CGS or MKS units are specified. Temperature can be given in KEV, EV, JOULES, or KELVIN.

The first density card will be interpreted as electron density. The last density card will be proton density. Likewise with temperatures. A card reading "END" ends the definition.

The cards for a maxwellian flux definition are then, the 'TYPE 2' card, one or more density cards, one or more temperature cards, and an 'END' card (optional).

### 7.3.3 Reverse Trajectory Particle Tracking - Type 3

Card 2 contains one of the two literals MAXWEL or DEFOR. Following 'MAXWEL' input is as in Type 2, (q.v.), except an END card is required. Following 'DEFOR', cards are required giving IUNIT, HOUR, IDAY. The data contained in the ELT NASCAP.DEFOR must have been copied onto file IUNIT.

Subsequent cards contain

NSPEC	Number of species
NENG	Number of energies
NTHET	Number of polar angles
NPHI	Number of azimuthal angles
NSTP	Maximum number of steps per particle
RMASS(1), CHARGE(1)	Mass (kg), Charge (C)
.	
.	
.	
RMASS(NSPEC), CHARGE(NSPEC)	
VCODE	Initial code velocity
STV(3)	Vector characterizing flux anisotropy

The present code requires NSPEC = 2, with species 1 being electrons and species 2 protons. The final card, STV, may be omitted, in which case the flux is assumed isotropic.

### 7.3.4 Double Maxwellian Flux - Type 4

Flux definition input file consists of the TYPE card specifying type 4, followed by up to four cards specifying maxwellian components, and (optionally) an END. Each

component card consists of five fields, each field containing a literal or a floating-point number.

The fields of the component cards and their permissible entries are:

<u>Field</u>	<u>Contents</u>	<u>Permitted Entries</u>
1	Species	'PROTONS', 'ELECTRONS', 'IONS', 'END'
2	Density	
3	Density Unit	'CGS', 'MKS'
4	Temperature	
5	Temperature Unit	'EV', 'KEV', 'JOULES', 'KELVIN', 'ERGS'

Note that in the current version of NASCAP the terms 'IONS' and 'PROTONS' are synonymous.

```

1.      TYPE      I
2.      Polar Run
3.      21.0
4.      .30
5.      2000.0
6.      .50E00
7.      9.0      9.0      9.0
8.      21.0
9.      8.40E-7
10.     10.010.0  9.0  8.3  7.6  6.6  4.7  3.2  1.5  0.5  0.0
11.     10.0  9.8  9.0  8.0  7.4  6.5  4.5  2.9  1.4  0.5  0.0
12.     10.0  9.7  9.0  8.0  6.9  5.8  4.4  2.8  1.4  0.5  0.0
13.     10.0  9.6  8.9  7.8  6.8  5.6  4.4  2.6  1.3  0.5  0.0
14.     10.0  9.6  8.8  7.5  6.3  5.3  3.9  2.3  0.9  0.5  0.0
15.     10.0  9.7  8.7  7.4  6.0  4.5  3.0  1.7  0.5  0.0  0.0
16.     10.0  9.8  8.6  7.5  5.7  3.9  2.7  1.0  0.5  0.0  0.0
17.     10.0  9.7  8.7  7.3  5.5  3.4  1.8  0.5  0.5  0.0  0.0
18.     10.010.0  8.9  7.4  5.5  3.3  1.7  0.3  0.5  0.0  0.0
19.     10.0  9.9  8.7  7.2  5.4  3.2  1.5  0.1  0.5  0.0  0.0
20.     10.0  9.8  8.5  6.8  4.9  2.7  1.1  0.5  0.0  0.0  0.0
21.     10.0  9.8  8.4  6.7  4.6  2.6  1.0  0.5  0.0  0.0  0.0
22.     10.0  9.8  8.5  6.7  4.7  2.7  1.1  0.5  0.0  0.0  0.0
23.     10.0  9.7  8.5  6.9  5.0  3.1  1.4  0.1  0.5  0.0  0.0
24.     10.0  9.9  8.6  7.1  5.2  3.5  1.7  0.6  0.5  0.0  0.0
25.     10.010.0  8.7  7.4  5.6  3.9  2.6  1.1  0.1  0.5  0.0
26.     10.010.0  9.0  7.7  6.3  4.8  3.2  1.8  0.4  0.5  0.0
27.     10.010.0  9.2  8.3  7.5  5.0  4.0  2.5  0.7  0.5  0.0
28.     10.010.0  9.6  9.0  8.5  7.5  5.5  3.5  1.5  0.5  0.0
29.     10.010.0  9.9  9.0  8.7  6.6  5.8  4.0  2.1  0.5  0.0
30.     10.010.0  9.6  9.0  8.9  6.9  5.0  3.8  1.9  0.5  0.0
31.     10.010.0  9.4  9.0  8.7  6.6  5.4  3.5  1.6  0.5  0.0
32.     10.010.0  9.4  9.0  7.8  6.6  4.7  3.0  1.4  0.5  0.0
33.     10.010.0  9.4  8.7  7.6  5.5  3.6  2.2  1.0  0.5  0.0
34.     10.010.0  9.3  8.5  6.6  5.2  3.0  1.6  0.5  0.0  0.0
35.     10.010.0  9.3  8.1  6.2  4.4  2.5  1.2  0.2  0.5  0.0
36.     10.010.0  9.4  8.2  6.3  4.3  2.4  1.1  0.1  0.5  0.0
37.     10.010.0  9.5  8.3  6.2  4.2  2.4  1.1  0.1  0.5  0.0
38.     10.010.0  9.4  8.1  6.2  4.3  2.5  1.2  0.2  0.5  0.0
39.     10.010.0  9.3  8.1  6.2  4.4  2.7  1.5  0.5  0.0  0.0
40.     10.010.0  9.2  8.2  6.5  4.8  3.4  2.0  0.8  0.5  0.0
41.     10.010.0  9.1  8.1  6.8  5.5  4.0  2.4  1.1  0.5  0.0
42.     10.010.0  9.1  8.2  7.3  6.3  4.5  2.7  1.5  0.5  0.0
43.     10.010.0  9.2  8.3  7.4  6.6  5.0  3.1  1.4  0.5  0.0
44.     10.010.0  9.1  8.4  7.5  6.5  4.7  3.4  1.5  0.5  0.0
45.     10.010.0  9.0  8.4  7.6  6.5  4.6  3.3  1.5  0.0  0.0

```

Example 7.1a. (Flux Definition). Defines a test tank electron beam flux using polar coordinates.

1	TYPE	1						
2		Cartesian Run						
3		21.0						
4		.150	.30					
5		2000.						
6		.50						
7		9.0	9.0	9.0				
8		21.						
9		8.40E-7						
10		7	11					
11		11.1803	10.5409	10.1379	10.0000	10.1379	10.5409	11.1803
12		9.4340	8.6667	8.1718	8.0000	8.1718	8.6667	9.4340
13		7.8102	6.8638	6.2272	6.0000	6.2272	6.8638	7.8102
14		6.4034	5.2068	4.3333	4.0000	4.3333	5.2068	6.4034
15		5.3852	3.8873	2.6034	2.0000	2.6034	3.8873	5.3852
16		5.0000	3.3333	1.6667	.0000	1.6667	3.3333	5.0000
17		5.3852	3.8873	2.6034	2.0000	2.6034	3.8873	5.3852
18		6.4034	5.2068	4.3333	4.0000	4.3333	5.2068	6.4034
19		7.8102	6.8638	6.2272	6.0000	6.2272	6.8638	7.8102
20		9.4340	8.6667	8.1718	8.0000	8.1718	8.6667	9.4340
21		11.1803	10.5409	10.1379	10.0000	10.1379	10.5409	11.1803

Example 7.1b. (Flux Definition). Defines a test tank electron beam flux using Cartesian coordinates.

1.		TYPE	2
2.		1.00	CGS
3.		1.0	CGS
4.		10.00	KEV
5.		10.0	KEV

Example 7.2. (Flux Definition). Defines a neutral 10 keV plasma for use in the Maxwell probe operating mode.

1.		TYPE	3	
2.		MAXWELL		
3.		1.00	CGS	
4.		1.0	CGS	
5.		10.00	KEV	
6.		10.00	KEV	
7.			END	
8.		2		NSPEC
9.		5		NENG
10.		5		NIHET
11.		5		NPHI
12.		100		NSTP
13.		9.1E-31	-1.6E-19	MASS, CHARGE
14.		16.7E-28	1.6E-19	MASS, CHARGE
15.		0.3		VCODE

Example 7.3a. (Flux Definition). Defines a neutral 10 keV maxwellian plasma for use in the reverse trajectory particle pushing mode.

1.	TYPE	3		
2.	DEFOR			
3.	9			
4.	9.998			
5.	73			
6.	2		NSPEC	
7.	5		NENG	
8.	5		NTHET	
9.	1		NPHI	
10.	200		NSTP	
11.	9.1E-31	-1.6E-19		MASS, CHARGE
12.	16.7E-28	1.6E-19		MASS, CHARGE
13.	0.3		VCODE	

Example 7.3b. (Flux Definition). Takes flux from DeForest environmental data for hour 9.998 of day 73. The data is read from LUN 9.

1.	TYPE	3		
2.	MAXWELL			
3.	0.53	CGS		
4.	0.6	CGS		
5.	4.114	KEV		
6.	0.43	KEV		
7.		END		
8.	2		NSPEC	
9.	05		NENG	
10.	5		NTHET	
11.	1		NPHI	
12.	100		NSTP	
13.	9.1E-31	-1.6E-19		MASS, CHARGE
14.	16.7E-28	1.6E-19		MASS, CHARGE
15.	0.3		VCODE	

Example 7.3c. (Flux Definition). Defines a non-neutral, non-equilibrium maxwellian plasma for use by the reverse trajectory particle pushing mode.

1	TYPE	4		
2	ELECTRONS	.6	CGS	.3 KEU
3	ELECTRONS	.4	CGS	20. KEU
4	PROTONS	.3	CGS	20. KEU
5	PROTONS	.7	CGS	.3 KEU
6	END			

Example 7.4. (Flux Definition). Defines a double maxwellian flux environment.

### 7.3.5 Multiple Reading of Flux Definition; Changing Environments

NASCAP attempts to read a flux definition each time TRILIN or DETECT is called. If the 'DEBYE' option is specified, it is also read when CAPACI is called. If the flux file contains only one flux definition, NASCAP will rewind the file and re-read the same specifications each time. An alternate mode of operation is to construct a flux file containing several successive flux definitions. This is particularly useful for simulation of a changing environment, or for a run having several TRILIN-DETECT cycles (as DETECT requires a TYPE 3 flux specification). For successive fluxes to work properly, each specification must end cleanly, so that NASCAP encounters a 'TYPE' card whenever it looks for a new environment. Thus types 2 and 4 require an 'END' card if another flux is to follow. Type 3 must have an STV card (a zero vector may be used to specify isotropic flux), or an '@EOF' card. Type 1 must have exactly the correct number of data cards. If an end-of-file condition is encountered when a 'TYPE' card is expected, NASCAP will rewind the file and begin the sequence of environments anew.

An additional consideration for changing environments is that if the 'DEBYE' option is specified a sudden environment change will cause a sudden potential change due to the difference in space charge screening. Also, the output of the CAPACI module is environment dependent on the 'DEBYE' case. NASCAP accounts for these effects in an approximate way to avoid the need to call CAPACI for each new environment. The accuracy of the approximations used may be gauged by calling CAPACI for the extreme environments used, and noting the variation of the spacecraft effective radius.

## APPENDIX B

### DEFAULT MATERIALS AND PARAMETERS

#### DEFAULT MATERIALS

##### Conductors

AQUADG	Conducting carbon coating (Aquadag)
ALUMIN	Aluminum
CPAINT	Conducting paint
GOLD	Gold
INDOX	Indium Oxide ( $\text{In}_2\text{O}_3$ )
MAGNES	Magnesium
SCREEN	Metallic screen

##### Insulators

KAPTON	Kapton
NPAINT	Nonconducting paint
SIO2	Quartz ( $\text{SiO}_2$ )
SOLAR	Solar cell cover material ( $\text{MgF}_2$ on $\text{SiO}_2$ )
TEFLON	Teflon

Note that the default properties are not necessarily the same as those used for the SCATHA model.

MATERIAL 1: ALUMIN

1  
11  
12  
13  
14  
15  
16  
17  
18  
19  
20

PROPERTY  
DIELECTRIC CONSTANT  
THICKNESS  
CONDUCTIVITY  
ATOMIC NUMBER  
DELTA MAX > COEFF  
-MAX > DEPTH\*\* -1  
RANGE  
EXPONENT > RANGE  
RANGE > EXPONENT  
EXPONENT  
YIELD FOR 1KEV PROTONS  
MAX DE/DX FOR PROTONS  
PHOTOCURRENT  
SURFACE RESISTIVITY  
SPACE DISCHARGE POT'L  
INTERNAL DISCHARGE POT'L

INPUT VALUE  
1 1.000+000 (NONE)  
1 1.000+000 METERS  
-1 1.000+000 MHO/M  
1 1.000+001 (NONE)  
9 9.700+001 (NONE)  
3 3.000+001 KEV  
2 2.000+002 ANG.  
2 2.000+002 ANG.  
2 2.000+002 ANG.  
1 1.000+001 (NONE)  
2 2.000+001 (NONE)  
2 2.000+002 KEV  
4 4.000+005 A/M\*\*2  
-1 1.000+000 OHMS  
2 2.000+003 VOLTS  
1 1.700+001 VOLTS  
1 1.800+001 VOLTS  
1 1.900+001 VOLTS  
2 2.000+001 VOLTS

CODE VALUE  
1 1.000+000 (NONE)  
-1 1.000+000 MESH  
1 1.000+001 MHO/M  
7 7.000+001 (NONE)  
3 3.000+001 (NONE)  
3 3.000+002 ANG-C1  
4 4.000+002 ANG.  
1 1.000+002 ANG.  
1 1.000+000 (NONE)  
1 1.000+001 (NONE)  
2 2.000+001 (NONE)  
2 2.000+002 KEV  
4 4.000+005 A/M\*\*2  
-1 1.000+000 V-S/C  
2 2.000+004 VOLTS  
1 1.700+001 VOLTS  
1 1.800+001 VOLTS  
1 1.900+001 VOLTS  
2 2.000+001 VOLTS

MATERIAL 2: AQUADG

1  
11  
12  
13  
14  
15  
16  
17  
18  
19  
20

PROPERTY  
DIELECTRIC CONSTANT  
THICKNESS  
CONDUCTIVITY  
ATOMIC NUMBER  
DELTA MAX > COEFF  
-MAX > DEPTH\*\* -1  
RANGE  
EXPONENT > RANGE  
RANGE > EXPONENT  
EXPONENT  
YIELD FOR 1KEV PROTONS  
MAX DE/DX FOR PROTONS  
PHOTOCURRENT  
SURFACE RESISTIVITY  
SPACE DISCHARGE POT'L  
INTERNAL DISCHARGE POT'L

INPUT VALUE  
1 1.000+000 (NONE)  
1 1.000+000 METERS  
-1 1.000+000 MHO/M  
6 6.000+000 (NONE)  
7 7.000+000 (NONE)  
3 3.000+001 KEV  
-1 1.000+000 ANG.  
2 2.000+000 (NONE)  
1 1.000+001 (NONE)  
3 3.000+001 (NONE)  
1 1.000+001 (NONE)  
2 2.000+002 KEV  
-1 1.000+000 A/M\*\*2  
-1 1.000+000 OHMS  
1 1.000+004 VOLTS  
2 2.000+003 VOLTS  
1 1.700+001 VOLTS  
1 1.800+001 VOLTS  
1 1.900+001 VOLTS  
2 2.000+001 VOLTS

CODE VALUE  
1 1.000+000 (NONE)  
-1 1.000+000 MESH  
1 1.000+000 MHO/M  
6 6.000+000 (NONE)  
7 7.000+000 (NONE)  
2 2.000+002 ANG-C1  
3 3.000+002 ANG.  
1 1.000+000 (NONE)  
1 1.000+000 (NONE)  
3 3.000+001 (NONE)  
1 1.000+001 KEV  
-1 1.000+000 A/M\*\*2  
-1 1.000+000 V-S/C  
1 1.000+004 VOLTS  
2 2.000+003 VOLTS  
1 1.700+001 VOLTS  
1 1.800+001 VOLTS  
1 1.900+001 VOLTS  
2 2.000+001 VOLTS

MATERIAL 3: CPAINT

1  
11  
12  
13  
14  
15  
16  
17  
18  
19

PROPERTY  
DIELECTRIC CONSTANT  
THICKNESS  
CONDUCTIVITY  
ATOMIC NUMBER  
DELTA MAX > COEFF  
-MAX > DEPTH\*\* -1  
RANGE  
EXPONENT > RANGE  
RANGE > EXPONENT  
EXPONENT  
YIELD FOR 1KEV PROTONS  
MAX DE/DX FOR PROTONS  
PHOTOCURRENT  
SURFACE RESISTIVITY  
SPACE DISCHARGE POT'L  
INTERNAL DISCHARGE POT'L

INPUT VALUE  
1 1.000+000 (NONE)  
-1 1.000+000 METERS  
1 1.000+000 MHO/M  
5 5.000+000 (NONE)  
1 1.000+001 (NONE)  
-1 1.000+001 KEV  
-1 1.000+000 ANG.  
3 3.000+000 (NONE)  
1 1.000+000 ANG.  
9 9.000+000 ANG.  
1 1.000+000 (NONE)  
3 3.000+001 (NONE)  
1 1.000+002 KEV  
-1 1.000+000 A/M\*\*2  
-1 1.000+000 OHMS  
1 1.000+004 VOLTS  
2 2.000+003 VOLTS  
1 1.700+001 VOLTS  
1 1.800+001 VOLTS  
1 1.900+001 VOLTS

CODE VALUE  
-1 1.000+000 (NONE)  
1 1.000+000 MESH  
1 1.000+000 MHO/M  
5 5.000+000 (NONE)  
1 1.000+001 (NONE)  
-1 1.000+001 ANG-C1  
1 1.000+003 ANG.  
0 0.000+000 ANG.  
1 1.000+000 (NONE)  
1 1.000+000 (NONE)  
3 3.000+001 (NONE)  
1 1.000+002 KEV  
-1 1.000+000 A/M\*\*2  
-1 1.000+000 V-S/C  
1 1.000+004 VOLTS  
2 2.000+003 VOLTS  
1 1.700+001 VOLTS  
1 1.800+001 VOLTS  
1 1.900+001 VOLTS

MATERIAL 4: GOLD

PROPERTY	INPUT VALUE	CODE VALUE
1 DIELECTRIC CONSTANT	1.000+00 (NONE)	1.000+00 (NONE)
2 THICKNESS	1.000+03 METERS	1.000+02 MESH
3 CONDUCTIVITY	-1.000+00 MHO/M	-1.000+00 MHO/M
4 ATOMIC NUMBER	79.00+01 (NONE)	79.00+01 (NONE)
5 DELTA MAX >COEFF	8.800+01 (NONE)	2.520+00 (NONE)
6 -MAX >DEPTH** -1	8.000+01 KEV	1.900+02 ANG -01
7 RANGE	9.500+01 ANG.	1.350+02 ANG.
8 EXPONENT > RANGE	1.630+00 (NONE)	1.420+02 ANG.
9 RANGE > EXPONENT	3.460+01 ANG.	1.770+00 (NONE)
10 EXPONENT	7.000+01 (NONE)	7.000+01 (NONE)
11 YIELD FOR 1KEV PROTONS	4.110+01 (NONE)	4.110+01 (NONE)
12 MAX DE/DX FOR PROTONS	1.900+02 KEV	1.900+02 KEV
13 PHOTOCURRENT	-2.000+05 A/M**2	-2.000+05 A/M**2
14 SURFACE RESISTIVITY	-1.000+00 OHMS	-1.000+03 V-S/O
15 SPACE DISCHARGE POT'L	1.000+04 VOLTS	1.000+04 VOLTS
16 INTERNAL DISCHARGE POT'L	2.000+03 VOLTS	2.000+03 VOLTS
17	1.700+01	1.700+01
18	1.800+01	1.800+01
19	1.900+01	1.900+01
20	2.000+01	2.000+01

MATERIAL 5: INDOX

PROPERTY	INPUT VALUE	CODE VALUE
1 DIELECTRIC CONSTANT	1.000+00 (NONE)	1.000+00 (NONE)
2 THICKNESS	1.000+03 METERS	1.000+02 MESH
3 CONDUCTIVITY	-1.000+00 MHO/M	-1.000+00 MHO/M
4 ATOMIC NUMBER	21.00+01 (NONE)	21.00+01 (NONE)
5 DELTA MAX >COEFF	1.440+00 (NONE)	1.020+00 (NONE)
6 -MAX >DEPTH** -1	8.000+01 KEV	1.490+02 ANG -01
7 RANGE	1.000+00 ANG.	1.570+02 ANG.
8 EXPONENT > RANGE	0.000+00 (NONE)	0.000+00 ANG.
9 RANGE > EXPONENT	7.180+00 ANG.	2.000+00 (NONE)
10 EXPONENT	3.550+01 (NONE)	3.550+01 (NONE)
11 YIELD FOR 1KEV PROTONS	3.300+01 (NONE)	3.300+01 (NONE)
12 MAX DE/DX FOR PROTONS	1.910+02 KEV	1.910+02 KEV
13 PHOTOCURRENT	-1.000+05 A/M**2	-1.000+05 A/M**2
14 SURFACE RESISTIVITY	-1.000+00 OHMS	-1.000+03 V-S/O
15 SPACE DISCHARGE POT'L	1.000+04 VOLTS	1.000+04 VOLTS
16 INTERNAL DISCHARGE POT'L	2.000+03 VOLTS	2.000+03 VOLTS
17	1.700+01	1.700+01
18	1.800+01	1.800+01
19	1.900+01	1.900+01
20	2.000+01	2.000+01

MATERIAL 6: MAGNES

PROPERTY	INPUT VALUE	CODE VALUE
1 DIELECTRIC CONSTANT	1.000+00 (NONE)	1.000+00 (NONE)
2 THICKNESS	1.000+03 METERS	1.000+02 MESH
3 CONDUCTIVITY	-1.000+00 MHO/M	-1.000+00 MHO/M
4 ATOMIC NUMBER	12.00+01 (NONE)	12.00+01 (NONE)
5 DELTA MAX >COEFF	9.200+01 (NONE)	7.790+00 (NONE)
6 -MAX >DEPTH** -1	2.500+01 KEV	2.790+02 ANG -01
7 RANGE	-1.000+00 ANG.	6.960+02 ANG.
8 EXPONENT > RANGE	0.000+00 (NONE)	0.000+00 ANG.
9 RANGE > EXPONENT	1.740+00 ANG.	1.750+00 (NONE)
10 EXPONENT	2.430+01 (NONE)	1.000+00 (NONE)
11 YIELD FOR 1KEV PROTONS	2.440+01 (NONE)	2.440+01 (NONE)
12 MAX DE/DX FOR PROTONS	2.300+02 KEV	2.300+02 KEV
13 PHOTOCURRENT	-2.000+05 A/M**2	-2.000+05 A/M**2
14 SURFACE RESISTIVITY	-1.000+00 OHMS	-1.000+03 V-S/O
15 SPACE DISCHARGE POT'L	1.000+04 VOLTS	1.000+04 VOLTS
16 INTERNAL DISCHARGE POT'L	2.000+03 VOLTS	2.000+03 VOLTS
17	1.700+01	1.700+01
18	1.800+01	1.800+01
19	1.900+01	1.900+01

MATERIAL 7: SCREEN

PROPERTY	INPUT VALUE	CODE VALUE
1 DIELECTRIC CONSTANT	1.000+00 (NONE)	1.000+00 (NONE)
2 THICKNESS	-1.000+00 METERS	-1.000+00 MESH
3 CONDUCTIVITY	-1.000+00 MHO/M	-1.000+00 MHO/M
4 ATOMIC NUMBER	1.000+00 (NONE)	1.000+00 (NONE)
5 DELTA MAX >COEFF	0.000+00 (NONE)	0.000+00 (NONE)
6 R-1 MAX >DEPTH** -1	1.000+00 KEV	1.000+00 ANG - C1
7 RANGE	1.000+01 ANG.	1.000+01 ANG.
8 EXPONENT > RANGE	0.500+00 (NONE)	0.500+00 ANG.
9 RANGE > EXPONENT	0.000+00 ANG.	0.000+00 (NONE)
10 EXPONENT	1.000+00 (NONE)	1.000+00 (NONE)
11 YIELD FOR 1KEV PROTONS	0.000+00 (NONE)	0.000+00 (NONE)
12 MAX DE/DX FOR PROTONS	1.000+00 KEV	1.000+00 KEV
13 PHOTOCURRENT	0.000+00 A/M**2	0.000+00 A/M**2
14 SURFACE RESISTIVITY	-1.000+00 OHMS	-1.000+00 V-S/O
15 SPACE DISCHARGE POT'L	1.000+04 VOLTS	1.000+04 VOLTS
16 INTERNAL DISCHARGE POT'L	2.000+03 VOLTS	2.000+03 VOLTS
17	1.100+01	1.100+01
18	1.800+01	1.800+01
19	1.900+01	1.900+01
20	2.000+01	2.000+01

MATERIAL 8: KAPTON

PROPERTY	INPUT VALUE	CODE VALUE
1 DIELECTRIC CONSTANT	3.500+00 (NONE)	3.500+00 (NONE)
2 THICKNESS	1.270+04 METERS	1.270+04 MESH
3 CONDUCTIVITY	1.000+14 MHO/M	1.000+14 MHO/M
4 ATOMIC NUMBER	5.000+00 (NONE)	5.000+00 (NONE)
5 DELTA MAX >COEFF	2.100+00 (NONE)	2.100+00 (NONE)
6 R-1 MAX >DEPTH** -1	-1.000+00 KEV	-1.000+00 ANG - C1
7 RANGE	0.000+00 ANG.	0.000+00 ANG.
8 EXPONENT > RANGE	1.000+00 (NONE)	1.000+00 ANG.
9 RANGE > EXPONENT	1.400+00 ANG.	1.400+00 (NONE)
10 EXPONENT	9.800+00 (NONE)	9.800+00 (NONE)
11 YIELD FOR 1KEV PROTONS	3.300+01 (NONE)	3.300+01 (NONE)
12 MAX DE/DX FOR PROTONS	1.910+02 KEV	1.910+02 KEV
13 PHOTOCURRENT	2.000+05 A/M**2	2.000+05 A/M**2
14 SURFACE RESISTIVITY	1.000+16 OHMS	1.000+16 V-S/O
15 SPACE DISCHARGE POT'L	1.000+04 VOLTS	1.000+04 VOLTS
16 INTERNAL DISCHARGE POT'L	2.000+03 VOLTS	2.000+03 VOLTS
17	1.700+01	1.700+01
18	1.800+01	1.800+01
19	1.900+01	1.900+01
20	2.000+01	2.000+01

MATERIAL 9: NPAINT

PROPERTY	INPUT VALUE	CODE VALUE
1 DIELECTRIC CONSTANT	3.500+00 (NONE)	3.500+00 (NONE)
2 THICKNESS	5.000+05 METERS	5.000+05 MESH
3 CONDUCTIVITY	5.900+14 MHO/M	5.900+14 MHO/M
4 ATOMIC NUMBER	5.000+00 (NONE)	5.000+00 (NONE)
5 DELTA MAX >COEFF	2.100+00 (NONE)	2.100+00 (NONE)
6 R-1 MAX >DEPTH** -1	-1.500+00 KEV	-1.500+00 ANG - C1
7 RANGE	1.000+00 ANG.	1.000+00 ANG.
8 EXPONENT > RANGE	0.000+00 (NONE)	0.000+00 ANG.
9 RANGE > EXPONENT	1.050+00 ANG.	1.050+00 (NONE)
10 EXPONENT	9.800+00 (NONE)	9.800+00 (NONE)
11 YIELD FOR 1KEV PROTONS	3.300+01 (NONE)	3.300+01 (NONE)
12 MAX DE/DX FOR PROTONS	1.910+02 KEV	1.910+02 KEV
13 PHOTOCURRENT	2.000+05 A/M**2	2.000+05 A/M**2
14 SURFACE RESISTIVITY	1.000+13 OHMS	1.000+13 V-S/O
15 SPACE DISCHARGE POT'L	1.000+04 VOLTS	1.000+04 VOLTS
16 INTERNAL DISCHARGE POT'L	1.000+03 VOLTS	1.000+03 VOLTS
17	1.700+01	1.700+01
18	1.800+01	1.800+01
19	1.900+01	1.900+01

MATERIAL 10: SiO2

1  
2  
3  
4  
5  
6  
7  
8  
9  
10  
11  
12  
13  
14  
15  
16  
17  
18  
19  
20

PROPERTY  
DIELECTRIC CONSTANT  
THICKNESS  
CONDUCTIVITY  
ATOMIC NUMBER  
DELTA MAX > COEFF  
E-MAX > DEPTH\*\* -1  
RANGE  
EXPONENT > RANGE  
RANGE > EXPONENT  
EXPONENT  
YIELD FOR 1KEV PROTONS  
MAX DE/DX FOR PROTONS  
PHOTOCURRENT  
SURFACE RESISTIVITY  
SPACE DISCHARGE POT'L  
INTERNAL DISCHARGE POT'L

INPUT VALUE  
4.00+00 (NONE)  
1.27-04 METERS  
1.00-14 MHO/M  
1.00+01 (NONE)  
2.40+00 (NONE)  
4.00+00 KEV  
-1.00+00 ANG.  
0.00+00 (NONE)  
0.00+00 ANG.  
2.00+01 (NONE)  
3.30+01 (NONE)  
1.91+02 KEV  
2.00-05 A/M\*\*2  
1.00+04 OHMS  
1.00+04 VOLTS  
2.00+03 VOLTS  
1.70+01  
1.80+01  
1.90+01  
2.00+01

CODE VALUE  
4.00+00 (NONE)  
1.27-03 MESH  
1.00-14 MHO/M  
1.00+01 (NONE)  
1.17+01 (NONE)  
7.11-03 ANG-C1  
1.18+03 ANG.  
0.00+00 ANG.  
0.00+00 (NONE)  
1.00+00 (NONE)  
3.30+01 (NONE)  
1.91+02 KEV  
2.00-05 A/M\*\*2  
1.00+04 V-S/C  
1.00+04 VOLTS  
2.00+03 VOLTS  
1.70+01  
1.80+01  
1.90+01  
2.00+01

MATERIAL 11: SOLAR

1  
2  
3  
4  
5  
6  
7  
8  
9  
10  
11  
12  
13  
14  
15  
16  
17  
18  
19  
20

PROPERTY  
DIELECTRIC CONSTANT  
THICKNESS  
CONDUCTIVITY  
ATOMIC NUMBER  
DELTA MAX > COEFF  
E-MAX > DEPTH\*\* -1  
RANGE  
EXPONENT > RANGE  
RANGE > EXPONENT  
EXPONENT  
YIELD FOR 1KEV PROTONS  
MAX DE/DX FOR PROTONS  
PHOTOCURRENT  
SURFACE RESISTIVITY  
SPACE DISCHARGE POT'L  
INTERNAL DISCHARGE POT'L

INPUT VALUE  
4.00+00 (NONE)  
1.27-04 METERS  
1.00-14 MHO/M  
1.00+01 (NONE)  
4.10+00 (NONE)  
4.10+01 KEV  
-1.00+00 ANG.  
0.00+00 (NONE)  
0.00+00 ANG.  
2.00+01 (NONE)  
1.36+00 (NONE)  
4.00+01 KEV  
-2.00+05 A/M\*\*2  
-1.00+00 OHMS  
1.00+04 VOLTS  
2.00+03 VOLTS  
1.70+01  
1.80+01  
1.90+01  
2.00+01

CODE VALUE  
4.00+00 (NONE)  
1.27-03 MESH  
1.00-14 MHO/M  
1.00+01 (NONE)  
1.96+01 (NONE)  
1.48+02 ANG-C1  
5.46+02 ANG.  
0.00+00 ANG.  
1.69+00 (NONE)  
1.00+00 (NONE)  
1.36+00 (NONE)  
4.00+01 KEV  
-2.00+05 A/M\*\*2  
-1.85-13 V-S/C  
1.00+04 VOLTS  
2.00+03 VOLTS  
1.70+01  
1.80+01  
1.90+01  
2.00+01

MATERIAL 12: TEFLON

1  
2  
3  
4  
5  
6  
7  
8  
9  
10  
11  
12  
13  
14  
15  
16  
17  
18  
19

PROPERTY  
DIELECTRIC CONSTANT  
THICKNESS  
CONDUCTIVITY  
ATOMIC NUMBER  
DELTA MAX > COEFF  
E-MAX > DEPTH\*\* -1  
RANGE  
EXPONENT > RANGE  
RANGE > EXPONENT  
EXPONENT  
YIELD FOR 1KEV PROTONS  
MAX DE/DX FOR PROTONS  
PHOTOCURRENT  
SURFACE RESISTIVITY  
SPACE DISCHARGE POT'L  
INTERNAL DISCHARGE POT'L

INPUT VALUE  
2.00+00 (NONE)  
1.27-04 METERS  
1.00-14 MHO/M  
7.00+00 (NONE)  
3.00+00 (NONE)  
3.00+01 KEV  
3.00+02 ANG.  
1.59+00 (NONE)  
1.00+02 ANG.  
2.00+00 (NONE)  
3.30+01 (NONE)  
1.91+02 KEV  
2.00-05 A/M\*\*2  
1.00+16 OHMS  
1.00+04 VOLTS  
2.00+03 VOLTS  
1.70+01  
1.80+01  
1.90+01

CODE VALUE  
2.00+00 (NONE)  
1.27-03 MESH  
1.00-14 MHO/M  
7.00+00 (NONE)  
1.98+01 (NONE)  
4.06+02 ANG-C1  
2.77+02 ANG.  
2.00+02 ANG.  
1.59+00 (NONE)  
2.00+00 (NONE)  
3.30+01 (NONE)  
1.91+02 KEV  
2.00-05 A/M\*\*2  
1.85+03 V-S/C  
1.00+04 VOLTS  
2.00+03 VOLTS  
1.70+01  
1.80+01  
1.90+01

## REFERENCES

1. Katz, I., J. J. Cassidy, M. J. Mandell, D. E. Parks, G. W. Schnuelle, P. R. Stannard and P. G. Steen, "Additional Application of the NASCAP Code. Volume II. SEPS, Ion Thruster Neutralization and Electrostatic Antenna Models," NASA CR-165350, February 1981.
2. Stannard, P. R., I. Katz, M. J. Mandell, J. J. Cassidy, D. E. Parks, M. Rotenberg and P. G. Steen, "Analysis of the Charging of the SCATHA (P78-2) Satellite," NASA CR-165348, December 1980.
3. Phys. Rev., B19, p. 121, 1979.
4. Katz, I., J. J. Cassidy, M. J. Mandell, G. W. Schnuelle, P. G. Steen, D. E. Parks, M. Rotenberg and J. H. Alexander, "Extension, Validation and Application of the NASCAP Code," NASA CR-159595, January 1979.
5. Cassidy, J. J., "NASCAP User's Manual - 1978," NASA CR-159417, August 1978.
6. McCoy, J. E. and A. Konradi, "Sheath Effects Observed on a 10 meter High Voltage Panel in Simulated Low Earth Orbit Plasma," Spacecraft Charging Technology-1978, p. 315, NASA Conference Publication 2071, AFGL-TR-79-0082, 1979.
7. Laframboise, J. G., "Theory of Spherical and Cylindrical Langmuir Probes in a Collisionless, Maxwellian Plasma at Rest," UTIAS Report No. 100, June 1966.

### DISTRIBUTION LIST

National Aeronautics and Space Administration  
Washington, D. C. 20546  
Attn: W. R. Hudson/Code RP 1 copy  
D. P. Williams, III/Code RS-5 1 copy

National Aeronautics and Space Administration  
Ames Research Center  
Moffett Field, CA 94035  
Attn: H. Lum, Jr./M.S. 244-7 1 copy

National Aeronautics and Space Administration  
Goddard Space Flight Center  
Greenbelt, MD 20771  
Attn: R. O. Bartlett/Code 408.0 1 copy  
A. Kampinsky/Code 727.0 1 copy  
E. G. Stassinopoulos/Code 601.0 1 copy  
R. S. Bever/Code 405.0 1 copy

Jet Propulsion Laboratory  
4800 Oak Grove Drive  
Pasadena, CA 91103  
Attn: Ray Goldstein 1 copy  
H. Garrett 1 copy  
E. V. Pawlik 1 copy  
Paul Robinson 1 copy

National Aeronautics and Space Administration  
Lyndon B. Johnson Space Center  
Houston, TX 77058  
Attn: J. E. McCoy/Code SN3 1 copy  
A. Konradi/Code SN3 1 copy

National Aeronautics and Space Administration  
Langley Research Center  
Hampton, VA 23665  
Attn: J. D. DiBattista/M.C. 158B 1 copy  
J. W. Goslee/M.C. 364 2 copies

National Aeronautics and Space Administration  
Lewis Research Center  
21000 Brookpark Road  
Cleveland, OH 44135  
Attn: Head, Mechanics, Fuels & Physics Section/  
M.S. 501-11 1 copy  
Technology Utilization Office/M.S. 7-3 1 copy  
Report Control Office/M.S. 5-5 1 copy  
Office of Reliability and Quality  
Assurance/M.S. 500-211 1 copy  
AFSC Liaison Office/M.S. 501-3 2 copies

DISTRIBUTION LIST (Continued)

Department of Electrical Engineering  
Pennsylvania State University  
121 Electrical Engineering  
East Building  
University Park, PA 16801  
Attn: J. Robinson 1 copy

Department of Physics  
University of California at San Diego  
P. O. Box 109  
La Jolla, CA 92037  
Attn: E. Whipple 1 copy

Aerojet Electrosystems Company  
1100 West Hollyvale Street  
Azusa, CA 91720  
Attn: C. Fischer/Dept. 6751 1 copy

Aerospace Corporation  
P. O. Box 92957  
Los Angeles, CA 90009  
Attn: J. R. Stevens 1 copy  
R. Broussard 1 copy  
J. F. Fennell 1 copy

Beers Associates, Inc.  
Post Office Box 2549  
Reston, VA 22090  
Attn: Dr. Brian Beers 1 copy

Boeing Aerospace Company  
P. O. Box 3999  
Seattle, WA 98124  
Attn: H. Liemohn/M.S. 8C-23 1 copy  
D. Tingey 1 copy

Communications Satellite Corporation  
Comsat Laboratories  
Clarksburg, MD 20734  
Attn: A. Meulenberg, Jr. 1 copy

European Space Agency  
ESTEC  
Zwartweg, Noordwijk  
Netherlands  
Attn: John Reddy, P.B. TTM, 1719 8 2883 1 copy

DISTRIBUTION LIST (Continued)

Ford Aerospace and Communications Corporation  
Western Development Laboratories Division  
3939 Fabian Way  
Palo Alto, CA 94303  
Attn: D. M. Newell/M.S. G-80 1 copy  
J. Pherson 1 copy

General Dynamics Convair  
Kearny Mesa Plant  
P. O. Box 80847  
San Diego, CA 92138  
Attn: J. I. Valerio 1 copy

General Electric Company  
Valley Forge Space Center  
P. O. Box 8555  
Philadelphia, PA 19101  
Attn: V. Belanger/U-2439 1 copy  
A. Eagles 1 copy

Grumman Aerospace  
Bethpage, NY 11714  
Attn: M. Stauber 1 copy

Hughes Aircraft Company  
P. O. Box 92919  
Los Angeles, CA 90009  
Attn: E. Smith/M.S. A620 1 copy

Hughes Research Laboratories  
3011 Malibu Canyon Road  
Malibu, CA 90265  
Attn: Dr. Jay Hyman 1 copy

IRT Corporation  
P. O. Box 80817  
San Diego, CA 92138  
Attn: J. Wilkenfeld 1 copy

JAYCOR  
P. O. Box 85154  
San Diego, CA 92138  
Attn: E. P. Wenaas 1 copy

Kaman Science  
1500 Garden of the Gods Road  
Colorado Springs, CO 80907  
Attn: F. Rich 1 copy

DISTRIBUTION LIST (Continued)

Lee W. Parker, Inc. 252 Lexington Road Concord, MA 01742 Attn: L. Parker	1 copy
Lockheed Palo Alto Research Laboratory 3251 Hanover Street Palo Alto, CA 94303 Attn: J. B. Reagan/Bldg. 205, Dept. 52-12 D. P. Cauffman	1 copy 1 copy
Martin Marietta Corporation P. O. Box 179 Denver, CO 80201 Attn: D. E. Hobbs K. Killian	1 copy 1 copy
Massachusetts Institute of Technology Lincoln Laboratory P. O. Box 73 Lexington, MA 02173 Attn: F. G. Walther	1 copy
McDonnell Douglas Astronautics Company 5301 Bolsa Avenue Huntington Beach, CA 92647 Attn: W. P. Olson	1 copy
Mission Research Corporation 1150 Silverado Street P. O. Box 1209 La Jolla, CA 92038 Attn: V. van Lint	1 copy
RCA Astroelectronics Division P. O. Box 800 Princeton, NJ 08540 Attn: H. Strickberger/M.S. 91	1 copy
Science Applications, Inc. 101 Continental Building Suite 310 El Segundo, CA 90245 Attn: D. McPherson	1 copy
Science Applications, Inc. 2860 S. Circle Drive Colorado Springs, CO 80906 Attn: E. E. O'Donnell	1 copy

DISTRIBUTION LIST (Continued)

Simulation Physics, Inc.  
41 B Street  
Burlington, MA 01803  
Attn: R. G. Little

1 copy

SRI International  
333 Ravenswood Avenue  
Menlo Park, CA 90425  
Attn: J. Nanevicz

1 copy

TRW Systems  
One Space Park  
Redondo Beach, CA 90278  
Attn: A. Rosen  
G. Inouye

1 copy

1 copy